

CRAIG
★
★
★

3

THEORETICAL AND APPLIED OBSIDIAN HYDRATION DATING:
Determining Rates From Environmental Temperatures, and
the Hydration Analysis of 4-SAC-29 Obsidian Artifacts

Larry David Arnold
A.B., (Sacramento State College), 1967

Thesis

Submitted in partial satisfaction of
the requirements for the degree of

MASTER OF ARTS
in
ANTHROPOLOGY

AT THE

SACRAMENTO STATE COLLEGE

Approved:

Howard P. Goldfried, Chairman

Gerald Jay Johnson
Advisory Committee

Date Aug 12, 1969

TABLE OF CONTENTS

Chapter	
I.	INTRODUCTION.....1
II.	THE EVOLUTION OF OBSIDIAN HYDRATION DATING.....6
III.	THE OBSIDIAN HYDRATION PHENOMENON IN THEORITICAL PERSPECTIVE: A Method for Determining Hydration Rates from Environ- mental Temperatures.....12
	The Molecular Diffusion of Water in Obsidian.....12
	Chemical and physical characteristics....13
	Diffusion mechanics.....16
	Derivation of Hydration Rates for Micro- climates by Temperature Analysis.....20
	Determination of hydration rates from the effective temperature.....22
	Determination of the effective temperature.....25
	Hydration rate solutions for three California microclimates: Sacramento- Davis, California; Fresno, California; Brawley, California.....35
	Verification of the Temperature Method through an Independent Rate Calibration by C-14.....43
IV.	THE QUANTATIVE ANALYSIS OF OBSIDIAN HYDRATION THROUGH MICROSCOPIC PETROGRAPHY.....48
	Preparation of Obsidian Thin-Sections.....48
	Cutting the section; grinding the section to mounting thickness; pol- ishing the mounting surface; mount- ing the section; grinding the sec- tion to final polishing thickness; polishing the section to viewing thickness; mounting the cover slip

	The Microscopic Analysis of Thin-Sections.....	64
	Calibrating the microscope; low power optical field insertion; general thin- section survey; selection of optimum rim location; high power optical field insertion; rim boundry determination; measurement of the hydration rim	
V.	THE APPLICATION OF OBSIDIAN HYDRATION DATING TO ARTIFACTS FROM THE KING BROWN SITE.....	81
	Site Discription and History of Excavation.....	81
	The Combined Error Function.....	82
	A Test of the Uniform Hydration Hypothesis and the Chronology of Burial-Associated Obsidian Lots.....	86
	Chronology of burial-associated obsidian lots.....	86
	A test of the uniform hydration hypothesis....	91
	General Chronology of the King Brown Obsidian Artifacts.....	93
	Geotemporal configurations.....	93
	Culturally significant temporal relation- ships.....	97
VI.	CONCLUSIONS.....	101
	BIBLIOGRAPHY.....	112
	APPENDIX A	
	APPENDIX B.	
	APPENDIX C	
	APPENDIX D	

Chapter One

INTRODUCTION

This thesis is concerned with the theory and application of a relatively new dating technique in the field of archaeology--obsidian hydration dating. Originally developed in 1958 by Friedman and Smith, the technique has since undergone a period of refinement in a number of research programs and currently is gaining tentative acceptance throughout the scientific community.

The Department of Anthropology at Sacramento State College itself became involved with the process through the efforts of Mr. William Pritchard in the final months of 1967. Following a departmental relocation over the summer of 1968, the hydration laboratory was established in its permanent location under the auspices of Dr. William Beeson. With Mr. Pritchard to relate the essentials of the technique, and with approximately 300 obsidian artifacts (excavated in the summer of 1967 from 4-SAC-29) as convenient subjects, an analysis was initiated in October of 1968 and completed in April of 1969.

The objective of this thesis is threefold: (1) to present a comprehensive view of obsidian hydration theory culminating in the derivation of a method for determining hydration rates from the environmental temperatures; (2) to develop an optimum procedure using the present petrographic equipment for the preparation and the analysis of

obsidian thin-sections; and (3) to provide a relative chronology (microns of hydration), and a tentative absolute chronology (years B.P.) for the SAC-29 obsidian artifacts.

A comprehensive view of obsidian hydration theory is necessary to understand the basis of many forthcoming analytical steps, and essential to endeavors aimed at applying the technique. The uniform molecular absorption of water along a definable front in obsidian is the foundation upon which the entire technique rests. The theoretical view then will be the first emphasis of this thesis and will cover (1) the process of hydration; (2) diffusion mechanics; and (3) the derivation of tentative hydration rates using temperature as the prime variable.

The second emphasis deals with the laboratory procedures for the preparation and analysis of the obsidian specimens. As there is presently no extensive publication specifically on the "art" of preparing obsidian thin-sections nor the technique of their microscopic analysis, this section will cover such procedure in considerable detail.¹ Hopefully, it will prove useful as a laboratory manual specifically for those using the present hydration equipment, and as a source of technical comparison in a more general sense.

The final emphasis of this work will be on the actual application of the process to obsidian artifacts from 4-SAC-29. Of approximately 300 projectile points and fragments from the Maidu Indian site in southwest Sacramento,

262 were analyzed to provide a relative chronology by degree of hydration. A tentative absolute chronology will be suggested and based on the theoretical derivation of the hydration rate for the Sacramento-Davis microclimate. The resulting chronology will then be utilized to establish the following: (1) the relationship between an artifact's age and its depth in the site; (2) the degree of soil disturbance reflected by the age versus depth correlation; and (3) the relative intensity of site occupation through time.

Within the 262 artifacts analyzed, there are 54 projectile points and fragments associated with seven burials. In decreasing numbers the lot sizes per burial are as follows: 25, 10, 6, 5, 4, 3, and 1. Each of these obsidian lots constitutes a unique grouping of similar materials exposed to similar conditions; they therefore provide a test for an important hypothesis in hydration theory: namely, the hypothesis that obsidians exposed to similar conditions will undergo uniform amounts of hydration. If the standard deviation of the burial lots in microns of hydration is not significantly different from that of the expected measurement error, then the uniformity hypothesis will be confirmed. Conversely, if the difference is probably or highly significant, then the hypothesis will respectively be either conditionally accepted or completely rejected, depending on the level of significance by the chi-square test. Finally, since

the burial-associated obsidian lots constitute such heavily weighted samples for particular points in time and space, their statistics will be handled separately from that of the general distribution of artifacts within the site's space-time continuum.

Preceding the above central text will be a short view of the evolution of obsidian hydration dating. The evolutionary sequence will follow the expansion of the process from its invention by Irving Friedman, a geochemist; and Robert Smith, a mineralogist, through its further development at Stanford to its consequent applications in other research programs in the past few years. By the completion of the sequence, the reader will have the information necessary to view this work in diachronic perspective, and also a sufficient background to ease the transition into the theoretical aspects of the hydration phenomenon.

Following the central text will be the final conclusions of the thesis. Here the findings of this research will be reviewed and evaluated. Suggestions to aid in verifying the temperature-based method of deriving hydration rates will be recommended. Finally, recommendations to set standards of accuracy between hydration dating laboratories will be presented.

Thus the format of this thesis will unfold in the following sequence: the introduction (Chapter I); the evolution of obsidian hydration dating (Chapter II); the theoretical aspects of the hydration phenomenon and the derivation

of hydration rates by temperature analysis (Chapter III); the quantitative analysis of obsidian hydration (Chapter IV); the application of the process to obsidian artifacts from the King Brown Site (Chapter V); and the concluding remarks (Chapter VI). In addition, photographs of the burial artifacts analyzed, a table of the resulting hydration measurements, a table of micron values in years B.P. for Sacramento and Davis, and a table of the micrometer conversion factors will be included in the appendices.

CHAPTER TWO

THE EVOLUTION OF OBSIDIAN HYDRATION DATING

Time is many things, but one of its chief manifestations is in rate of change. When the rate of change of any irreversible process is constant within specified parameters, and the amount of change is quantifiable, then that process is a potential dating device. In 1955, Ross and Smith, while conducting a study of volcanic glasses, observed that freshly exposed surfaces of obsidian will take up water from the environment to form an observable hydrated surface layer. By 1960, subsequent research by Friedman and Smith (starting in 1958) demonstrated that the hydration process was continuous, irreversible, and proceeded at a uniform rate within specified parameters according to the equation $D = (kt)^{1/2}$. In their well known pioneering work, suggesting the use of obsidian as a dating device, Friedman and Smith reported the following observations:

Using artifacts from archaeological sites of known age, the influence of temperature, relative humidity, chemical composition of the obsidian, burning and erosion of the obsidian on the rates of hydration was determined. Temperature and chemical composition are the main factors controlling the rate of hydration. Obsidian hydrates more rapidly at a higher temperature, and thus progresses at a faster rate in tropical than in arctic climates. Rhyolitic obsidian hydrates more slowly than does trachytic obsidian. Using archaeological data from various parts of the world, several tentative hydration rates were determined for tropical, temperate, and arctic climates. The method in its present state of development is especially suited to determine relative chronologies in layered sequences of artifacts from a single site, or region (1960:476).

Immediately following the article by Friedman and Smith, Clifford Evans and Betty Meggers offered an archaeological evaluation of the new dating method. In their article Evans and Meggers (1960:523) pointed out two categories of potential error: the geotechnical uncertainties covered by Friedman and Smith; and errors in archaeological context. The principle source of context error reported at that stage resulted from the reuse of significantly older artifacts by more recent cultures. If the artifact was never reworked during the period of reuse, then no new surfaces would have been exposed to register its bicultural context. Additional archaeological problems reported were the tendency for diachronic mixing of artifacts within a site; and the possibility of erroneous rates of hydration derived from faulty C-14 correlations. In concluding their work, Evans and Meggers indicated that dating of archaeological horizons by the method shows considerable promise within present geotechnical and archaeological limitations. "If continued research can resolve some of the geological problems of the hydration of obsidian and permit the establishment of reliable rates of hydration, archaeology will have a new dating method that will be at least as accurate as many of the methods now in use" (1960:537).

The next major contribution to the development of obsidian hydration dating was the first intensive analysis of a fairly homogeneous petrological and archaeological area. The work of Friedman and Smith utilized a heterogeneous world-wide sample of approximately 600 obsidian artifacts and specimens.

c

In the next contribution, Donavan Clark utilized approximately 300 artifacts from 15 sites in Central California. This selection constituted an intensive sampling of one fairly homogeneous area, and thus provided a specific test of Friedman and Smith's more encompassing research. Conducted as a Stanford University doctoral project between 1959 and 1961, Clark's work was designed to accomplish three major objectives: (1) to verify the reliability of hydration measurements; (2) to determine the degree of variance between contemporary samples within burial lots, and the extent of variance between such lots; and (3) to determine a tentative Central California hydration rate for absolute dating (Clark, 1961:95). The results of Clark's three objectives were: (1) a measurement error or reliability of $\pm .26$ microns between two analysts at the one sigma level (Friedman reported $\pm .20$); (2) a within burial lot variance of less than $\pm .2$ microns (one sigma) with the variance between non-contemporary lots being significantly different (1961:95); and (3) a tentative hydration rate based on C-14 correlation in the form $\bar{D}^x = (kt)^{3/4}$, where \bar{D}^x is hydration thickness in microns, k is a constant chiefly depending on the environmental temperature, and t is the time in years. The "best" compromise for the constant k was (later) given as 0.0105 (Clark, 1964:177). The expression for the hydration rate was the main variation from the findings of Friedman and Smith ($\bar{D}^x = (kt)^{1/2}$); subsequent findings, however, have tended to support the latter classical expression for diffusion rates.¹

After the publication of Clark's dissertation, the emphasis rapidly switched from the research and development phase to that of development and application. Furthermore, in view of the complexities in determining the hydration rates, the general orientation became one of utilizing the process more as a precise method in relative dating. Being a fairly inexpensive and rapid process, the number of laboratories began to spread. In 1959 there were two: the laboratory directed by Friedman and Smith at the U.S. Geological Survey, Washington, D.C., and Donavan Clark's at Stanford University. By 1963 there were six, and by 1967 eleven laboratories were in operation (Michels, 1967: 211). With the addition of the University of Hawaii (Roger Green), the University of Oregon Museum of Natural History (LeRoy Johnson, Jr.) and finally Sacramento State College, the total known to date is thirteen. The following are the laboratories now in operation (listed in order of establishment):

- | | |
|--|--|
| 1. U.S. Geological Survey,
(I. Friedman) | 8. University of Calif.
Davis (Baumhoff) |
| 2. Stanford University,
(B. Gerow) | 9. Pennsylvania State
University (Michels) |
| 3. Smithsonian Institute
of Anthropology,
(C. Evans) | 10. University of Oregon
Museum of Natural
History (LeRoy
Johnson, Jr.) |
| 4. University of Auckland,
New Zealand,
(R.C. Green) | 11. University of Manitoba
(W.J. Mayer-Oakes) |
| 5. Brown University,
(D.D. Anderson) | 12. University of Hawaii
(Roger Green) |
| 6. University of Hokkaido
(Katsui and Kondo) | 13. Sacramento State College
(Larry David Arnold
and William Pritchard) |
| 7. University of Calif.
Los Angeles (Meighan) | |

Note: Numbers 1-11 were reported by Michels (1967: 214)
Numbers 12-13 are from personal knowledge.

Following the republication of part of Clark's doctoral dissertation in 1964,² the next major contribution was Michels' 1965 Ph.D dissertation³ which covered various archaeological applications of relative obsidian hydration dating in great detail. Namely: (1) relative time-ordering of artifact styles at a site; (2) artifact reuse; (3) testing of site stratigraphy; (4) relative intensity of occupation through time; (5) discovery of commercial focus within a particular artifact class; and (6) the use of dated obsidian artifacts to segregate their associated materials in poorly stratified sites, or mixed surface samples.

In addition to Michels' Ph.D. dissertation, various applied articles have appeared in a number of professional journals. In the applied category were articles by: Roger Green (1962 and 1964); Evans (1965); Dixon (1966); Michels (1967); Adams (1968); Meighan, Foote and Aiello (1968); and Michels (1969). Of theoretical importance were works (mainly prior to 1965) by: R.R. Marshall (1961); Friedman, Smith and Long (1963); Friedman, Smith and Clark (1963); and again Friedman, Smith and Long (1966).

The majority of the above articles will be utilized in subsequent chapters on theoretical and applied aspects and will therefore be covered at that time.

In concluding this section, I wish to emphasize that the chief archaeological value at present lies in the relative dating aspects of the method. Absolute dating aspects have

11

lagged due to the complexity of making accurate C-14/hydration correlations, and the uncertainties resulting from the effects of environmental temperature and small variations in chemical composition of the obsidian. The publication of the 1966 article by Friedman, Smith and Long, however, has contributed needed valuable information regarding the effects of temperature, and is helping in the establishment of reliable rates of hydration. This article will be utilized as the basis of a theoretical derivation of the local hydration rate presented in the following chapter.

Chapter Three

THE OBSIDIAN HYDRATION PHENOMENON IN THEORETICAL PERSPECTIVE: A Method for Determining Hydration Rates from Environmental Temperatures

I. THE MOLECULAR DIFFUSION OF WATER IN OBSIDIAN

Within samples of glassy rhyolitic rocks, often two phases of glass are observed: one is typical obsidian, and the other is perlite. The boundary between the two is very sharp and implies a sequence of formation. As Ross and Smith observed: "The only interpretation that seems possible is that the entire mass was originally obsidian and the perlite was formed as a result of some secondary process" (1955: 1074). This secondary process, identified in their article as hydration, was the subject of the later intensive research by Friedman and Smith (1960) which verified the obsidian to perlite conversion by continual diffusion of H_2O and led to the utilization of the process as a dating device. In effect, when dating obsidian samples one is either measuring the width of the perlite layer, or the depth to which water has diffused into the obsidian sample. In other words, the only difference between perlite and obsidian chemically is the percentage of water and the way it is held; and physically the difference in refractive index and a small degree of mechanical strain, which gives the perlite generally a lighter color (especially in cross-polarized light). Let us now examine the chemical and physical characteristics of the two phases in greater detail.

A. Chemical and Physical Characteristics

First, and most important, for diffusion there is a discrete difference in water concentration between the two phases. For obsidian the water content by weight is about 0.3 percent, whereas for perlite the content is about 3.5 percent (Ross and Smith, 1955:1075). This difference in concentration (about ten times more water for perlite) provides the driving force for the diffusion process.

Of secondary importance is the source of and the manner in which the water is held in the two phases. The exact nature of the bonding is not defined for either phase due mainly to the high number of possible combinations between water and the silica and other constituents of the glass; however, experiments have demonstrated that the pristine water content of obsidian (.3%) is held at a much higher energy level than the meteoric water (3.5%) of the hydrated or perlite phase. "The fact that the H₂O of obsidian is held tenaciously and released almost explosively at temperatures of 800° to 1000° C. indicates fixation at temperatures characteristic of magmas" (Ross and Smith, 1955:1086). On the other hand, continued heating at temperatures from 200° to 600° C. is sufficient to drive off the water of hydration. In such an experiment then, at temperatures near 600° C. water will be driven off until about .3% remains; thereafter the concentration remains stable as the temperature is increased until the fixation level is reached (800° to 1000° C.)--then the pristine water is finally and

almost explosively released. Thus the source of water in the two phases is also distinct. Later experiments (Friedman and Smith, 1958:218) demonstrated conclusively by isotopic comparison (deuterium) that the water in the hydrated (perlite) layer was related to meteoric (surface) water, whereas the water in nonhydrated obsidian was different. "The probable explanation of water in normal obsidian is that it was inherited directly from the magma, that is, it represents pristine H₂O" (Ross and Smith, 1955:1086).

The important implication derived from the geochemical research is that hydration: (1) proceeds under normal atmospheric temperatures and pressures by the diffusion of meteoric water, and (2) as Friedman and Smith (1960) demonstrated, it is a continuing process to be expected anywhere obsidian is exposed to normal atmospheric conditions.

The physical difference between perlite and obsidian, as mentioned above, is chiefly manifested by a variation in the index of refraction: obsidian has a ^{average} refractive index of 1.486 whereas that of perlite is 1.497 (Ross and Smith, 1955: 1075). Furthermore, the refractive index is directly related to the water content in both phases; in fact, the amount of water has about twice the effect on the index in obsidian than in perlite (again an indication of the difference in the nature of the water bonding between the two phases). It is this difference in the refractive index which causes the contrast between the two phases under normal light. The contrast observed under cross-polarized light results from mechanical strain

produced by the addition of water with very little change in the obsidian's volume (the H_2O molecules can nearly fit in the space within the silica tetrahedrons). Such strain birefringence disappears as the water content is driven from the hydrated layer. In addition, after the hydration reaches a thickness of 40-60 μ the strain tends to cause the rim to spall off (Friedman and Smith, 1960:487).

With the essential chemical and physical aspects of both phases covered, let us now focus on the boundary area between the two. Such boundary areas or diffusion fronts in many substances are transitional or gradational and thus ill-defined. "However, in obsidians this diffusion front is sharp, varying only in the order of 0.1 micron in depth" (Friedman and Smith, 1960:482). Figure 3.1 is a graph showing the relationship between the water content and depth from surface across the diffusion front. This illustrates the very sharp transitional distance (.1 μ) between the hydrated and non-hydrated obsidian: if the amount of hydration increased, the graphical illustration would advance to the right (deeper into the obsidian) while retaining the same form.

The sharpness of the diffusion front is one of the essential characteristics enabling accurate measurements of the amount of hydration. It is also then a primary factor in the theoretical limit of measurement accuracy. Curiously enough, the measurement error determined from the 4-SAC-29 obsidians and by Friedman and Smith (1960) was in the order of \pm .1 microns or about twice the width of the diffusion front. The

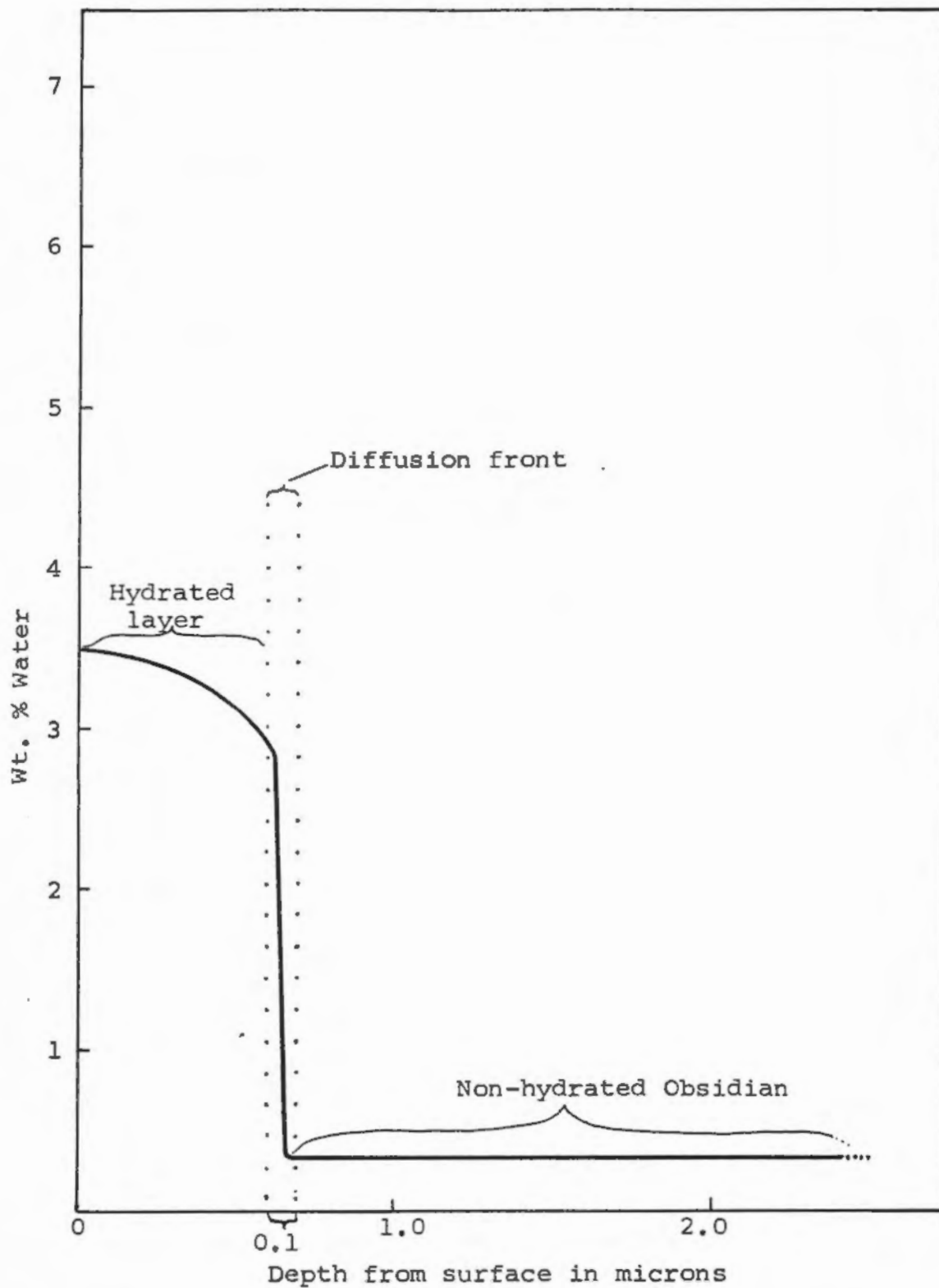


Fig. 3.1. Diagram showing the high water content of the saturated hydrated phase, the sharp diffusion front, and the low water content of the non-hydrated obsidian phase. (From Friedman and Smith, 1960:483)

probable explanation for this is that measurements vary randomly about the extremes of the diffusion front for the majority of trials. The theoretical limit of the measurement error would then seem to be in the order of $\pm .05$ microns, or the width of the diffusion front itself. So far the nearest reported to that limit is $\pm .07$ (Michels, 1967:213). The explanation of the visibility of the diffusion front under magnification (see Plate 3.1) along with some other interesting aspects of the hydrated layer was furnished through the use of an electron microscope. "An electron photomicrograph image of the hydrated region reveals a sector exhibiting parallel microfractures all running perpendicular to the exterior surface of the stone and terminating at approximately the same point. The sharply demarcated front seen through an ordinary light microscope is an optical smear of the interior ends of the microfracture lines" (Michels, 1967:214).

Having outlined the essential chemical and physical differences between phases along with the characteristics of the diffusion front, let us now proceed to a simple description of the mechanics of diffusion and thereafter to the determination of rates of hydration by temperature.

B. Diffusion Mechanics

As indicated above, the concentration of water in perlite is about ten times that in the non-hydrated obsidian. Consider a water molecule as an impurity in either side of the diffusion front and "trapped" within a cage formed by the

atoms of the relatively large silica tetrahedron making up the majority of the obsidian (rhyolitic obsidians are 75-78% silica, SiO_4). Now at temperatures above absolute zero atoms are in a continual state of thermal oscillations about their average positions with the amplitude being directly proportional to temperature. Such also is the case with the silica tetrahedron and its "caged" water molecule. The water molecule vibrates in the cage formed by the adjacent atoms of the tetrahedron and each time it approaches the walls of the cage, strong repulsive forces set in to force it back to the center of its cell. However, if it has sufficient thermal energy to overcome the repulsive forces it can jump to an adjacent cage. The energy E necessary to accomplish this jump is called the activation energy. It should be evident that such jumps are in part dependent on temperature and the surrounding crystal geometry. Figure 3.2 illustrates the change in energy as the water molecule moves between cells. The energy of the water molecule is minimum at the cell center A, maximum at the midway point between cells B, and drops again to a minimum as it reaches the adjacent cell center C. If the impurity molecules are homogeneously distributed within the obsidian crystal structure, then one can easily see that random jumps will result in no net movement of matter. A jump in one direction will simply balance a jump in the other direction. However, for our particular case the distribution of water is far from homogeneous between phases. Obsidian is capable of absorbing up to 3.5% of its weight in water and during its formation

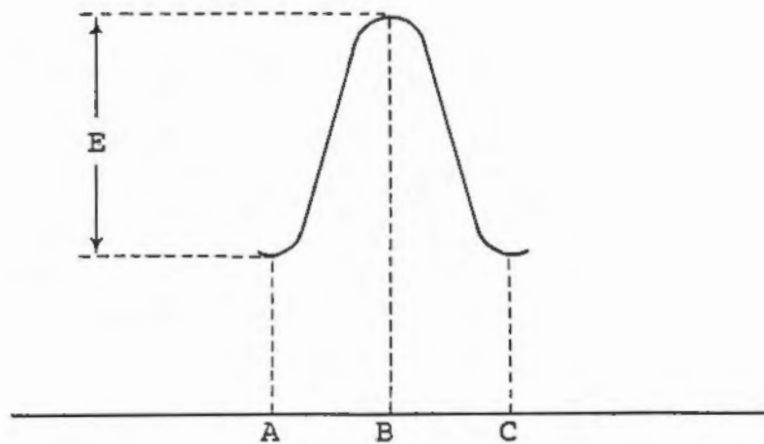


Fig. 3.2. Energy of an impurity molecule as it moves from an initial position A in one cage to a final position C in an adjacent cage. (From Girifalco, 1964:39)

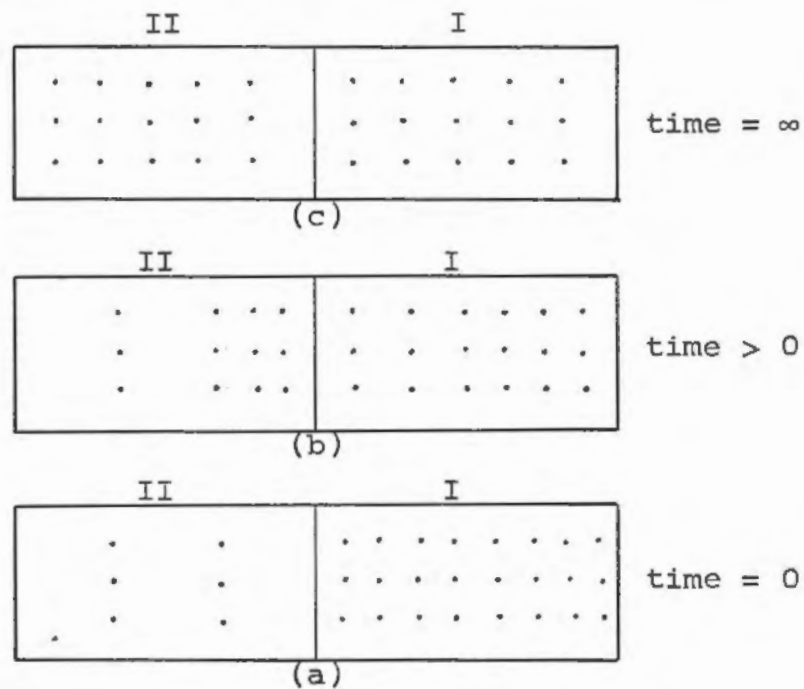


Fig. 3.3. Schematic diagram of the net transport of matter under the influence of a concentration gradient. (From Girifalco, 1964:43)

only around one-tenth of that is achieved. Thus water is taken on from the environment by diffusion until that saturation point is achieved. Figure 3.3 is a simplified illustration of the situation existing between the two phases in obsidian. Part I (a) has a higher impurity concentration (3.5%) than Part II (a) (0.3%). If we assume this section is suddenly isolated from a further supply of impurities (H_2O) at time $t=0$, then the illustration depicts the diffusion of the water throughout the section from $t=0$ to $t=\infty$. Since there are more impurities per unit volume in region I than region II, the number of them that initially jump from I to II is greater than the number that jump from II to I. Thus in time, region II acquires impurities at the expense of I so that eventually there is an even distribution throughout the material. Hence for diffusion across a concentration gradient there is a net movement of material. For the actual case where the section is not isolated from a further supply of impurities, one can easily see that the diffusion front will simply advance in the direction of lowest concentration as the area immediately behind approaches saturation, i.e., the concentration gradient acts as a driving force.

The mathematical equations relating the matter flow to the concentration are essentially based on this net exchange or flux across the gradient, and known as Fick's First and Second Laws of Diffusion. The net flux, J , depends on the jump frequency, the geometry of the crystal, and the difference in concentration of impurity atoms on adjacent planes.

Without going through the derivation (see Girifalco, 1964:45) the expression relating the net flux J to the concentration (c) relative to displacement (x) is given by Fick's First Law:

$$J = -D \frac{\partial c}{\partial x}, \text{ where } D = D_0 e^{-E/kT}$$

and E is the activation energy, k is Boltzmann's constant, and T is absolute temperature. D , the diffusion coefficient, is the essential item that must be determined in describing a given diffusion process. "The most important single fact that can be known about the diffusion coefficient is its variation with temperature" (Girifalco, 1964:54). (The work of Friedman, Smith, and Long in 1966 was essentially devoted to the determination of "D" for rhyolitic obsidians and plays a key role in the derivation of hydration rates for microclimate in the following section of this chapter.)

The expression relating the concentration c , the displacement x , and the time t is given by Fick's Second Law:

$$\frac{\partial c}{\partial t} = D \frac{\partial^2 c}{\partial x^2} + \frac{\partial D}{\partial x} \frac{\partial c}{\partial x}$$

The Second Law is an expansion of Fick's First Law (see Girifalco, 1964:50) and the basic equation used in diffusion work. It is derived by combining the First Law with the Law of the Conservation of Matter; the essential difference being that the Second Law establishes concentration profiles as a function of time in any particular case. Thus when the value of D is known for a particular case, then the time t , and

displacement x are given by the following solution to Fick's Second Law (see Barrer, 1951:9):

$$x^2 = Dt \quad (1)$$

This, of course, is in agreement with publications on diffusion rates: "According to the data of Friedman and Smith (1960), the hydration rate at a given temperature is defined by the equation:

$$x^2 = kt$$

where x = depth of penetration of water in microns, k = constant for a given temperature, and t = time in years" (Friedman and Smith and Long, 1966:323). The distinction between k and D in the two equations may be interpreted as meaning k is D for a given temperature, i.e., k is a special case of D . (~~Often there is no distinction, with either being used interchangeably.~~)

II. DERIVATION OF HYDRATION RATES FOR MICROCLIMATES BY TEMPERATURE.

As previously mentioned (Page 10), absolute dating aspects of the hydration method have come to play the minor role in actual field use. Starting with the work of Friedman and Smith (1960), C-14 has been the only practical means of defining hydration rates (or D) in years thereby enabling the process to be used as an absolute dating device. However, C-14 correlations do have their complications: (1) the number of C-14 dates at a site is not always sufficient; (2) the range

of dates available often is not dispersed well enough for an accurate description of the rate curve; (3) the question of the obsidian and the item dated by C-14 being contemporaneous often presents a problem; (4) the accuracy of the C-14 date is at times in question; (5) the number of geographical areas with C-14/hydration correlations is vastly insufficient; and (6) the expense of the C-14 process itself is prohibitive. Although there have been a number of accurate C-14/hydration correlations, one can appreciate the difficulty involved. Another major problem in using the method for absolute dating is its sensitivity to the environmental temperature. As stated in the preceding section on diffusion mechanics, temperature is the most important single fact in a diffusion process. The diffusion rate is chiefly dependent on temperature; hence in absolute dating one can not take a rate determined in one microclimate and apply it to an adjacent area having a different annual temperature. When the effective temperatures of two areas correspond, then and only then can one rate be used for both; however, we will cover this in detail shortly.

Recalling the general expression for the diffusion coefficient, $D = D_0 e^{-E/kT}$, we can see that once the activation energy E and constant D₀ for the particular material are empirically defined, then D for any particular temperature T can be determined. The implication should be obvious--one need know only the temperature of the area from which the obsidians were recovered to determine their hydration rate.

Thus rates can, theoretically, be determined by: (1) temperature through one approach, or (2) by C-14 (or other calibration means) from the opposite approach. Regardless of the approach, however, the objective is still the determination of D , the diffusion or rate coefficient. Friedman, Smith, and Long (1966) after several years of experiments successfully determined the diffusion coefficient of rhyolitic glass over a temperature range from 5° C. to 100° C. What remained to be defined following their publication was the relationship between the effective temperature T_e in the diffusion coefficient, and the environmental temperatures to which the obsidians have been continually exposed at the site. We will shortly turn, hopefully, to the determination of that relationship.

A. Determination of Hydration Rates From the Effective Temperature.

First of all, should the temperature relationship be successfully determined, we will need to know the expression equating the effective temperature T_e to the diffusion coefficient D . Although the publication by Friedman et al (1966) does not contain the equation, there is sufficient data to determine it by the method of least squares.

Utilizing their experimentally determined hydration rate at 100° C. in conjunction with the rates determined by C-14 calibration from five different areas of the world by

Friedman and Smith (1960) we have the following data (Friedman et al, 1966:324):

<u>Source</u>	<u>T_e °C</u>	<u>D (μ²/1000 years)</u>
1. Experimental	100	10,000.0
2. Coastal Ecuador	30	11.0
3. Egypt	28	8.1
4. Temperate No. 1	25	6.5
5. Temperate No. 2	20	4.5
6. Sub-arctic	5	0.9

With the vertical axis being the log of D, the horizontal axis the effective temperature T_e in °C, and the slope of the line log D vs. T_e being the activation energy E, we now use the method of least squares to determine the equation of the line best fitting the data.

In the general equation of a straight line, $y = bx + a$, we designate $y = \log D$ and $x = T_e$ or $\log D = bT_e + a$; where,

$$b = \frac{n \sum (T_e \log D) - (\sum \log D) \sum T_e}{n(\sum T_e^2) - (\sum T_e)^2} \quad (2)$$

$$a = \frac{\sum \log D - b \sum T_e}{n} \quad (3)$$

Note: n = the number of trials or degrees of freedom.

Making the necessary computations we find that:

$$\begin{aligned} \sum T_e &= 208.0 & \sum T_e^2 &= 12,734 \\ \sum \log D &= 7.3702 & \sum (T_e \log D) &= 489.837 \end{aligned}$$

Now solving for b and a in equation (2) and (3) we find:

$$\begin{aligned} b &= .0424, \text{ and} \\ a &= -.2410 \end{aligned}$$

Substituting a and b into the expression $\log D = bT_e + a$, we thus have the desired equation best fitting the empirical data:

$$\log D = .0424T_e - .2410 \quad (4)$$

Given any effective temperature of hydration, equation (4) can then be used to find the corresponding D in microns squared per thousand years. For example, if the effective temperature T_e at a given location is 25°C . then:

$$\begin{aligned} \log D &= .0424 T_e - .2410 \\ \log D &= .0424 (25) - .2410 \\ \log D &= 1.0600 - .2410 \\ \log D &= .8190, \text{ finding the antilog then} \\ D &= 6.5 \mu^2/1000 \text{ years} \quad (\text{Temperate No. 1}) \end{aligned}$$

Finally, recalling equation (1), $x^2 = Dt$, we substitute D determined for $T_e = 25^\circ \text{C}$. and arrive at the rate equation needed for absolute dating within that particular microclimate.

$$x^2 = 6.5 \mu^2/10^3 t$$

Given any depth of hydration x in microns, one can use the above equation to determine t in thousands of years. For example, if x is found to be one micron for a certain obsidian artifact, then:

$$\begin{aligned} x^2 &= 6.5 \mu^2/10^3 t \\ (1)^2 &= 6.5 t \\ 1 &= 6.5 t \\ t &= 1/6.5 = .1540 \times 10^3 \text{ years, or} \\ t &= 154 \text{ years} \end{aligned}$$

The artifact is about 154 years old (\pm the measurement error).

From the preceding information, the two main expressions for defining hydration in years B.P. given T_e are:

$$\log D = .0424 T_e - .2410 \quad (4)$$

$$x^2 = D t \quad (1)$$

What remains, then, is the determination of T_e , the effective temperature of hydration.

B. Determination of the Effective Temperature

The objective of this section is to determine the relationship between the effective temperature T_e and the environmental temperatures to which the obsidians were exposed during hydration. Since artifacts are normally recovered from the ground, soil may be considered as the primary environment of hydration for obsidian artifacts. The behavior of soil temperatures relative to these artifacts is, therefore, first in the order of investigation. It is to be noted from the onset that the following derivation holds only for temperate and tropical climates.

1. Determining the Effective Thermal Energy Level

During an artifact's stay in the soil, three factors work together to influence hydration: time, temperature, and depth. The temperature at a given point is a function of both depth and time (chiefly time of year). As one might expect, the subsoil temperatures near the surface very closely reflect the degree of solar radiation. Over the summer

months soil temperature will rapidly decrease within the first foot from the surface and thereafter decrease very much more slowly with depth while approaching a constant. Conversely, during cold winter months soil temperatures increase (more linearly) with depth as they approach a constant. From numerous tables of soil temperatures compiled from approximately 800 locations around the world (Chang, 1958), soil-temperature profiles seem to have the following general characteristics in temperate and tropical climates:

- (1) The mean annual temperatures at all depths below approximately one foot are statistically equal.
- (2) The temperature constant approached during the summer and winter months (see above) is the mean annual soil temperature.

Figure 3.4 (a) shows a temperature profile by depth for one summer day near the University of Leipzig. The skewing towards the high end is especially evident in this display. Such a skewing characteristic plays an important role on a monthly basis as illustrated in Figures 3.5 (a & b).

Figure 3.4 (b) shows a series of geotherms taken throughout the year and is in support of the first general characteristic derived from Chang's data. As Geiger has observed: "one might conclude from the positions of the curves that the mean annual temperature scarcely alters with depth" (Geiger, 1965:65).

Figure 3.5 (a) is a temperature-depth time profile by month from Temple, Texas. Figure 3.5 (b) is also such a profile by month from Brawley, California. The two typical

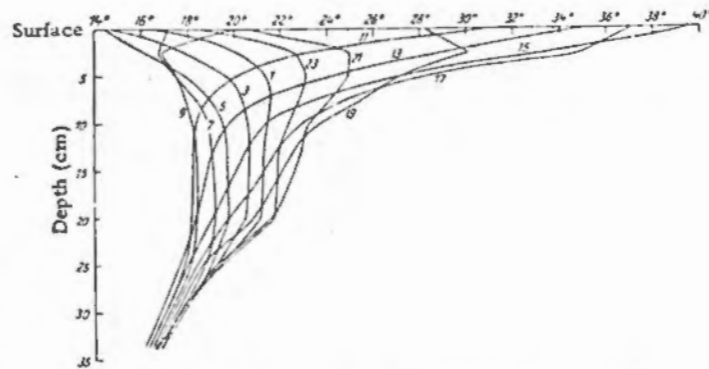


Fig. 3.4(a). Temperature profile by depth showing the rapid skewing of highs near the surface. (From Geiger, 1965:57)

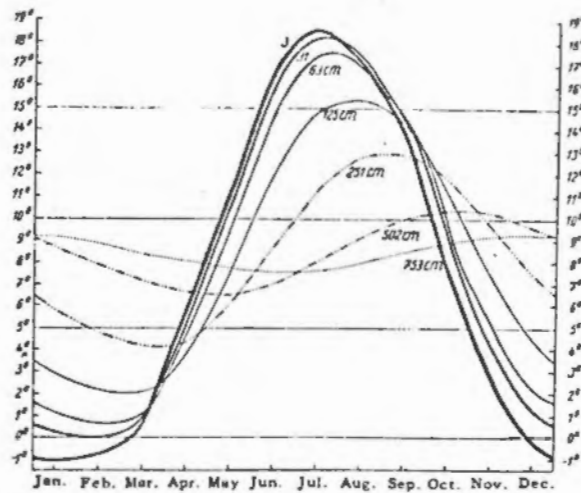


Fig. 3.4(b). Geotherms indicating temperature behavior at a given depth over one year. From the symmetry of each geotherm one can see there is little variation in the annual means by depth. (From Geiger, 1965:65)

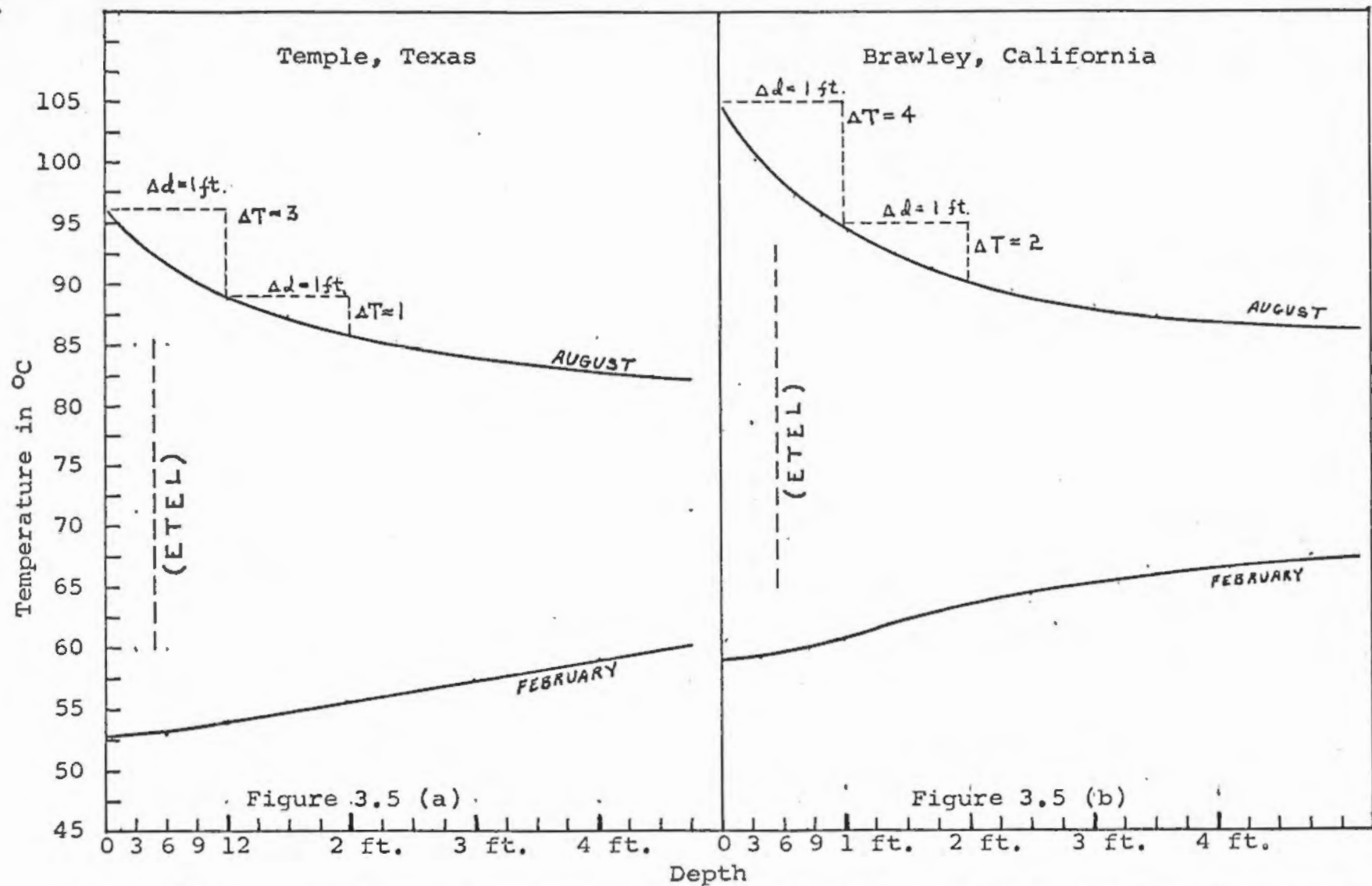


Fig. 3.5 (a&b). Tautochrone profiles showing the variation of temperature with depth for the highest and lowest months of the year. The ETEL line indicates the approximate depth of the effective thermal energy level.

21

profiles provide a different perspective than Fig. 3.4 (b) and illustrate both general characteristics listed above. As can easily be seen, the decrease in temperature with depth during the summer maximum is very rapid within the first foot. Thereafter the change becomes increasingly slower. For the winter minimums the change is slow and nearly linear with depth (as mentioned previously) without the rapid surface change characteristic of summer. The effect of the asymmetrical minimum and maximum tautochrones¹ on the mean is evident at a glance. Above a certain point, the thermal demarcation point, the mean temperatures accelerate toward the surface, while below that point the change becomes slow and often hard to detect within a certainty of half a degree. In view of our desired relationship, the first essential question is: which level most accurately reflects the range of temperatures to which an artifact has been exposed within the ground? Once that most effective level is defined, then the monthly temperatures for that level will be integrated to determine T_e , the effective temperature of hydration.

To define the effective level one must first know how many readings per unit of depth are needed to give a meaningful average. If the tautochrones were linear, then the readings would be evenly spaced by depth and a simple average would complete the task. Then, once the average was computed, the level nearest that average would be selected as the representative one. However, the tautochrones are exponential, not linear; therefore, the number of readings per

unit of depth is not constant and must be determined. From what has previously been stated about temperatures above and below the thermal demarcation point, one might expect the number of readings above it to be large and then decrease rapidly per unit of depth. That, in fact, is the case. To determine the number of readings per unit depth we inspect the rate of change, $\Delta T/\Delta d$, using one foot increments. Referring to Fig. 3.5 (a) we see for the first foot $\Delta T/\Delta d = 3/1 \text{ ft.}$; thus 3 readings are necessary for the first foot. For the next foot we find $\Delta T/\Delta d \approx 1/\text{ft.}$ or only one reading per foot; and then about one reading for the next three feet. In general the readings for several such profiles follow somewhere between an inverse square and inverse cube law regardless of soil types. In other words, between:

- (a) 3 readings /0-1 ft.; 1 reading /1-2 ft.;
1 reading /2-5 ft.
- or
- (b) 4 readings /0-1 ft.; 2 readings /1-2 ft.;
1 reading /2-3 ft.

Since the majority of cases follow closer to (a), the inverse cube relationship will be used. One might note, however, that using (b) would hardly introduce much error. Thus for determining the representative level we will need three readings within the first foot; one for the next foot; and finally, one at the midpoint of the next three feet. This would be effective for an artifact found anywhere between zero and about five feet. Practically speaking, the change is so small that disregarding the two readings over the next 36 feet

would be negligible. Thus the process is generally effective for depths encountered in archaeology.

We are now ready to determine the effective level in Fig. 3.5 (a) and 3.5 (b), and in two additional examples to show the level trend. From the inverse cube rate (a) we select the following readings:

Temple, Texas
(Chang, 1958:195)

1 in.	71.5
3 in.	71.0
6 in.	70.9
2 ft.	70.7
4 ft.	70.5
	<hr/>
	354.6

$$354.6/5=70.92^{\circ} \text{ F.}$$

$$3'' < d < 6''$$

Brawley, California
(Weather Bureau, 1966)

1 in.	84.0
4 in.	79.0
12 in.	77.0
20 in.	76.6
4 ft.	76.0
	<hr/>
	392.6

$$392.6/5=78.5^{\circ} \text{ F.}$$

$$4'' < d < 6''$$

Faucett, Missouri
(Chang, 1958:187)

1 in.	55.1
3 in.	54.3
6 in.	54.0
2 ft.	53.6
4 ft.	53.4
	<hr/>
	270.4

$$270.4/5=54.1^{\circ} \text{ F.}$$

$$3'' < d < 6''$$

Lincoln, Nebraska
(Chang, 1958:190)

1 in.	58.0
3 in.	55.3
6 in.	54.6
1 ft.	52.9
3 ft.	52.5
	<hr/>
	273.3

$$273.3/5=54.7^{\circ} \text{ F.}$$

$$3'' < d < 6''$$

From the above typical examples one can see the effective level generally lies between 3 inches and 6 inches ($3 < d < 6$). The most readily available source of temperatures is called

Climatological Data (published by the Weather Bureau), and it lists the four-inch level, if any level at all; so expediency and probability dictate it to be the appropriate choice. Thus the four-inch depth is the most probable and readily available measure of sub-surface thermal energy, i.e., it is the desired effective level from which T_e can be integrated within temperate climates.

For tropical and arctic climates the former is trivial, but the latter is complex. In tropical climates soil temperatures, like atmospheric temperatures, change very little during the year, and very slowly with depth. For example, at Chinchina, Colombia the annual range at four inches is only around 6° F, while the temperature range between four inches and six feet for the warmest month is only 4° F (Chang, 1958:167). In comparison, the same ranges for Brawley, California are respectively 45° F and 25° F. With so small a range the effective soil temperature in tropical climates can essentially be determined from any one month at any level between three inches and three feet. However, for purposes of standardization, using the annual monthly sequence at about a four-inch depth is recommended.

Finally, for the case of arctic climates no attempt will be made to derive hydration rates since the work by Friedman et al (1966) does not extend below 5° C; in addition, the arctic soil characteristics are complex, making generalizations exceedingly difficult to formalize.

From the preceding we have selected four inches as the most probable depth of the effective thermal energy level (ETEL), and limited the environmental range to tropical and temperate climates. Having selected the appropriate ETEL we are now left with one final but essential problem in the determination of T_e , the effective temperature of hydration: how can the ETEL monthly temperatures be combined to give one effective annual temperature?

2. Finding T_e by Approximate Integration of ETEL Temperatures

In determining T_e , the problem is to somehow combine a number of different temperatures into one representative of all. In a special sense the problem is to find the "average" of the ETEL monthly temperatures. However, finding the simple (arithmetic) average is not the correct method: such an average ignores the time duration of each temperature. In other words, diffusion is proportional to both temperature and time, and each is an essential factor in determining T_e . What method, then, does one apply to a series of temperatures held over their respective exposure times to arrive at the effective temperature? Fig. 3.6 illustrates the following general situation, and will help to clarify the question. During a hypothetical experiment, an obsidian specimen is exposed to a temperature T_1 for t_1 months, T_2 for t_2 months, and T_3 for t_3 months. Referring to Fig. 3.6, temperature (T) is represented by the vertical axis, and time (t) is represented by the horizontal axis. To graph the three

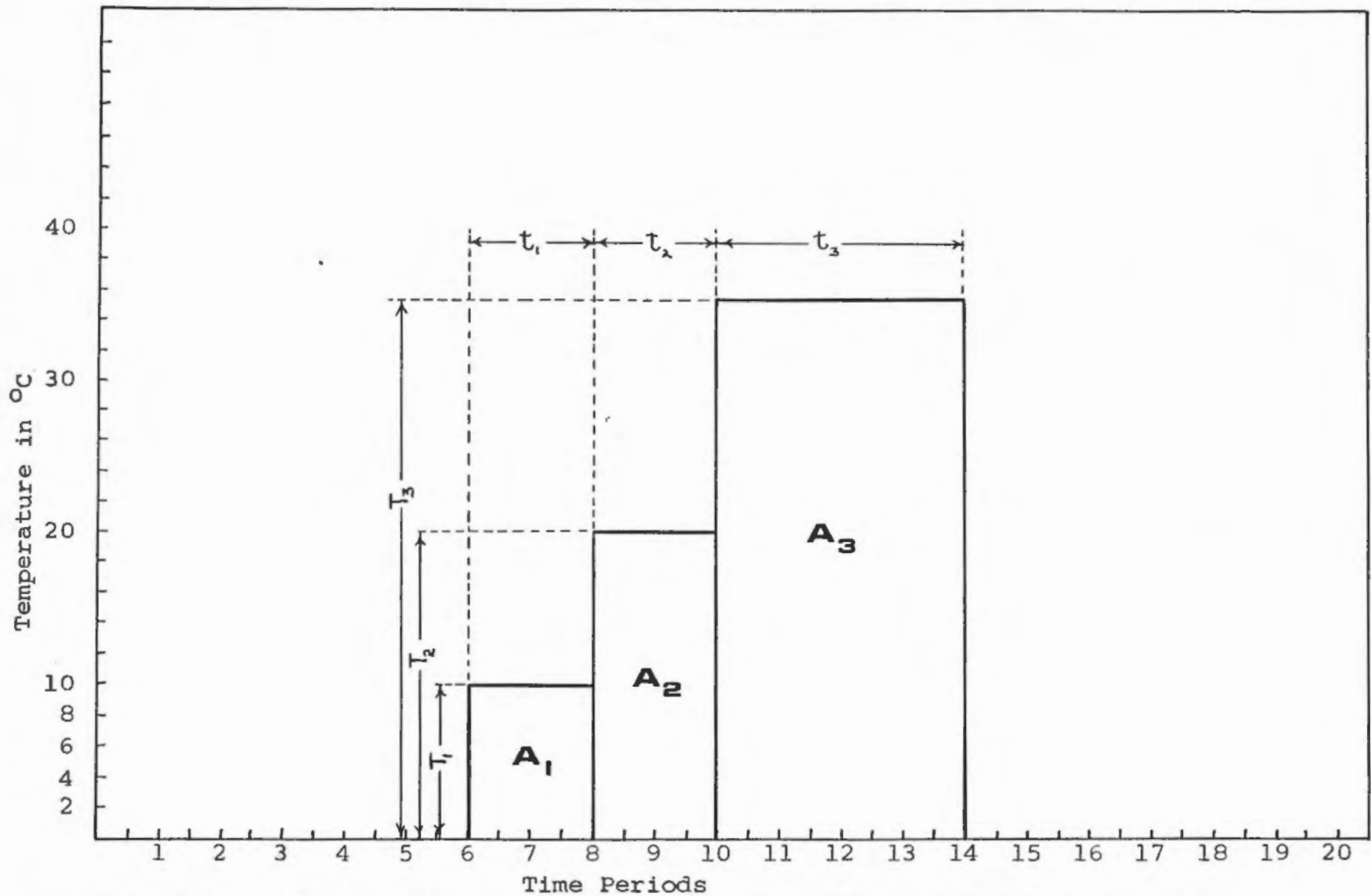


Fig. 3.6. Temperature-time relationship with areas illustrating the relative affect of each temperature during hydration.

temperature exposures we begin at some arbitrary starting time and proceed up to T_1 °C and then across t_1 months of exposure time. The area A_1 now represents the time-temperature product at T_1 °C. Next, at the end of t_1 months the temperature is raised to T_2 and held for t_2 months: area A_2 represents the time-temperature product at T_2 °C. In the same manner, A_3 represents the t_3 months exposure at T_3 °C. The graph represents the integral of the various temperatures over $t_1 + t_2 + t_3$ months. Each area represents the effect its temperature has within the whole. The relative effect of each temperature, therefore, is found by multiplying the ratio of its area to the whole times the temperature itself.

Finally, once the relative effect of each temperature is known, all of them can be summed to give the total effective temperature, or T_e . The method, in general then, is to find the total ($T \times t$) area by approximate integration, "weigh" each temperature by the ratio of its area to the whole, and then sum the "weighted" temperatures to give the integrated temperature for the entire period. If we designate a general series of temperatures as $T_1, T_2, T_3, \dots, T_n$, their respective ($T \times t$) areas as $A_1, A_2, A_3, \dots, A_n$, and the total area ($A_1 + A_2 + \dots, A_n$) as A_t , then the general expression for T_e is:

$$T_e = \frac{t_c}{t_n} \left(\frac{A_1}{A_t} T_1 + \frac{A_2}{A_t} T_2 + \frac{A_3}{A_t} T_3 + \dots + \frac{A_n}{A_t} T_n \right) \quad (5)$$

$$T_e = \frac{t_c}{t_n} \sum_{n=1}^{\infty} \frac{A_n}{A_t} T_n \quad (5a)$$

$$n = 1 \rightarrow \infty$$

The first factor, t_c/t_n , is the ratio of the number of time periods above 0°C (t_c) to the total number of time periods (t_n). For most cases $t_c = t_n$ and the ratio is unity; however, in colder temperate climates where some time periods are below freezing, the ratio operates to adjust for the 0°C null periods. Since water solidifies from 0°C , diffusion becomes rather difficult!

To illustrate a specific case, let (T_1, t_1) , (T_2, t_2) , and (T_3, t_3) in Fig. 3.6 assume the following values (which they actually are):

(1)	(2)	(3)
$T_1 = 10^\circ\text{C}$	$T_2 = 20^\circ\text{C}$	$T_3 = 35^\circ\text{C}$
$t_1 = 2$ months	$t_2 = 2$ months	$t_3 = 4$ months

To find T_e using equation (5) we first solve for the individual areas.

(1)	(2)	(3)
$A_1 = T_1 \times t_1$	$A_2 = T_2 \times t_2$	$A_3 = T_3 \times t_3$
$A_1 = 10^\circ \times 2$	$A_2 = 20^\circ \times 2$	$A_3 = 35^\circ \times 4$
$A_1 = 20^\circ\text{C-m}$	$A_2 = 40^\circ\text{C-m}$	$A_3 = 140^\circ\text{C-m}$

The total area, A_t , then is:

$$A_t = A_1 + A_2 + A_3$$

$$A_t = 20 + 40 + 140$$

$$A_t = 200^\circ\text{C-m}$$

Inspecting the temperatures we find there are no time periods (months in this case) at or below 0°C so $t_c = t_n$ or $t_c/t_n = 1$.

Substituting the above results into equation (5):

$$T_e = t_c/t_n \left(\frac{A_1}{A_t}T_1 + \frac{A_2}{A_t}T_2 + \frac{A_3}{A_t}T_3 + \dots + \frac{A_n}{A_t}T_n \right), \text{ we have}$$

$$T_e = 8/8 \left(\frac{20^{\circ}\text{C}-\text{m}}{2000\text{C}-\text{m}}10^{\circ}\text{C} + \frac{40^{\circ}\text{C}-\text{m}}{2000\text{C}-\text{m}}20^{\circ}\text{C} + \frac{140^{\circ}\text{C}-\text{m}}{2000\text{C}-\text{m}}35^{\circ}\text{C} \right)$$

$$T_e = 1 \left(1^{\circ}\text{C} + 4^{\circ}\text{C} + 24.5^{\circ}\text{C} \right)$$

$$\underline{T_e = 29.5^{\circ}\text{C}}$$

To contrast the difference between the simple average temperature (\bar{T}), and the integrated effective temperature, we now solve for the former:

$$\bar{T} = \frac{2(10) + 2(20) + 4(35)}{8}$$

$$\bar{T} = 25.0^{\circ}\text{C}$$

The simple average is in error by 15.5% for this case. Thus one can see why T_e can not be found by simply averaging the various monthly temperatures.

In conclusion, given the temperature-time values at about a four inch depth throughout each month of the year, the rate of hydration can be found through the following equations:

$$T_e = t_c/t_n \left(\frac{A_1}{A_t}T_1 + \frac{A_2}{A_t}T_2 + \frac{A_3}{A_t}T_3 + \dots + \frac{A_n}{A_t}T_n \right) \quad (5)$$

$$\log D = .0424 T_e - .241 \quad (4)$$

$$x^2 = Dt \quad (1)$$

C. Hydration Rate Solutions for Three California Microclimates

Fortunately for the 4-SAC-29 hydration analysis, the Weather Bureau reports four-inch soil temperatures taken from the nearby city of Davis. In addition, the publication reports like readings from two other locations: Fresno in Central California, and Brawley in Southern California. The three locations provide a contrast in climates which will prove most useful in the next section on the relationship between soil and atmospheric temperatures. But now we proceed with the section at hand: the hydration rate solutions for the above locations.

1. Sacramento and Davis, California

Climatological Data, published by the Weather Bureau, contains the average maximum and minimum temperatures for each month. As the duration of the daily highs and lows are very nearly equal on a monthly basis, each month then consists of one time period at the average high, and one time period at the average low. Thus there are two periods per month or 24 periods in the total (yearly) cycle. Weather Bureau records show the choice of year has little effect as illustrated by the annual mean with standard deviation over 34 years at Sacramento: $61.2 \pm .5^{\circ} F$ or $16.2 \pm .25^{\circ} C$. As the variation does not appear to be significantly different for California in general, annual readings within $.5^{\circ} F$ will be considered statistically equivalent. Using the monthly soil temperatures for any one year at Davis (1966 in this case) we proceed with the rate solution.

First T_e is found through equation (5):

$$T_e = \frac{t_c}{t_n} \left(\frac{A_1}{A_t} T_1 + \frac{A_2}{A_t} T_2 + \dots + \frac{A_n}{A_t} T_n \right), \text{ where}$$

$$A_n = T_n \times t_n, \text{ and } t_c/t_n = 24/24 = 1$$

Month	T_n °F	t_n	A_n	A_n/A_t (%)	$(A_n/A_t)T_n$ °F
1	50.0	1	50.0	3.05	1.5
	41.1	1	41.1	2.50	1.03
2	53.6	1	53.6	3.27	1.75
	43.6	1	43.6	2.66	1.16
3	65.6	1	65.6	3.98	2.62
	51.8	1	51.8	3.16	1.64
4	79.1	1	79.1	4.83	3.82
	62.5	1	62.5	3.80	2.38
5	87.3	1	87.3	5.32	4.64
	69.8	1	69.8	4.25	2.96
6	96.4	1	96.4	5.87	5.65
	78.0	1	78.0	4.76	3.70
7	93.8	1	93.8	5.72	5.36
	76.3	1	76.3	4.65	3.54
8	96.7	1	96.7	5.89	5.67
	80.1	1	80.1	4.88	3.90
9	89.7	1	89.7	5.46	4.90
	79.5	1	79.5	4.85	3.85
10	77.5	1	77.5	4.72	3.65
	62.3	1	62.3	3.79	2.36
11	60.4	1	60.4	3.68	2.22
	51.5	1	51.5	3.14	1.62
12	50.4	1	50.4	3.04	1.53
	44.8	1	44.8	2.73	1.22

$$A_n = 1641.4 = A_t$$

$$\frac{A_n}{A_t} T_n = 72.70 \text{ °F} = T_e$$

The effective temperature for the Sacramento-Davis microclimate by equation (5) is: 72.70°F . Converting to degrees Centigrade:

$$C = \frac{5}{9} (F - 32)$$

$$C = \frac{5}{9} (72.70 - 32)$$

$$C = 22.6$$

$$\underline{\underline{T_e = 22.6^\circ\text{C}}}$$

Next, having T_e in $^{\circ}\text{C}$, we find the diffusion coefficient, D , from equation (4):

$$\log D = .0424 T_e - .241$$

$$\begin{aligned}\log D &= .0424 (22.6) - .241 \\ &= .958 - .241\end{aligned}$$

$$\log D = .717$$

$$D = 5.21 \mu^2/1000 \text{ years}$$

Finally, substituting D (for 22.6°C) in equation (1) we have the desired rate expression for the Sacramento-Davis micro-climate:

$$x^2 = Dt \quad (1)$$

$$\underline{x^2 = 5.21 t}$$

Note: Since D has units of $\mu^2/1000$ years, t will be in thousands of years.

2. Fresno, California

Referring to Climatological Data for the monthly soil temperatures at Fresno (1968-69 is the only annual sequence as yet available) we proceed in the same manner as above:

From equation (5)

$$T_e = \frac{t_c}{t_n} \left(\frac{A_1}{A_t} T_1 + \frac{A_2}{A_t} T_2 + \dots + \frac{A_n}{A_t} T_n \right),$$

using the climatological data we find:

$$T_e = 76.4^{\circ}\text{F}, \text{ or}$$

$$T_e = 24.8^{\circ}\text{C}$$

From equation (4): $\log D = .0424 T_e - .241$, using $T_e = 24.8^\circ C$
the diffusion coefficient is:

$$\log D = .0424 T_e - .241$$

$$\log D = .0424 (24.8) - .241$$

$$\log D = .811$$

$$D = 6.46 \mu^2/1000 \text{ years}$$

From the general rate equation, $x^2 = Dt$, the expression for the
Fresno microclimate using $D = 6.46 \mu^2/1000 \text{ years}$ is:

$$x^2 = 6.46 t$$

3. Brawley, California

Referring, once more, to Climatological Data for the
monthly soil temperatures at Brawley (1968), we again proceed
in the same manner as above:

From equation (5)

$$T_e = \frac{t_c}{t_n} \left(\frac{A_1}{A_t} T_1 + \frac{A_2}{A_t} T_2 + \dots + \frac{A_n}{A_t} T_n \right),$$

using the climatological data to find:

$$T_e = 83.6^\circ F, \text{ or}$$

$$T_e = 28.8^\circ C$$

From equation (4): $\log D = .0424 T_e - .241$, using $T_e = 28.8^\circ C$
the diffusion coefficient is:

$$\log D = .0424 T_e - .241$$

$$\log D = .0424 (28.8) - .241$$

$$\log D = .960$$

$$D = 9.12 \mu^2/1000 \text{ years}$$

Finally, from the general rate equation $x^2 = Dt$, the expression for the Brawley microclimate using $D = 9.12 \mu^2/10^3$ years is:

$$x^2 = 9.12 t$$

D. An Empirically Derived Relationship Between Soil and Atmospheric Temperatures in California

As the method now stands, the chief limiting factor in determining hydration rates by temperature results from the extreme scarcity of soil temperature records. Since taking such measurements requires a minimum of one year's daily observations (with the proper equipment), the archaeologist will rarely have the opportunity to gather the data while at a particular site location. Thus if the site's annual temperature does not correspond to one of the three computed above, C-14 correlation then becomes the only method of rate determination. The one practical solution to the dilemma is to find some way of equating soil temperatures to the extensively reported atmospheric readings.

To accomplish this task we have three temperature sets, the bare minimum necessary to establish an equation. Using the effective soil temperature from the three California locations, a comparison was made between each temperature and the respective atmospheric readings reported by the Weather Bureau. Because of the wide number of variables, finding such a relationship seemed rather dubious, and the results, therefore, were expected to be anything but consistent. However, the results were just the opposite--they were amazingly consistent.

The first problem in making the comparison was to inspect the listed atmospheric temperatures of each area for any consistencies between them and the soil readings. Of the monthly average, the average low, and the average high, the monthly average high seemed to hold the greatest potential for a soil-to-atmospheric temperature relationship. There seemed to be a consistent increase between each location's atmospheric average high and soil temperature when proceeding south from Sacramento to Brawley in Southern California. As observations strongly suggest atmospheric heat-dissipating elements to be more varied than in the case of heat supply (the sun), it follows that atmospheric highs would be more consistent than lows. With the indicated consistency as a basis, the atmospheric highs and soil temperatures were thus selected for the forthcoming comparison.

Using Climatological Data as a source, the average atmospheric highs from each location are first integrated to provide the necessary pair members for the soil temperatures (T_e) determined in the preceding section:

1. Integration of Atmospheric Average Highs

Using equation (5a), the general form of equation (5), the solutions for each integrated atmospheric temperature, T_A , follows:

$$T_A = \frac{t_c}{t_n} \sum_{n=1}^{\infty} \frac{A_n}{A_t} T_n$$

Sacramento-Davis (Davis-1966)			Fresno (1966)		
A_n	$A_n/A_t(\%)$	$(A_n/A_t) T_n \text{ } ^\circ\text{F}$	A_n	$A_n/A_t(\%)$	$(A_n/A_t) T_n \text{ } ^\circ\text{F}$
54.5	6.12	3.33	54.5	5.84	3.17
57.2	6.41	3.66	59.1	6.36	3.76
65.8	7.39	4.86	70.4	7.56	5.32
77.8	8.72	6.78	82.2	8.83	7.25
82.2	9.22	7.56	87.4	9.39	8.20
88.5	9.92	8.76	93.2	10.03	9.35
88.7	9.95	8.83	96.1	10.32	9.93
93.9	10.53	9.90	99.5	10.68	10.63
87.5	9.82	8.58	89.2	9.58	9.18
79.6	8.93	7.10	80.9	8.69	7.03
63.7	7.16	4.56	67.9	7.30	4.95
51.9	5.83	3.02	50.4	5.42	2.73
$A_t=891.3$		$T_A=76.9 \text{ } ^\circ\text{F}$	$A_t=930.7$		$T_A=81.5 \text{ } ^\circ\text{F}$

Brawley (1966)		
A_n	$A_n/A_t(\%)$	$(A_n/A_t) T_n \text{ } ^\circ\text{F}$
66.0	6.25	4.15
68.9	6.53	4.51
79.4	7.52	5.98
88.8	8.42	7.46
95.5	9.04	8.63
102.0	9.67	9.89
106.0	10.04	10.65
106.8	10.12	10.80
101.2	9.59	9.71
89.4	8.47	7.57
79.6	7.54	6.00
72.0	6.82	4.90
$A_t=1056.6$		$T_A=90.4 \text{ } ^\circ\text{F}$

2. Comparison of the Integrated Atmospheric and Soil Temperatures, and Derivation of Their Relationship by Inspection

<u>Location</u>	<u>T_e (soil)</u>	<u>T_a (atm.)</u>
Sac-Davis	72.7 ^o F	76.9 ^o F
Fresno	76.4 ^o F	81.5 ^o F
Brawley	83.6 ^o F	90.4 ^o F

With the three point sets displayed the essential question may now be asked: what equation, if any, expresses the relationship between T_e and T_a ? For example, if Fresno reported only atmospheric readings, what relationship could be used to determine the effective soil temperature, T_e ? By inspection the relationship is found to be both linear and trivial and to have the form:

$$T_e = 4/5 T_a + 11.2 \quad (6)$$

To demonstrate the empirically derived relationship we will use T_a from each location and see if equation (6) gives T_e within the expected $\pm .5^\circ$ F accuracy (see Page 35).

Sac-Davis	Fresno	Brawley
$T_a=76.9^\circ$ F	$T_a=81.5^\circ$ F	$T_a=90.4^\circ$ F
$T_e=4/5 T_a + 11.2$	$T_e=4/5 T_a + 11.2$	$T_e=4/5 T_a + 11.2$
$T_e=4/5(76.9)+11.2$	$T_e=4/5(81.5)+11.2$	$T_e=4/5(90.4)+11.2$
$T_e=61.5+11.2$	$T_e=65.2+11.2$	$T_e=72.3+11.2$
$T_e=72.7^\circ$ F	$T_e=76.4^\circ$ F	$T_e=83.5^\circ$ F
Expected $T_e=72.7^\circ$ F, there is no detectable error.	Expected $T_e=76.4^\circ$ F, there is no detectable error.	Expected $T_e=83.6^\circ$ F, the .1 error is well within the accuracy limits.

For the only available soil temperatures in California the empirically derived relationship equating T_e to T_a is amazingly consistent. Theoretically two points define a linear relationship and additional points then verify that relationship. We have one strong verification. As the locations are rather

evenly spaced and widely distributed over the State, the relationship appears valid for California in general; however, an additional point lying outside the present distribution would help greatly to increase one's confidence in such a generalization.

The following, final, section of this chapter contains the only verification presently available for the method of rate determination by temperature. It is a check on the interdependent equation system upon which the method depends, and, if positive, will add the needed additional point mentioned in the preceding paragraph.

E. Verification of the Temperature Method through an Independent Rate Calibration by C-14.

The theoretically based method of rate determination by temperature now stands complete but to this point untested. One diffusion rate, independently and accurately determined by C-14 calibration, and originating in either the extreme northern or southern areas of California would provide an essential test. Recalling the three derived equations:

$$\text{(from soil) } T_e = \frac{t_c}{t_n} \left(\frac{A_1}{A_t} T_1 + \frac{A_2}{A_t} T_2 + \dots + \frac{A_n}{A_t} T_n \right) \quad (5)$$

$$\text{(from air) } T_e = 4/5 T_a + 11.2 \quad (6)$$

$$\log D = .0424 T_e - .241 \quad (4)$$

and the general diffusion equation:

$$x^2 = D t \quad (1)$$

one critical observation becomes apparent. Each equation in

the system depends upon all the preceding ones i.e., if the relationship in equation (5) is invalid then (6), (4), and (1) will carry the error and so on. Thus the entire derived system must be valid for its end result, D, to equal the results of an accurate and completely independent method of determining the diffusion coefficient.

One such diffusion coefficient, independently and accurately determined by C-14 calibration, and originating in an extreme northern area of California was provided by LeRoy Johnson, Jr. through the efforts of Professor Jerald Johnson at Sacramento State College.

With ten C-14 dates and ten associated obsidian lots (107 artifacts) from a site (4-Sk-4) adjacent to Tulelake, California, LeRoy Johnson has accomplished one of the most well-based and accurate rate calibrations to date (see Johnson, 1969). As was evident from his manuscript of computations, the dates were well dispersed and more than adequate to cover the rate curve. Using the method of least squares in logarithmic form to derive the rate equation best fitting the 4-Sk-4 data, Johnson found the following diffusion coefficient for the Tulelake region:

$$D = 3.5 \mu^2/10^3$$

Note: From the data $D = 3.49 \mu^2/10^3$, the above of course was rounded.

At this time, then, comes the obvious but critical question: will the system of temperature-based equations give an equivalent answer for the diffusion coefficient?

In view of the question we present the following hypothesis: if the soil-to-atmospheric relationship is valid; if the general depth of the effective thermal energy level is accurate; if the temperature integration technique is correct; and if the relationship between the effective temperature and diffusion coefficient is valid, then the answers will agree. From the expected sigma variation of $\pm .5^{\circ}\text{F}$ in annual temperature, a variation of $\pm .15 \mu^2/10^3\text{y}$ can be expected for D; hence, equivalent means agreement within $\pm .15 \mu^2/10^3\text{y}$. What then does the temperature method provide for an answer?

The initial step in determining any rate is to consult Climatological Data for the temperature reading. As the Weather Bureau does not provide soil temperatures for Tulelake, T_e will have to be found from the integrated atmospheric temperature T_a . The above source gives the following atmospheric average highs for each month in order from January through December of 1966: 40.3, 43.9, 54.6, 66.2, 75.2, 74.2, 82.6, 85.8, 79.8, 69.4, 48.1, and 43.0°F . T_a as determined by equation (5):

$T_n^{\circ}\text{F}$	x	t_n	=	A_n	$A_n/A_t(\%)$	$(A_n/A_t) T_n^{\circ}\text{F}$
40.3		1		40.3	5.26	2.12
43.9		1.		43.9	5.75	2.52
54.6		1		54.6	7.16	3.91
66.2		1		66.2	8.68	5.75
75.2		1		75.2	9.86	7.40
74.2		1		74.2	9.73	7.22
82.6		1		82.6	10.80	8.93
85.8		1		85.8	11.24	9.65
79.8		1		79.8	10.46	8.36
69.4		1		69.4	9.10	6.32
48.1		1		48.1	6.32	3.04
43.0		1		<u>43.0</u>	5.64	<u>2.42</u>
				$A_t=763.1$		$T_a=67.64^{\circ}\text{F}$

thus for Tulelake $T_a = 67.6^{\circ}\text{F}$.

Next the effective temperature of hydration T_e is found by equation (6):

$$T_e = 4/5 T_a + 11.2$$

$$T_e = 4/5(67.6)+11.2$$

$$T_e = 54.1 + 11.2$$

$$\underline{T_e = 65.3^{\circ}\text{F}}$$

To find the diffusion coefficient D , we first convert T_e into $^{\circ}\text{C}$:

$$C = 5/9(F-32)$$

$$C = 5/9(65.3-32)$$

$$C = 18.5^{\circ}$$

$$\underline{T_e = 18.5^{\circ}\text{C}}$$

Finally, equation (4) provides D :

$$\log D = .0424 T_e - .241$$

$$\log D = .0424(18.5) - .241$$

$$\log D = .543, \text{ and}$$

$$\underline{D = 3.49 \mu^2/10^3 \text{ years}}$$

Comparing the two results we find there is no detectable difference between the unrounded answers by C-14 and temperature analysis:

Johnson, Jr.	$D = 3.49 \mu^2/10^3 \text{ years}$	C-14
Arnold	$D = 3.49 \mu^2/10^3 \text{ years}$	Temperature

Thus by using two completely independent methods each has provided a check on the other. The above hypothesis is verified by the equality, and the temperature method stands for the first time upon a tested foundation. The exactness of the

agreement was a most welcome surprise but not essential: since the expected sigma variation was $\pm .15 u^2/10^3$ years, an answer between $3.34 u^2/10^3$ years and $3.64 u^2/10^3$ years would still confirm the agreement. Finally, the agreement has extended the soil-to-atmospheric relationship to the northern border of California, and provided an additional point check to further substantiate its validity.

The theoretically based method of hydration rate determination by temperature is now complete. The derivation has extended into many disciplines, and in places has proceeded through rather unfamiliar environments to arrive at its conclusion. As is so often the case, time will provide the needed tests and, hopefully, they will clarify and substantiate the method as a practical means for finding hydration rates through temperature analysis.

Next the "art" of microscopic petrology provides us with specimens to measure, and measurements upon which to apply the results of the Sacramento-Davis hydration rate: in short, the technique used, and the results of the 4-SAC-29 obsidian hydration analysis.

Chapter Four

THE QUANTITATIVE ANALYSIS OF OBSIDIAN HYDRATION THROUGH MICROSCOPIC PETROGRAPHY

The laboratory procedures used in the quantitative analysis of obsidian hydration fall into two major divisions:

- I. The Preparation of Obsidian Thin-Sections
- II. The Microscopic Analysis of Obsidian Thin-Sections

In turn, each major division is composed of a series of operational phases which form the heart of the analytical process. These phases will each be presented with a detailed discussion under their respective major divisions. Hopefully, the techniques used and the refinements developed during this research will be of assistance to future work carried out specifically within this department, and will also be of assistance as a source of reference to others with similiar endeavors.

I. The Preparation of Obsidian Thin-Sections

As the accuracy of hydration measurements directly depends on the quality of the obsidian thin-section, correct procedure must be followed to ensure that quality. The analyst must perfect the technique of thin-section preparation to as high a degree as possible, and, while there are certain basic steps, each individual must seek his own best refinement of those steps. To a certain degree, then, such work might well be classified as art.

13

The preparation of obsidian thin-sections may be divided into the following seven operational phases:

1. Cutting the Section
2. Grinding the Section to Mounting Thickness
3. Polishing the Mounting Surface
4. Mounting the Section
5. Grinding the Section to Final Polishing Thickness
6. Polishing the Section to Viewing Thickness
7. Mounting the Cover Slip

Phase 1: Cutting the Section

Removing a small section of obsidian from the artifact is the first objective. This is accomplished by means of a diamond cut-off saw blade (.020" thick by 6" in diameter). The obsidian specimen is first carefully inspected to determine the optimum location for removing a small V-shaped section. The artifact is next secured in the castoloy clamp, adjusted for the correct cutting angle, and then rotated into the water-cooled blade from below (Plate 4.1). When a depth of about four millimeters is reached, the artifact is rotated out of the blade and the main axle with clamp is moved horizontally to the opposite thickness stop. The artifact is then rotated into the blade for the parallel and final cut to the same depth. Finally, the artifact is removed from the clamp. The isolated section is now broken from the artifact by inserting a flat metal blade into one of the cuts and increasing pressure until separation occurs. The second phase is then ready to commence.

Discussion of Phase 1

Determining the optimum location for removing the V-shaped section depends often on a compromise between preserving identifying cultural features and providing the most diagnostic thin-section for analysis. In the case of projectile points, the base often is the chief identifying feature so generally the cut is made away from that area. For non-serrated points the cut is "usually" made into the middle one-third of the leading edge. For serrated points the cut is "usually" made between the first serration and the point tip whenever possible. Any further specification will depend on the particular point and one's archaeological orientation. The initial diagnostic value of a section, however, depends on one important rule: the cut must always be made at right angles to the absorbing surface. The closer a cut approaches a right angle the more well-defined will be the hydration boundary when viewed through the microscope. Hazy boundaries or boundaries shifting position under a changing focus are generally traced to oblique cuts across the diffusion vector.

In order to minimize oblique cuts, to ensure parallel cuts, and to standardize section thickness, a mechanism designed around a castaloy clamp was built, and attached to the Felker cut-off machine (Plate 4.1 & 4.2). When using this mechanism, the angle of cut is varied by rotating the jaws about the clamp's threaded center shaft until it is 90°

to the absorbing surface. The center shaft locking nut (Plate 4.1 #1) is then tightened to secure the cutting angle. The sectioning cuts will then be parallel to each other and 90° to the absorbing surface. The depth of cut is controlled by adjusting the cut-off blade to the desired height. As indicated above, 4mm is normally the optimum depth. The base then is usually the shortest leg of the triangular section and hence the hydration rims will be located adjacent to the section's major axis--a useful relationship in later phases.

To standardize section thickness, and to prevent lateral drift during cutting, locking collars (Plate 4.3, #1) were fitted to each end of the main axle. The collars articulate with the inside surface of the machine's mounting framework, and are adjusted via set screws.

The question of minimizing initial section thickness was found to be a function of two variables for any saw: (1) the amount of surface chipping caused by the diamond saw (Fig. 4.1), and (2) the degree of lateral vibration in the saw. The thickness stops then must be set wide enough to ensure that chipping does not overlap from each side (the middle $1/3$ ' of the surface will remain intact), and that the section will be sufficiently thick to prevent its being broken off by lateral vibration in the saw. Chipping and breaking tolerances then must be determined for each blade to set the minimum section thickness-- 1.5mm was found to be optimum section thickness for the

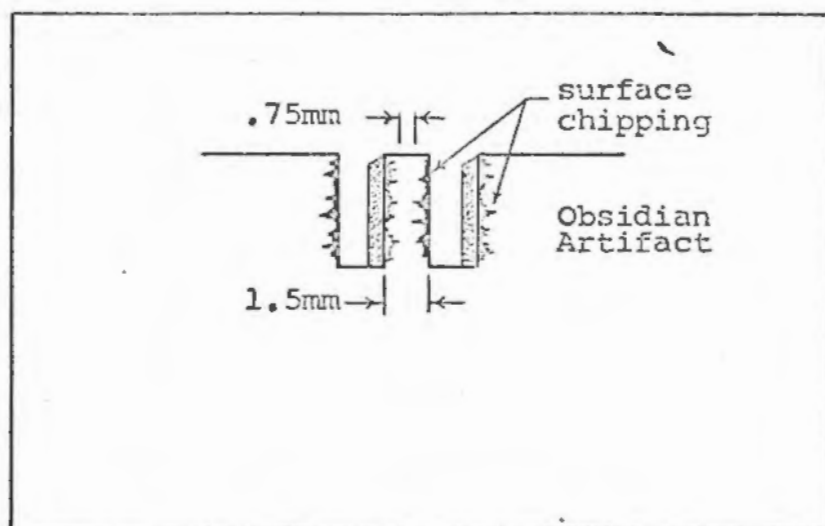


Fig. 4.1. Surface chipping caused by the diamond blade during cutting. The section is cut to 1.5 mm to insure an unchipped middle area \approx .75 mm wide from which the actual thin-section surface is ground.

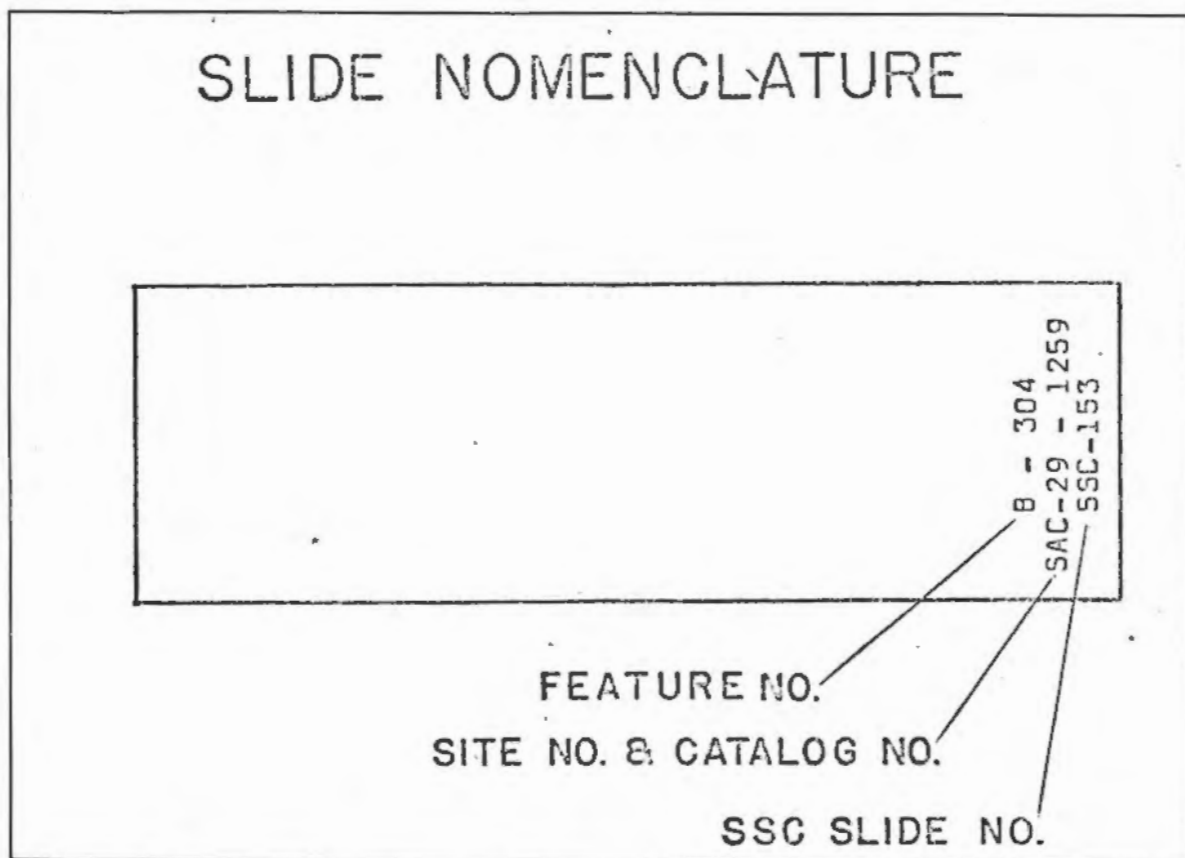


Fig. 4.2. Nomenclature system developed for inscribing slides with the proper identifying markings for each thin-section.

.020 x 6" blade. For our equipment a section greater than 1.5mm only added unnecessary grinding; however, a section less than 1.5mm resulted in an excessively chipped absorbing surface. The latter, of course, removes the hydrated surface and thereafter renders the entire procedure useless.

Finally comes the minor problem of separating the isolated section from the artifact. Utilizing a flat metal blade (Plate 4.4, #1) which is the same thickness as the cut-off saw proved most effective. When this shearing tool is inserted into the cut (behind the section) and rotated forward, the tightness of fit distributes the shearing force so that the section tends to separate at the base. Thinner shearing tools concentrate the force towards the top of the section, often resulting in mid-section fractures. Once separated, the section is ready to be ground to mounting thickness. The average preparation time for ten sections was three minutes per section.

Phase 2: Grinding the Section to Mounting Thickness

The primary objective of the second phase is twofold: (1) to reduce the section to the optimum uniform mounting thickness, and (2) to ensure the section is ground on both faces past the chipped areas to the intact surface. The resulting section will then have an intact hydration surface, uniform working thickness, and be ready for polishing and mounting.

Reducing the section to mounting thickness is accomplished by means of a horizontal lap wheel charged with

a slurry of #400 corundum powder and water. The obsidian section is held against the revolving wheel and periodically rotated to grind each face equally until the desired thickness is reached. After this point the third phase commences.

Discussion of Phase 2

After the section is removed from the artifact, it is placed on the tip of the index finger, and held against the lap wheel (revolving at about 100 RPM). Charged with the slurry of #400 abrasive powder and water, the twelve inch diameter wheel (Plate 4.5) can generally reduce a section six square millimeters in area (1.5mm thick) to a mounting thickness of 3/10 to 5/10 of a millimeter in ten minutes. During grinding, the section must periodically be rotated to reduce both faces equally--this will remove the surface area chipped when cutting and thereby ensure an intact rim throughout the absorbing surface of the finished section. Also during this phase, care must be taken to ensure the faces continually remain parallel. Over-grinding one edge can be corrected if the fault is noted sufficiently early in the phase. The corrective technique is to orient the thinnest part away from and the thickest towards oneself. Back pressure along the index finger then concentrates the greatest force on the thickest part to equalize the overall thickness. Since the rear of the hand normally drifts down during grinding, a good procedure is to always start with the widest edge to the rear. The sequence for this phase is grind,

rotate, check for evenness, and grind. When the uniform thickness is reduced to .3 to .5mm, the section is washed and finally ready for phase three. The average preparation time for 10 sections is 10 minutes per section.

Phase 3: Polishing the Mounting Surface

Polishing the mounting surface is the simplest of the seven operational phases. The objective is to optically finish one surface with the very fine #1000 corundum abrasive; this optical face will later be mounted against the micro-slide surface in Phase 4.

Discussion of Phase 3

Polishing one section face is accomplished by tracing figure eights through a slurry of #1000 powder and water on an 8 x 8 x .5" pyrex plate (Plate 4.6, #2). Each section, held against the index finger, is polished for 30 seconds using 4 inch figure eights (30 on the average) to ensure even grinding. After grinding, the polished surface is immediately marked with a No. 2 pencil for identification. The slurry is then washed from the section, and the section is ready for mounting. The average preparation time for ten sections is 1.5 minutes per section.

Phase 4: Mounting the Section

After being cut, ground, and polished, the obsidian specimen is now ready for mounting on a microslide. A microslide, inscribed with identification markings, is placed face down on a hot plate; a quantity of Lakeside #70

cement is then melted on the slide surface to accommodate the section. The section, polished face down, is placed on the melted cement and pressed into contact with the slide surface. When all air bubbles adhering to the section's circumference have been "cooked" out, the slide (microslide with specimen) is then removed from the hot plate and set aside to cool.

Discussion of Phase 4

As this phase necessitates the use of microslides directly in the process, a few suggestions relative to them are now in order. When one section only is to be analyzed, a slide is not essential until the mounting phase. However, when two or more are to be analyzed the slide then becomes the only practical means of identifying each thin-section. For this reason, each slide must be clearly inscribed with identification markings. The slide nomenclature will, of course, vary but for this research each slide was first marked at one end according to the following system: (1) feature or burial number, (2) site, and artifact catalogue number, and (3) number of each slide within a given site (Fig. 4.2). A carbide scriber was used to make the identifying inscriptions; these inscriptions are preserved from later grinding by mounting the section against the opposite slide surface.

Returning again to mounting procedure, the first concern is applying the Lakeside #70 cement.¹ The cement is somewhat liable to boil or vaporize at temperatures above

150°C. It is too viscous below 140°C, so the hot plate must maintain a temperature around 145°C. For the thermolyne hot plate (Plate 4.4) used during this phase, a control dial setting of 2.75 proved best.² Using this setting, the slide is placed, inscribed face down, on the hot plate. A corner of the Lakeside #70 bar (Plate 4.4, #2) is applied to the slide center until a pool large enough to accommodate the section has melted. It is recommended that pool size be no larger than 1.5 to 2 times the cross-sectional area of the thin-section; larger pools tend to collect abrasive powder during the next step of grinding, resulting in cloudy or dirty mounts. The next step is to place the optically finished section face on the cement pool. This polished face is identified via the carbon pencil marks which shine when reflecting light. The carbon marks do not shine when viewed through the thin-section and this fact is often the only means of verifying the true polished face. Using the forceps, the section is placed on the cement, and then pressed into contact with the slide surface. The section should be pressed a few more times during "cooking" to free any trapped bubbles. Cooking time usually takes from 3 to 5 minutes (or until all bubbles disappear), after which the slide is removed and cooled to room temperature for about an hour.

A final comment regarding mounting orientation: when the section is placed on the slide, the major axes of the section and the slide should be parallel. This procedure

aligns the hydration rims of the section with the general direction of the rotating lap wheel during grinding and thus minimizes chances of shearing rim segments due to cross grinding. The rim is already under mechanical strain relative to the rest of the section (due to its water content) and therefore should be exposed to minimum stress--and increasingly so from the mounting phase on. The average preparation time for ten sections is 4 minutes per section.

Phase 5: Grinding to Final Polishing Thickness

After the slide has cooled to room temperature, the section is ready to be ground to the final polishing thickness. The slide, secured by means of a suction dart (Plate 4.6, #3), is held, specimen down, against the lap wheel and ground with a slurry of #400 abrasive powder. When the section reaches a thickness approximating .006 inches, the slide is washed and is ready for the final polishing phase.

Discussion of Phase 5

The suction dart (purchased from any dime store) is the least expensive but one of the most useful tools of this phase. If kept clean, it will remain tightly secured to the slide as a handle, yet can be easily removed when desired. Grinding a mounted section would be nearly impossible without the dart.

Using a slurry of #400 corundum powder spread evenly across the lap wheel, the mounted section is now ground,

measured, and ground until it reaches a thickness around .006 inches. During grinding, the slide should be horizontally rotated 180° about every 30 seconds to ensure maintaining uniform thickness. In addition, over-grinding is a continual problem due to the section's thinness at this point; the only exact means of preventing this is through frequent checks on the dial test indicator (Plate 4.6, #1). Such checks, however, require washing as well as measuring and thus frequent checks expend a considerable amount of time. To limit such measurements, one can possibly use his index finger to estimate thickness. The author found (after many trials) he could estimate thickness to within .002 inches by passing the index finger over the section. With this technique only a few exact measurements near the end are needed and the time saved is considerable--especially when preparing many thin sections at a time. In any event, when the section approximates .006 inches (between .006 and .005) the slide is washed, and ready for polishing to viewing thickness.

A final comment regarding the abrasive slurry: with continual use the slurry accumulates particles sufficiently gross to detect when passing one's fingers over the wheel. These particles can easily mar the thin-section and when detected the slurry should be flushed from the wheel. Gross particle impurities are the chief argument against

reusing old and dehydrated slurry. The average preparation time for ten sections is 3 minutes per section.

Phase 6: Polishing to Viewing Thickness

The objective of this last grinding phase is to reduce the thin-section from .006 inches to a polished, viewing thickness of .0035 inches. This task is accomplished by once again utilizing a slurry of the very fine #1000 abrasive and water on the pyrex plate. The slide, secured again with a suction dart, is placed specimen down on the plate and manually ground until the section measures .0035 inches thick. After this point, the slide is carefully washed, and is then ready for the seventh and final operational phase--mounting the cover slip.

Discussion of Phase 6

The most critical problem of Phase 6 is destroying the thin-section by over-grinding. Frequent checks with the dial test indicator and experience eventually combine to minimize such losses; however, caution at this final point can not be over emphasized. The polishing (fine grinding) technique used here is the same as that of Phase 3--four inch figure eights. In addition, the slide should be periodically rotated 180° to minimize uneven grinding. When the specimen reaches .0045 inches in thickness, frequent checks (about once every five

cycles) should be made until the final .0035 inches is reached. This final viewing thickness of .0035 inches was empirically determined after examining approximately 150 thin-sections. When grinding within the .0045 to .0030 range recommended by Clark (1969:15), thin-sections equal to or greater than .004 inches had increasingly hazy hydration rims; conversely, .003 inches was found to be the fracturing border below which little remained of the rim to be examined. Thus .0035" appears to be the optimum thickness for the equipment system used at this laboratory. Upon reaching this thickness, the slide is washed with soap and water, and now is ready for the cover slip.

Finally, a word of caution relative to the suction dart: the fine grade abrasive (#1000) tends to work under the section cup and occasionally breaks the seal. To restore the seal one should rinse the slide and cup, and then attach the dart with the slide in hand. Never attach the dart while the slide rests on the pyrex plate -- the pressure can easily fracture a thin-section at this stage. The average preparation time for ten sections is 3 minutes per section.

Phase 7: Mounting the Cover Slip

Having successfully completed the first six phases, only the cover slip remains to be positioned. The slide (carefully cleaned) is placed, specimen up, on the hot plate; Canada balsum is then applied over and around the

thin-section; next, a cover slip is removed from the hot plate, carefully placed edge first into the balsum and slowly lowered onto the specimen. Finally, any trapped air bubbles should be immediately and carefully forced out under the nearest cover slip edge; however, removing all the bubbles is often impossible without exceeding pressure limits and thereby endangering the thin-section. Hence, a compromise is frequently the best procedure. The thin-section, now permanently suspended in an optical medium, is ready for microscopic analysis.

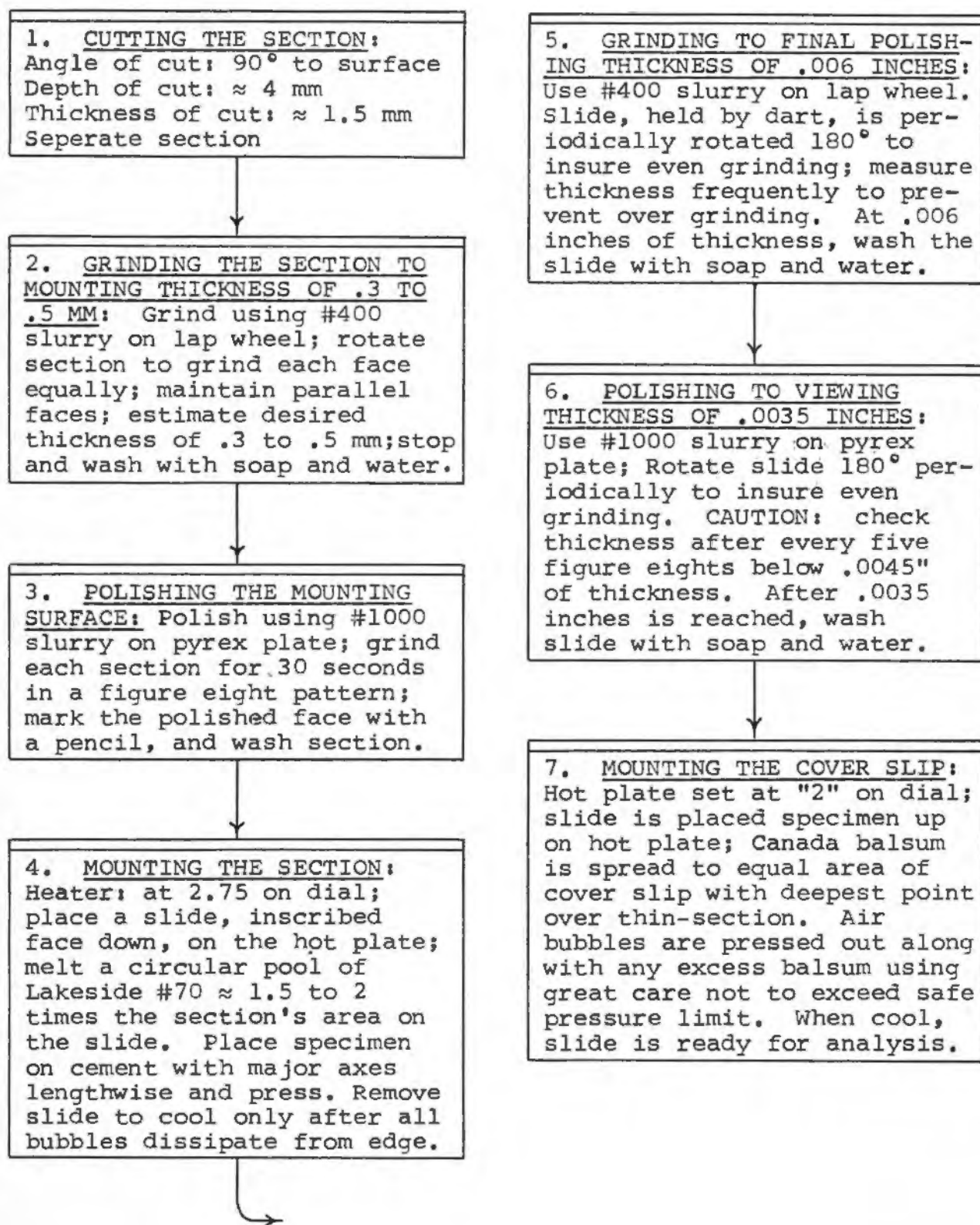
Discussion of Phase 7

Preventing or minimizing air bubbles when mounting cover slips is a continual problem. Bubbles form as a result of several factors but the following two seem especially significant: (1) depressions throughout the balsum's surface, and (2) a temperature differential between the cover slip and slide. The latter can be solved by heating the cover slip along with the slides; usually four or five cover slips at a time can be maintained on the hot plate. The former problem (depression in the balsum) has no sure solution but the author found the following technique gave best results: with a setting of "2" on the hot plate, the Canada balsum (Plate 4.4, #5) is first liberally applied to the thin-section and then brushed out and around as it becomes more fluid. The balsum should form a circle having an area about equal to the cover slips; it should be deepest directly

over the thin-section and gradually decrease out to the perimeter. When the cover slip is applied, one edge should be set in the cement's perimeter and then gently lowered allowing a small wall of fluid to precede the contact line across the surface. If done correctly, and bubbles formed should be located near the edges and easily forced out. Should a few bubbles prove difficult, it is usually better to leave them (as mentioned above) rather than endanger the thin-section by exceeding pressure limits. Once the bubbles and excess cement have been gently forced from beneath the cover slip, the slide is cooled to room temperature, and thereafter ready to be analyzed. The average preparation time for ten sections is 2 minutes per section.

The following procedural flow chart (Fig. 4.3) has been included to facilitate an understanding of the above preparation sequence, and to provide easy access to major steps and specifications within each operational phase. Obviously, when using different equipment the above operational sequence can hardly be an optimum procedure; however, for individuals using the same equipment the author found the above procedure gave optimum results in the final test of quality--thin sections having consistently complete and well-defined hydration rims under microscopic analysis.

Fig.4.3 THIN-SECTION PROCEDURAL FLOW CHART



II. The Microscopic Analysis of Thin-Sections

Before proceeding, a few words are needed concerning proficiency. It should be emphasized that proficiency in hydration analysis is not simply a matter of following steps--it is much more a result of experience. True proficiency in evaluating thin-sections most probably only starts when the number examined exceeds 50% of their possible varieties--thereafter the encounters become less a matter of "newness", and more a matter of repeating similar experience. Fortunately obsidian samples from most sites contain homogeneous groupings enabling the analyst to rapidly enlarge his sphere of similar experiences and refine his own analytical procedure.

Calibrating the Microscope

The microscopic analysis of thin-sections has one primary objective: the accurate measurement of hydration rims. To accomplish this the principle instrument, a petrographic microscope, must be fitted with some device for measuring lateral displacement and that device must be calibrated against a known source. In addition, the variation between individuals sometimes introduces small changes in the optical system, and therefore the calibration factor must be verified for each analyst. If the variation is significant, of course the individual must use his particular calibration factor. Calibration is an easy

but essential first step, and the procedure used in this first step will now be described. Following this procedure will come the presentation on microscopic analysis by operational phases.

A Leitz stage Micrometer (.01mm) provided the calibrating source. The Leitz Research Microscope (Labolux-8116) and the ten-power Filar Screw Micrometer Eyepiece (Plate 4.7) as a unit provide three optical magnification fields (10 x 10, 10 x 40, 10 x 100); each field used must be calibrated and thus there are three potential calibration factors, or one factor for each objective. The procedure for each field is the same.

The stage micrometer is a slide upon which is machined one millimeter divided into 100 parts having ten microns between each minor division. The objective of the calibration procedure is to determine the number of microns per division on the micrometer drum (Plate 4.7, #1) for each magnification field used. To accomplish this one simply records the drum's starting position; next advances the sweep-hairline over a known number of microns on the slide; and lastly records the drum's end position. The differences between the two drum positions gives the number of divisions turned to traverse the known distance. When five to ten trials have been completed over the known distance, the average number of drum divisions over that distance is computed. This average is finally divided into the number of microns

traversed giving the number of microns per drum division for the particular objective used. For example, when using the x40 objective the average number of drum divisions (ten trials) over 100 microns was 854.0 divisions. My calibration factor for the x40 objective then is:

$$\frac{100 \mu}{854.0} = .1175 \mu/\text{div.}$$

To minimize error one must always start and end with the sweep-hairline over the same location on a marker (be consistent). Also to minimize error, the sweep should traverse within the middle three-fourths of each field to eliminate any spherical aberation, and cover enough distance to provide three significant figures³ in the answer.

Having been calibrated, the microscope can now be employed in the analysis of thin-sections. Persons not entirely familiar with the use of a complex microscope should definitely consult some text on the function and use of microscope elements prior to any serious analysis of thin-sections: an accurate scope and an unqualified analyst commonly yield more frustration than results. (The Use and Care of the Microscope: 1949, by Bausch and Lomb Optical Co., N.Y. is recommended. The booklet covers the major theoretical and applied topics, and will facilitate microscope use throughout the forthcoming operational phases.)

The operational phases under "The Microscopic Analysis of Thin-Sections", can be divided into the following sequence for the Labolux-8116:

- 1.0. Low Power Optical Field Insertion (LFI)
 - 1.1. General Thin-Section Survey (GTS)
 - 1.2. Selection of Optimum Rim Location (SRL)
- 2.0. High Power Optical Field Insertion (HFI)
 - 2.1. Rim Boundary Determination (RBD)
 - 2.2. Measurement of the Hydration Rim (MHR)

Phase 1.0: Low Power Optical Field Insertion (LFI)

Low power optical field insertion (LFI) involves completing all optical adjustments necessary to examine the thin-section. Specifically, LFI deals with the following: placing the slide and centering the subject on the stage; bringing the subject into focus; and, finally, focusing the light condenser to provide maximum resolving power (ability to produce separate images of objects very close together). Figure 4.4 illustrates all main elements and shows the path of light through the microscope, while Plate 4.7 shows the elements on the Labolux scope itself. The LFI procedure will now be presented.

First, set the x10 objective in position, the illuminator control at "2", and the light condenser within five millimeters from the stage top. The slide is placed under the spring clips with the thin-section as nearly as possible over the center of the opening in

THE MICROSCOPE

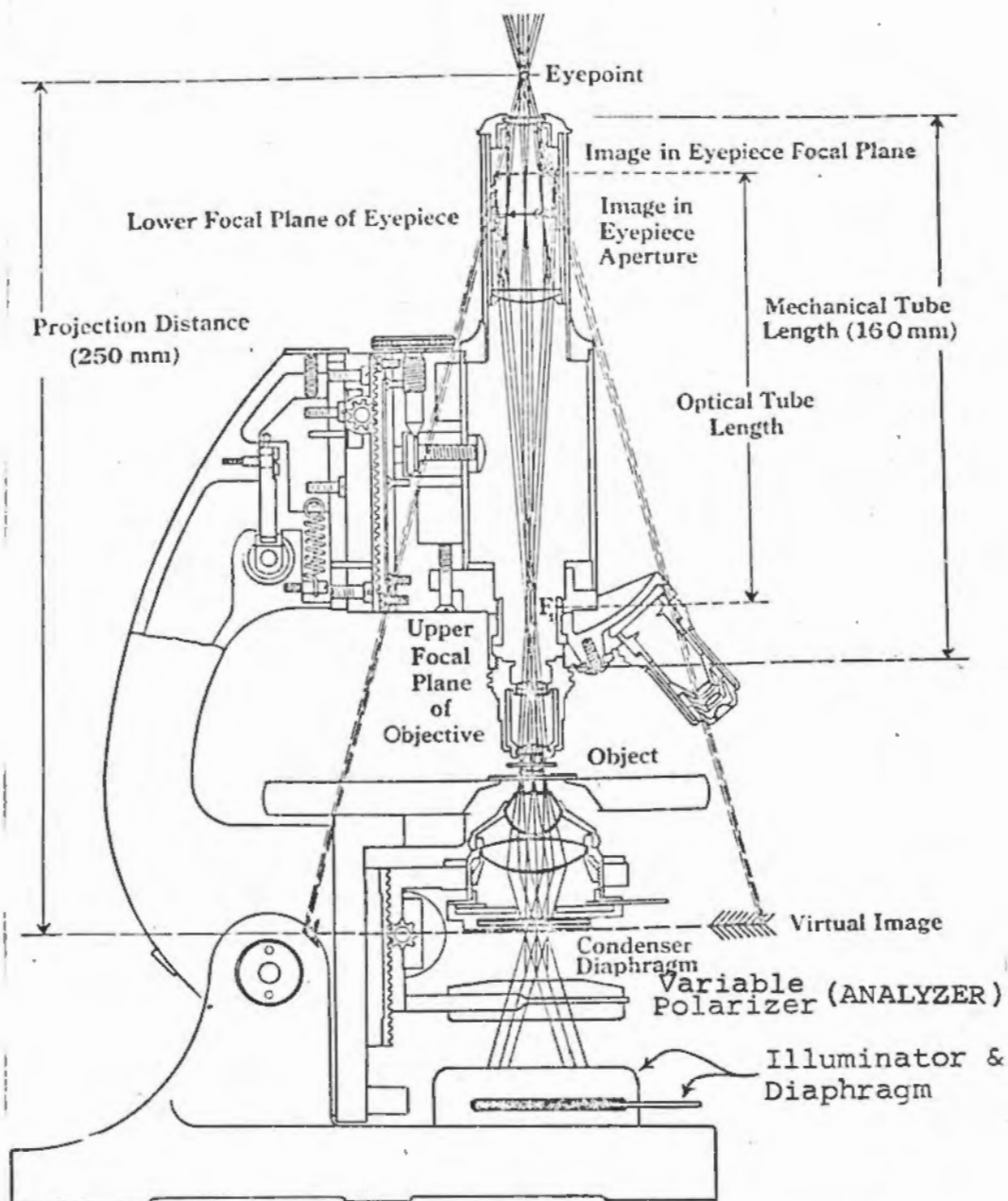


Fig. 4.4. The microscope and its main elements. The fixed-angle polarizer (not shown) is located just above point F_1 in the Labolux-8116 (see Plate 4.7, #2). Modified from Bausch and Lomb (1949:15).

the stage. A disk of light should be seen in the thin-section if properly centered. Next the x10 objective is racked within 5mm of the subject and backed off slowly (using first the course and then the fine control) until the thin-section is clearly focused. Now the illuminator diaphragm (Fig. 4.4) is set to minimum, and while looking through the microscope, the light condenser is racked up and down until the diaphragm image appears in clearest focus when viewed through or adjacent to the thin-section. The condenser has now been set to provide maximum resolving power and should not be moved while using the same objective. Finally, the illuminator diaphragm is opened until the entire field is covered. This completes the LFI phase.

Phase 1.1: General Thin-Section Survey (GTS)

The purpose of the GTS phase is to determine the general characteristics of the thin-section. The quality of preparation and rim characteristics (if any) are surveyed during this phase and will provide the information necessary to either reject the specimen or continue a more refined investigation.

With the optical field already at maximum resolution and the thin-section focused, the only remaining adjustment is to set the polarization analyzer, and quartz wedge (Plate 4.7, #3). This adjustment, largely a matter of personal preference, is accomplished by rotating the analyzer (with the wedge at different positions) until

the various structures within the thin-section are at maximum contrast and sharpest definition. The fixed-angle polarizer (second element of the polariscope⁴) can be removed by simply pulling out the control rod (Plate 4.7, #2) when viewing under normal light is desired.

The slide is now maneuvered on the stage until one edge of the thin-section bisects the optical field. Keeping the edge centered in the x100 field, a survey is made of the entire perimeter with attention directed to the degree of fragmentation, and the size and characteristics of any hydration rim (or rims) present. If the edge is fragmented throughout its circumference, the specimen is rejected and another prepared. Such fragmentation is a result mainly of over-grinding but can also result from excessive pressure on the cover slip during mounting. If the edge is generally intact (for at least one field diameter at different areas) and a hydration rim (also designated OH-rim) is present, then the specimen should be again surveyed to ensure the length of both surfaces contains the same OH-rim. Should a secondary OH-rim be detected, then the smaller is completely analyzed first, and thereafter the larger--such a choice is mainly arbitrary. Approximately one out of twenty SAC-29 points analyzed contained secondary OH-rims.

Assuming the specimen is well prepared and there is at least one rim, the next problem is to select the optimum rim

location for later measurement using the x40 objective (400 power). If no rim is visible and the edge is well defined, the absence is verified under 400x by slow perimeter search using Phase 2.0 and 2.1.

Phase 1.2: Selection of Optimum Rim Location (SRL)

Selecting an optimum OH-rim location before switching to the x40 objective is not merely staying with optical convention--such practice saves a considerable amount of "search" time due to the wider field of the x10 objective. The selection of the optimum location can arbitrarily be anywhere along a clear and continuous rim for some specimens, while for other specimens there might be few clearly defined areas due to fragmentation or crystallites, microbites, and other inclusions obscuring the OH-rim. In any event, a fairly straight segment of rim approximately one-quarter optical field diameters (OFD) in length, and offering the greatest relative degree of resolution is selected as the subject for measurement under the x40 objective. This subject is then placed at the optical field center.

Phase 2.0: High Power Optical Field Insertion (HFI)

The HFI phase involves switching from the x100 to the x400 field and completing the necessary adjustments to bring the selected subject back to optimum viewing conditions. First, the illuminator dial is set to "5"; second, the nosepiece is rotated until the x40 objective

is seated; and third, the distance between the subject and objective is narrowed (using the fine control) until the subject is clearly in focus. Next the light condenser is focused using the same procedure outlined during LFI (Phase 1.0). Any further light adjustment must be made either by varying the illuminator dial or adjusting the condenser diaphragm (Fig. 4.3). Finally, although usually not immediately necessary, the quartz wedge and or polariscope analyzer may be adjusted to personal preference.

The length of rim (formerly occupying about one-quarter of the x100 field) should now occupy the entire x400 field. After any final minor adjustments in centering or resolution, a point within that length of rim will be selected for measuring.

Phase 2.1: Rim Boundary Determination (RBD)

The objective of the RBD phase is to select and define OH-rim boundaries for measurement. No matter how accurate and consistent the measuring technique, the results can never exceed the accuracy with which the rim boundaries are themselves determined. Given a well prepared thin-section, the complexity of such determinations varies similar to a positively skewed distribution curve with about 25% being exceedingly easy to define, 70% presenting few problems, and 5% being borderline or useless. The factors influencing complexity

are of two basic types: (1) the optical characteristics of obsidian thin-section, and (2) the petrographical characteristics of obsidian thin-sections. Because of the critical nature of this phase, these characteristics will now be presented in some detail.

The optical characteristics affecting boundary determinations arise from the production of false OH-rims by the combination of two phenomena: double refraction (birefringence) and diffraction. Double refraction is a result of transparent crystalline substances having optical properties different in different directions. "Crystals having this property are said to be doubly refracting, or to exhibit birefringence" (Sears, 1949: 177). When one parallel beam of light strikes such an optically anisotropic substance, it will separate into two beams of light traveling at different angles through the crystal. "If the crystal is in the form of a plate with parallel surfaces [the thin-section], the two beams will emerge from the crystal in a direction parallel to that of the incident beam" (Rossi, 1957:297). Figure 4.5 illustrates such a phenomena and partially explains the weak bands of light (false rims) surrounding a thin-section. Thus the edge of the thin-section corresponds to one ray (the ordinary), and the edge of the band around the section (false rim) to the other (the extraordinary).

OPTICAL PHENOMENA IN THIN-SECTIONS

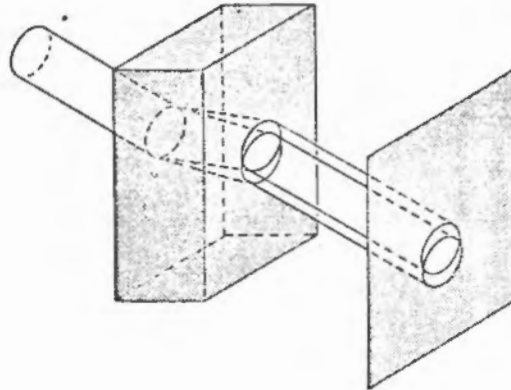


Fig. 4.5. Path of light through an optically anisotropic plate with parallel faces (thin section). The beam is doubly refracted producing a real and false image of the thin section edge (birefringence). Such false images can be mistaken for OH-rims. From Bruno (1957:297).

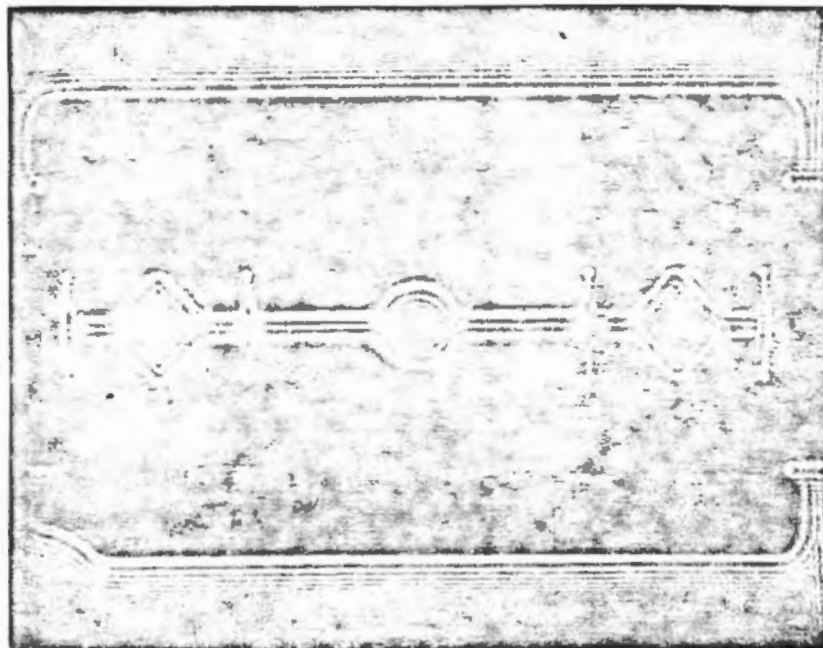


Fig. 4.6. Diffraction patterns produced by light passing perpendicular to the edges of a razor blade. Light reacting with the fine edges of a thin-section results in similar wave interference bands to complicate rim boundary determination. From Sears (1957: Fig. 9-8).

Diffraction, playing the minor role, manifests itself in diminishing secondary bands superimposed on the primary birefringence around the section. Figure 4.6 illustrates a classical diffraction pattern produced by the edge of a razor blade. Light reacting with the edge of a thin-section results in a similar wave interference phenomena but is complicated by the doubly refracting nature of the section. The resulting combination of birefringence and diffraction patterns adjacent to a carefully focused edge is often seen as a nearly perfect "counterfeit" OH-rim, occasionally followed by increasingly smaller and weaker bands. The obvious question then arises: how does one differentiate between real and false OH-rims?

The answer to the question of differentiating between real and false rims is mainly provided by varying the focal point within the thin-section. "As the microscope is adjusted in and out of focus, the inner edge of hydrated layer (the point where it contacts the non-hydrated obsidian) should not shift its position if the section has been cut perpendicular to the surface" (Friedman and Smith, 1960:479). There in fact may be a very small shift but a real rim will maintain the same width and nearly always the same position as the focus is slowly varied up and down through the thin-section.⁵ However, this is not the case for diffraction and birefringence bands. These bands are horizontally displaced

12

and become weaker in intensity as the focus is varied up and down past the optimum focal point of the thin-section edge. Normally, if a well defined OH-rim is present birefringence can be easily identified; however, where there is no rim present, birefringence can appear very much like the expected rim--especially when working in the area of 1.71 microns. The primary birefringence band standing adjacent to a carefully focused edge was found to have a characteristic width of 1.71 microns with a range between 1.64 and 1.78 microns. Should a well prepared thin-section exhibit a rim which: (1) is about 1.71 microns thick, and (2) is displaced more than its width by varying the focus within the section, then there can be little doubt the rim is false. In addition to the above, a simple check to eliminate birefringence is in the petrological make-up of the section: both the section and OH-rim must have a similar microlite and crystallite content. If the "Rim" is clear but the section has many inclusions, then the rim can hardly be part of that thin-section. In the case where the thin-section also is clear this check is indeterminate.

The petrographical characteristic affecting boundary determination arises from (1) physical alteration of the absorbing surface, and (2) the material content of the obsidian. The physical alteration of the obsidian surface destroys some or all of the hydrated layer and always has a detrimental effect. Common causes are burning and

abrasion (see also Friedman and Smith, 1960:485-486) of the artifact; an even more common cause is over-grinding during preparation. On the other hand, the material content of the obsidian rarely will physically alter the surface; however, it can certainly obscure or completely hide some or all of the diffusion front (inner edge of the OH-rim). The earlier work of Donovan Clark is in complete agreement with the observations made during the present research. "Petrographic features which may make the hydration obscure include the presence of abundant crystallites, microlites, magnetite grains, or inclusions (see Fig. 4.7). Compounds such as iron oxides, which color the section, also may affect the quality of measurement..." (Clark, 1961:18).

Of the 262 specimens analyzed from 4-SAC-29, the degree of obscurity varied similar to the above mentioned positively skewed distribution curve: about 20% were "crystal" to moderately clear, 75% contained a variety of inclusions but offered few problems and 5% were heavily to completely obscured. For specimens exhibiting no measurable rim due to a high degree of physical destruction, or complete obscuration of the OH-rim, an additional thin-section should be prepared. If a well prepared second specimen is the same, the artifact may justifiably be considered undatable.

To conclude the RBD phase, it will be assumed a thin-section with moderate inclusions has been clearly

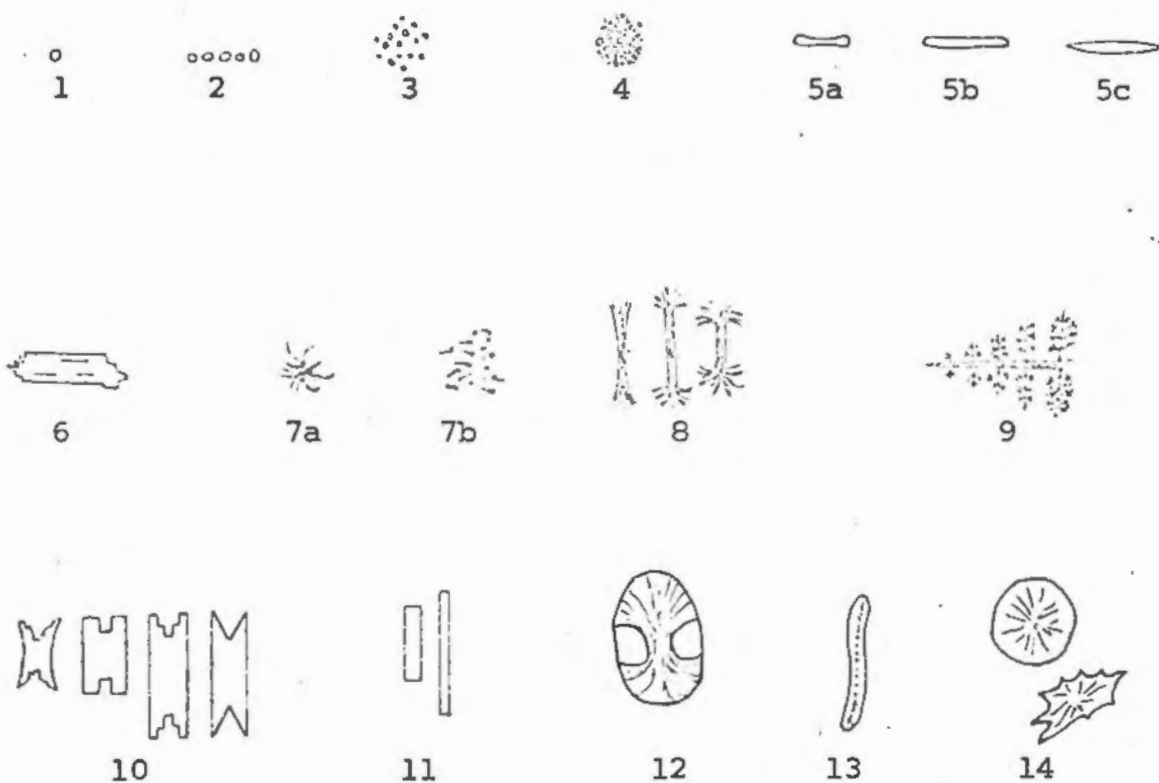


Fig. 4.7. Types of Crystallites and Microlites in thin-sections

- | | | |
|------------------|-----------------------------|--------------------------------|
| 1. Globulite | 7. Trichites | 11. Lath-crystal
Microlites |
| 2. Margarite | a. Asteroidal | 12. Scopulitic
Spherulite |
| 3. Cumulite | b. Acicular | 13. Axiolite
Microlite |
| 4. Globospherite | 8. Scopulites | 14. Spherulites |
| 5. Belonites | 9. Scopulitic
Growth | |
| a. Clavalite | 10. Crenulite
Microlites | |
| b. Longulite | | |
| c. Spiculite | | |
| 6. Bacillite | | |

Note: Numbers 1 - 9 are Crystallites
 Numbers 10 - 14 are Microlites

From Clark (1961:106)

70

focused and exhibits a discernible hydration rim (Plate 3.1). The bands of birefringence and diffraction have been identified through focal variation and thus are distinguished from the actual OH-rim boundaries. Furthermore, it will be assumed that the rim's diffusion front (inner edge) shifts very little under focal variation; and the edges are well defined being about twice the width of the micrometer hairline (very thin). Finally, a straight segment of the rim is centered in the x400 field, and the micrometer unit is rotated until the sweep-hairline parallels the rim. The rim is now positioned for measurement.

Phase 2.2: Measurement of the Hydration Rim (MHR)

With the rim boundaries now clearly determined, the final phase is ready to commence. The objective of the MHR phase is to measure in micrometer drum divisions the distance between the centers of the two rim boundaries. When five total measurements at two positions have been carefully made and each recorded on the artifact identification card (see below), their average is computed and multiplied by the appropriate calibration factor. The resulting product is the width of the hydration rim in microns.

The artifact identification card (Plate 4.9), tentatively designed by Mr. William Pritchard, was modified to its present form after analyzing two hundred artifacts. The only procedural change made was to decrease the number of trial readings from ten to five trials. After analyzing the two hundred

artifacts, an accuracy comparison using five against ten trials proved negligible⁶; therefore, ten trials were judged excessive and the number modified to five. Donavan Clark (1961:17) recommended one trial for a given location over 3 locations. This author only differs by taking three trials at the first location, and then two trials at another for verification. As stated above, the five trials are averaged and the mean is multiplied by the calibration factor to provide an answer in microns. A reliability (or repeatability, see Ch. V) test for a single observer using this procedure indicated 68.3% of the measurements would not differ more than $\pm .09$ microns. Michels (1967:213) reports a reliability of $\pm .07$ microns, while Friedman and Smith (1960:481) report a reliability of $\pm .10$ microns. Clark did not list the reliability for a single observer. Finally, Meighen (1968:1072) reports a maximum measurement error of $\pm .20$ microns but does not specify its standard deviation base or whether it is for a single observer or several. The $\pm .09$ micron measurement error is in close agreement with both Friedman and Smith, and Michels, and thus supports their finding at the one standard deviation level.

The measurement error in this work by convention will be based on one standard deviation (1σ) or a probability of 68.3% that the error will not vary more than $\pm .09$ microns. Thus all rim measurements will be in the form: $\bar{X} \pm .09 \mu$, and carry a statistical certainty of 68.3%. A 95.5% certainty would take into account two standard deviations ($2\sigma = .18\mu$), and be in the form: $\bar{X} \pm .18 \mu$.

Returning to the mechanics of measuring, the procedure is essentially the same as that for calibration. The x40 objective is used except in the following: (1) if the rim exceeds six microns, the x10 objective is used, and (2) if the rim is less than one micron, using a x100 objective is better procedure. With the sweep-hairline placed parallel to the carefully focused length of rim the procedure is as follows:

1. The sweep-hairline is slowly advanced to the exact center of one rim boundary.
2. The drum zero-position is then mentally noted or recorded on paper.
3. From the zero-point the sweep-hairline is advanced to the exact center of the second rim boundary.
4. The corresponding drum position for the second boundary is then noted.
5. The difference between the two drum readings is then recorded on the data card. The difference represents number of drum divisions between the rim boundaries.
6. After three trials at one location and two verification trials at a second location, the five are averaged and the mean recorded.
7. The average drum divisions is then multiplied by the x40 calibration factor, and the product recorded on the data card. This product is the average width of the hydration layer in microns.

During the measuring procedure, the sweep-hairline must be tracked in the same direction until the reading is completed. "In taking a reading always turn the screw in the direction of increasing numbers of the scale and wheel. To repeat a reading turn the wheel back at least one whole turn and make the setting approaching again from the same direction"

(Minor, 1956:192). Finally, good procedure dictates releasing the drum (or wheel) while still observing the hairline. This will prevent accidentally off-setting the hairline before recording its position.

In concluding, a few remarks concerning a simple thin-section reference system will be offered. The technique proved very helpful in rapidly relocating special features within the section, and has the often added feature of marking the rimless leg of the thin-section. Before placing the slide under the microscope, the shortest leg of the thin-section is marked (using a red Micropoint Fine-Stick 549) by placing a small red ink dot directly over it on the cover slip. This designates the base of the section and generally is the side coming from the artifact's interior, i.e., it is rimless. The other two legs are searched first, and if each contains a rim, the third (marked) leg can not contain a rim and thus has been eliminated. As for the reference system, all coordinates are given in distance from the base on either the port or the starboard side. For example, if a section contains only one short segment its position is designated to the nearest fifth of an optical field diameter (OFD) from the base on one side or the other. Specifically, a location would be designated: rim segment, $2\frac{2}{5}$ OFD, port side. The rim segment then could be later located without having to search the entire thin-section. Finally, recording a short general description of each rim under "comments" on the data card is

also recommended. The information should indicate the rim being: (1) continuous, or broken over one OFD; (2) clear, moderately clear, or obscured; and (3) edges sharply defined, or hazy. For example, a rim might be designated: continuous, moderately clear, and sharply defined.

A final suggestion before proceeding to the application of the dating method is now in order. From the necessity of removing a test-section from the artifact comes the problem of how to disguise the resulting gap. This problem was best solved for the typically black obsidians from SAC-29 by first filling the gap with modeling clay to within about one millimeter of the absorbing surface; next a polymer latex emulsion compound with ground marble (Hyplar Modeling Paste: \$1.25/pt.) and with Mars Black plastic color (Hyplar Plastic Colors: 60¢/2fl.oz.) mixed in is spread over the clay until flush with the obsidian surface; after the compound has dried for about three hours, straight plastic color may then be applied to match the gloss of the obsidian. The end of a small stick provides a means of application, while an index finger moistened with water is most practical for smoothing. After a few trials, one will find the gaps can be well disguised; and for artifacts having display potential this is an important consideration. The results of such restoration on two obsidian blades are pictured in Plate 4.9 (a&b) in Appendix D.

Chapter Five

THE APPLICATION OF OBSIDIAN HYDRATION DATING TO ARTIFACTS FROM THE KING BROWN SITE

I. SITE DESCRIPTION AND HISTORY OF EXCAVATION

The King Brown Site, 4-SAC-29, is located on the flood plain of the Sacramento River within the southwestern limits of the City of Sacramento.¹ Situated on the east side of the Sacramento River, this Maidu Indian site overlies the geologically recent Columbia silt deposit, and has soil generally characterized by a light grey-brown color with a relatively unconsolidated nature (Olsen, 1963: 10).

Excavations at SAC-29 (also known as the Roeder Site) were first conducted between 1939 and 1940 by Sacramento Junior College under the direction of Dr. J.B. Lillard and Mr. Franklin Fenenga. Following WW II, Sacramento State College initiated the second project at the King Brown Site. Commencing in 1955, their work continued through the summer of 1956 with Dr. Brigham Arnold as the project supervisor (Olsen, 1963: 8). After the 1955-56 project, no further excavations were carried out until 1967. In the summer of 1967 the third and final excavation was initiated, this time by the State of California, as a salvage archaeology project directed by Mr. William Fritchard. The excavation continued through the duration of the summer and was terminated in September of 1967 due to initial freeway construction over part of the site location.

The materials recovered during the final project are currently being used to generate masters theses within the Department of Anthropology at Sacramento State College. The obsidian specimens recovered from this project were familiar to the writer as a member of the 1967 excavation team, and constitute an adequate sample for a single site hydration analysis.

Using the methods described in Chapter Four and the Sacramento-Davis hydration rate from Chapter Three, the following analysis results were obtained from the SAC-29 obsidians recovered during the 1967 project.

II. THE COMBINED ERROR FUNCTION

The measurement reliability (or measurement error) is an essential first specification in hydration analysis: it specifies the limits within which a single artifact can not chronologically be distinguished with certainty from another. Thus ungrouped artifacts having hydration rims within this limit are not distinguishable in age. On the other hand, three or more grouped artifacts (from a burial for instance) will carry their own standard deviation error.

The approach used in determining the measurement component of the combined error function was to compute the standard deviation of the measurement variations for two trials each on thirty artifacts. The readings were taken at random locations, and spaced no less than one month between trials. The

above approach yielded the following results:

Table 5.1. Determining the Measurement Error

<u>SSC Slide #</u>	<u>Trial 1(μ)</u>	<u>Trial 2(μ)</u>	<u>($\Delta \mu$)</u>	<u>($\Delta \mu$)²</u>	<u>n</u>
11	4.70	4.70	.00	.0000	1
12	3.76	3.94	.18	.0324	2
21	1.63	1.62	.01	.0001	3
25	2.57	2.58	.01	.0001	4
32	2.09	2.07	.02	.0004	5
41	3.21	3.10	.11	.0121	6
43	1.86	1.84	.02	.0004	7
240	1.88	1.86	.02	.0004	8
45	4.18	4.20	.02	.0004	9
45B	3.52	3.35	.23	.0529	10
46	2.49	2.40	.09	.0081	11
47	2.14	1.99	.15	.0225	12
209	2.91	2.66	.25	.0625	13
154	2.01	2.04	.03	.0009	14
50	2.23	2.14	.09	.0081	15
51	1.88	1.89	.01	.0001	16
193	2.07	1.93	.14	.0196	17
53	1.87	1.88	.01	.0001	18
55	2.02	1.99	.03	.0009	19
56	1.98	1.99	.01	.0001	20
57	2.08	2.04	.04	.0016	21
243	1.22	1.24	.02	.0004	22
59	2.09	2.12	.03	.0009	23
60	2.13	2.08	.05	.0025	24
76	1.84	1.75	.09	.0081	25
252	4.88	4.84	.04	.0016	26
79	2.46	2.44	.02	.0004	27
84	1.58	1.53	.05	.0025	28
131	1.46	1.51	.05	.0025	29
44	1.89	1.87	.02	.0004	30

$$\Sigma(\Delta \mu)^2 = .2430$$

$$\sigma = \sqrt{\frac{\Sigma(\Delta \mu)^2}{(N-1)}} = \sqrt{\frac{.2430}{29}} = \sqrt{83.8 \times 10^{-4}} = \pm .09 \mu$$

The measurement error, E_m , is, therefore, $\pm .09 \mu$. As indicated earlier (Page 77), all ungrouped rim measurements will be given in the form $\bar{X} \pm .09 \mu$. The main characteristic

of the measurement error is its static nature: whether the reading is one or ten microns, the measurement is still only certain to within $\pm .09 \mu$. The significance of such a characteristic is readily seen: the percentage of error decreases with increasing age, e.g., at 9/10 of a micron the error is 10% while at 9 microns the error is down to 1%. The error change for the rate relationship, however, is just the opposite and will now be determined.

To define the error limits for the Sac-Davis hydration rate we use the $\pm .3^{\circ}\text{C}$ ($.25^{\circ}\text{C}$ actually) temperature error, and find D for the upper temperature limit using equation (2), i.e., $\log D = .0424 T_e - .241$. By this method the rate error, E_r , (at one S.D.) is found to be $\pm .15 \mu^2/10^3$ years, or expressed in the diffusion rate:

$$D = 5.21 \pm .15 \mu^2/10^3 \text{ years.}$$

It would seem that each age determination in years should have two \pm error limits: (1) the rate error, and (2) the measurement error. That, in fact, is correct. As Table 1 in Appendix C lists the micron-year equivalents in $.1 \mu$ intervals for $D = 5.21 \mu^2/10^3$ years, the most practical expression for the rate error is in a micron relationship (the measurement and rate errors will thus have the same units). Since $\pm .15 \mu^2/10^3$ years is the rate error, we find from $x^2 = Dt$ that the expression for E_r in microns is:

$$\pm .012 \times \mu$$

The general expression for a hydration measurement must account

for each error, and this is accomplished by combining both into one variance error function E_{m+r}^2 , and then taking the square root to provide the needed S.D. error function, E_{m+r} :

$$E_m = \pm .09\mu \qquad E_r = \pm .012x$$

$$E_m^2 = .0081\mu^2 \qquad E_r^2 = .000144x^2\mu^2$$

$$E_{m+r}^2 = E_m^2 + E_r^2$$

$$E_{m+r} = \pm \sqrt{E_m^2 + 1.44 \times 10^{-4} x^2} \qquad (7)$$

$$E_{m+r} = \pm \sqrt{.0081 + .000144x^2}$$

$$\underline{E_{m+r} = \pm .012 \sqrt{x^2 + 56.30} \mu} \qquad (8)$$

All hydration measurements then will have error limits set by the general relationship in equation (7), and ungrouped or isolated specimens will carry limits set by equation (8). At small measurement values, equation (8) will give a combined error differing little from E_m ($\pm .09\mu$); however, at seven microns E_r is rapidly approaching E_m , and by eight microns it has equalled it. Since the inaccuracy in equation (8) is just 7% at three microns by using only the measurement error (E_m), and since the inaccuracy rapidly decreases below that point, E_m ($\pm .09\mu$) only will be used for all readings at and below 3μ of hydration. Thus measurements will have one of two general forms depending on the amount of hydration:

$$\bar{X} \pm .09\mu \qquad (\leq 3\mu)$$

$$\bar{X} \pm .012 \sqrt{x^2 + 56.30} \mu \qquad (> 3\mu)$$

III. A TEST OF THE UNIFORM HYDRATION HYPOTHESIS, AND THE CHRONOLOGY OF BURIAL-ASSOCIATED OBSIDIAN LOTS

As previously stated (Page 3), within the 262 artifacts analyzed there are 54 projectile points and fragments associated with seven burials. The significance of the burial associated obsidian lots is that each lot has a high probability of containing obsidians which: (1) are contemporaneous, and (2) have been continually exposed to the same temperature. If the working hypothesis that obsidians exposed to similiar conditions undergo uniform amounts of hydration is correct, then the combined standard deviations of the lots should not be significantly greater than the expected measurement error. First we will describe the burial analysis results, and then test the validity of the hypothesis.

A. Chronology of the Burial-Associated Obsidian Lots

The rim measurements for all lot members analyzed are located under the column headed "OH-Rim in u" in Appendix B. In addition, Fig. 5.1 shows their distribution by .2 μ class intervals. The number of obsidian samples per burial lot can be determined from Fig. 5.1; however, for ease of reference, that data is furnished along with each lot's mean and standard deviation in the following table:

Table 5.2. Burial Lot Means and Standard Deviations

<u>Burial</u>	<u>Sample Size</u>	<u>Mean and S.D. μ</u>
301 & 304	25	2.12 \pm .19 *
305	1	3.13 \pm .10 **
306	4	1.87 \pm .02
307	6	2.01 \pm .25
308	5	1.97 \pm .06
313	10	2.07 \pm .04
315	3	1.78 \pm .06

- * Corrected mean (see below): uncorrected mean was 2.17 \pm .33 μ
 ** The S.D. can not be computed for one sample so the combined error applies.

The combined burial 301 and 304 consisted of two individuals as one unit having a total of 26 associated obsidian artifacts. One projectile point (Catalog #.6235; SSC #45) was excluded on unquestionable statistical grounds: its reading, 3.52 μ , lies over four standard deviations above the uncorrected lot mean, and over six standard deviations above when excluded from the mean's calculation. In other words, the artifact is statistically unrelated to the other lot members by age.

Since two standard deviations (S.D.) leaves only a 4.5% probability that it should be included and 3 S.D.'s only a .3% probability, one can appreciate such a 4 S.D. anomaly. It will be the policy of this thesis to exclude a group member if it is greater than two standard deviations above the uncorrected mean. The exclusion can be further substantiated on cultural grounds from a comparison of the points pictured in Appendix D: SSC #45 is of a type associated with greater

antiquity than its other lot members. Referring to Fig. 5.1, the anomaly is easily visible standing isolated in the 3.5 μ class center. Another reading, SSC #69, represented at the 2.7 μ class center lies just within the two S.D. cut-off for the uncorrected mean.

The exact reasons for the high age variance of the lot members in B-301 & 4 are uncertain. Which of the 26 projectile points should be associated with each individual and whether they are of equal age appears even more uncertain. Since the variety of point types and the extreme age of one point and high difference in another suggest culturally rather than geologically related explanations, this burial can not be used either to verify or disprove the hypothesis test.

Burial 307 with six obsidian specimens is the second and last to have an unexpectedly large variance. Referring once again to Fig. 5.1, one can see that two of the specimens are separated from the others by a full class interval. The measurements themselves are as follows: 2.35 μ , 2.31 μ , 1.90 μ , 1.90 μ , 1.81 μ , and 1.81 μ . First, neither the first two nor the last four can be excluded on statistical grounds as they are all well within the two S.D. level. Yet by referring to the points pictured in Appendix D under their SSC #: 37, 36, 186, 187, 185, and 188 respectively, one can see the obvious similarity between SSC # 36 and 37, and the difference between them and the last four. Whether the former or latter more accurately reflects the true age of the burial is impossible

to judge: thus the burial mean must include all samples resulting in a greater error factor.

The remaining burial means are all well within the expected $\pm .09 \mu$ measurement error and require no discussion regarding variance. Using the accepted means and their standard deviation, the final step before applying the age in years B.P. is to determine the 95% confidence limits for the actual age based on Student's t distribution (see Spiegel, 1961:188). The 95% confidence limits are given by $\bar{X} \pm t_{.975} (S/\sqrt{N-1})$, where N = sample size, S = standard deviation, \bar{X} = the burial mean, and $\pm t_{.975}$ are the 95 percentile values for Student's t distribution for a given number of degrees of freedom (found in standard statistical tables). Upon investigation one can see the confidence limits (at a given percentage) for a mean are a function of the samples' standard deviation and size (N). From the data in Table 5.2, the 95% confidence limits are computed using a t distribution table:

Table 5.3. The 95% Confidence Limits for Burial Means

Burial	$\bar{X} \pm t_{.975} (S/\sqrt{N-1}) \mu$	$\bar{X} \pm 95\% t \text{ Limits } \mu$
301 & 4	$2.12 \pm 2.06 (.19/\sqrt{24})$	$2.12 \pm .08$
305	no S.D., N = 1	N/A
306	$1.87 \pm 3.18 (.02/\sqrt{3})$	$1.87 \pm .04$
307	$2.01 \pm 2.57 (.25/\sqrt{5})$	$2.01 \pm .29$
308	$1.97 \pm 2.78 (.06/\sqrt{4})$	$1.97 \pm .08$
313	$2.07 \pm 2.23 (.04/\sqrt{9})$	$2.07 \pm .03$
315	$1.78 \pm 4.30 (.06/\sqrt{2})$	$1.78 \pm .18$

Reviewing the S.D.'s for the various burials, one can see that a small sample increases the error range above the standard deviation, whereas a large sample (B-301 & 4 and B-313) decreases the error range at the 95% confidence level. Thus it is obviously important to have as many samples as possible. For the normal S.D. encountered in hydration measurements, seven (7) seems "about" the breaking point between small and large samples. With the above computations, then, there is 95% confidence that the actual age lies within the limits set by the \pm values. The equivalent age in years may now be determined from Table 1, Appendix C.

Table 5.4. Chronology of Burials in Years B.P.

Burial	$\bar{X} \pm 95\% \text{ t Limits } (\mu)$	Years B.P.
301 & 4	2.12 \pm .08	863 \pm 66
305	3.13 \pm .10 *	1881 \pm 125
306	1.87 \pm .04	672 \pm 28
307	2.01 \pm .29	776 \pm 239
308	1.97 \pm .08	745 \pm 60
313	2.07 \pm .03	823 \pm 23
315	1.78 \pm .18	609 \pm 129

* The combined error applies as this is a single artifact over 3 μ .

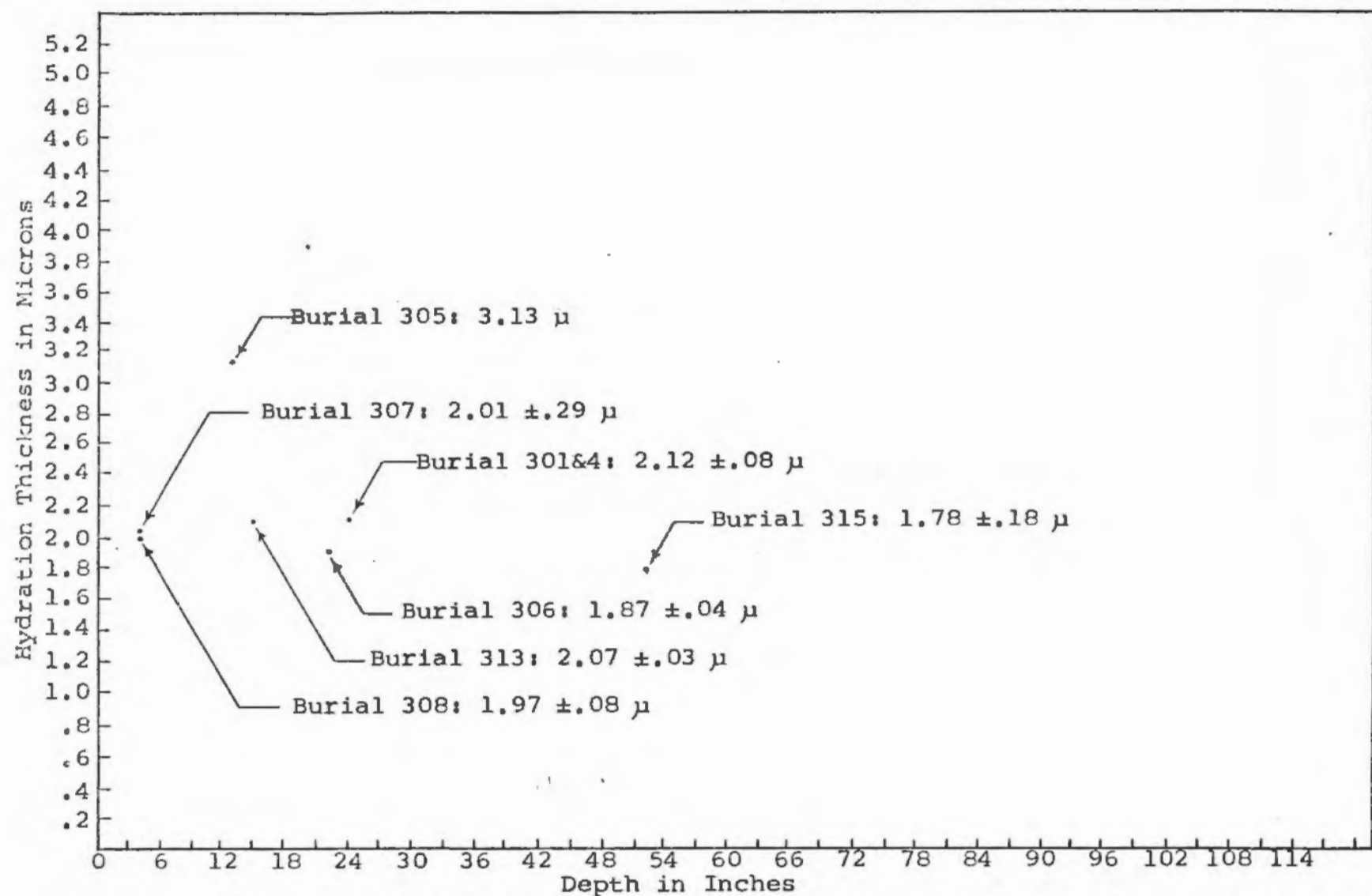
The seven burials then range from an average age of 1881 B.P. (88 A.D.) to 609 B.P. (1360 A.D.) with error limits from ± 23 years to ± 239 years. From Fig. 5.1 and Table 5.4 the burials are seen to be most heavily clustered between the 1.8 and 2.2 micron class intervals which corresponds well with the class interval high concentrations of unassociated artifacts (see Fig. 5.6).

The relationship between age and depth for the burials is plotted in Fig. 5.2. There seems to be no correlation between the two variables, and the explanation chiefly lies in the lack of sufficient data to provide meaningful results. This, however, is not the case for the unassociated artifacts as will be covered (see Fig. 5.5) after the following test to verify the uniform hydration hypothesis.

B. A Test of the Uniform Hydration Hypothesis

To test the hypothesis of uniform amounts of hydration for obsidians in like environments, it is necessary to have a group of artifacts of equal age and confined to equal environmental conditions. As the normal volume of a burial is very small, its environmental variation can be considered negligible; furthermore, the artifacts associated with the life or death of the individual will normally have negligible difference in age. Thus the obsidians associated with any one burial should have equivalent hydration rims, i.e., their deviation in measurement should not exceed the expected measurement error of $\pm .09 \mu$. To minimize the effects introduced by anomalies in age or environmental equivalencies and to maximize confidence, procedure necessitates investigating many burial lots to determine their combined standard deviation. If the combined S.D. of the lots is significantly greater (by the chi-square test) than $\pm .09 \mu$, then the test is negative. If their combined S.D. is equal to or less than $\pm .09 \mu$, then the results are positive and the hypothesis is

Fig. 52 MEAN HYDRATION THICKNESS OF BURIAL LOTS VS DISPLACEMENT FROM SURFACE



Note: There is 95% confidence that the true mean lies within the limits set by the \pm value.
 Burial 305 contained only one obsidian artifact; thus, the confidence limits for it can not be computed.

verified. From the burial lot standard deviations listed in Table 5.2, one can well anticipate a close test. The combined S.D. (S) for the five lots is:

$$s^2 = (\Delta x)^2 / N - 1$$

$$s^2 = .3322 / 27$$

$$s^2 = .012$$

$$s = \pm .10 \mu$$

Since the combined S.D. is $\pm .01 \mu$ higher than the expected measurement error, the final problem is to determine if the difference is significant at the 95% and 99% confidence levels following the practice in statistical decision theory: results significant (1) at levels less than 95% are not significant; (2) at 95% but not 99% are probably significant; and (3) at 99% are highly significant (Spiegel, 1961:174). Using the chi-square test:

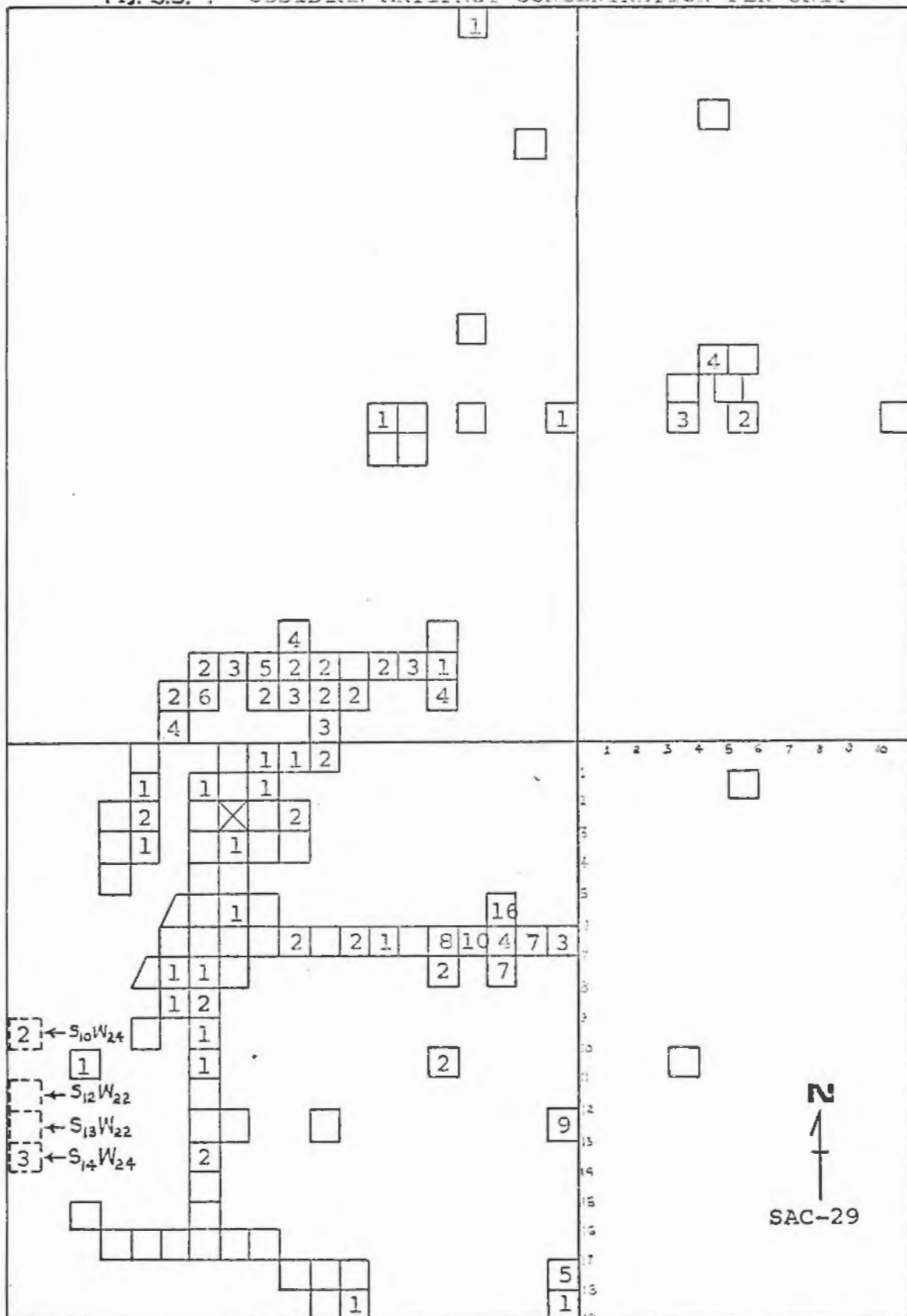
$$\chi^2 = Ns^2 / \sigma^2 \quad N=28, S=.11, \sigma=.09$$

$$\chi^2 = 28 (.012) / .0081$$

$$\chi^2 = 41.5$$

From the chi-square tables (Spiegel, 1961:345) at $N-1=27$ degrees of freedom, we find χ^2 must at least equal 47.0 to be significant, and must equal 43.2 to be probably significant. Since from the computations $\chi^2 = 41.5$, the difference is not significant with a confidence of greater than 99%. The uniform hydration hypothesis is therefore verified.

Fig. 5.3. . OBSIDIAN ARTIFACT CONCENTRATION PER UNIT



Note: The numbers designate the concentration per unit of obsidian artifacts analyzed. The four broken line squares designate units located as indicated beyond the limits of the chart.

IV. GENERAL CHRONOLOGY OF THE KING BROWN OBSIDIAN ARTIFACTS

The general chronology of the King Brown obsidian artifacts is divided into two main categories: (1) geologically significant temporal relationships, and (2) culturally significant temporal relationships. The former, or geotemporal configurations, is an investigation into the age versus soil depth correlation, and the evidence of soil disturbance at SAC-29 through such a correlation. The latter is concerned with culture in time, and deals with the intensity of the site's occupation through time.

A. Geotemporal Configurations

The investigation of the age versus soil depth relationship at a site necessitates having a sufficiently large sample (see Page 90) of artifacts from each depth increment used during the excavation. In addition, the sample should sufficiently represent the total surface area excavated. Using the results of the hydration analysis, the number of OH-values within each 2 μ interval are grouped within their respective levels, and plotted on a three-dimensional scatter diagram: this illustrates the frequency distribution of hydration values by level. Fig. 5.4 is such a scatter diagram for the SAC-29 samples. From such an array of data one can easily see the range of values by level, and also any tendency for these values to cluster within their respective levels. The first question then becomes: what is the mean hydration

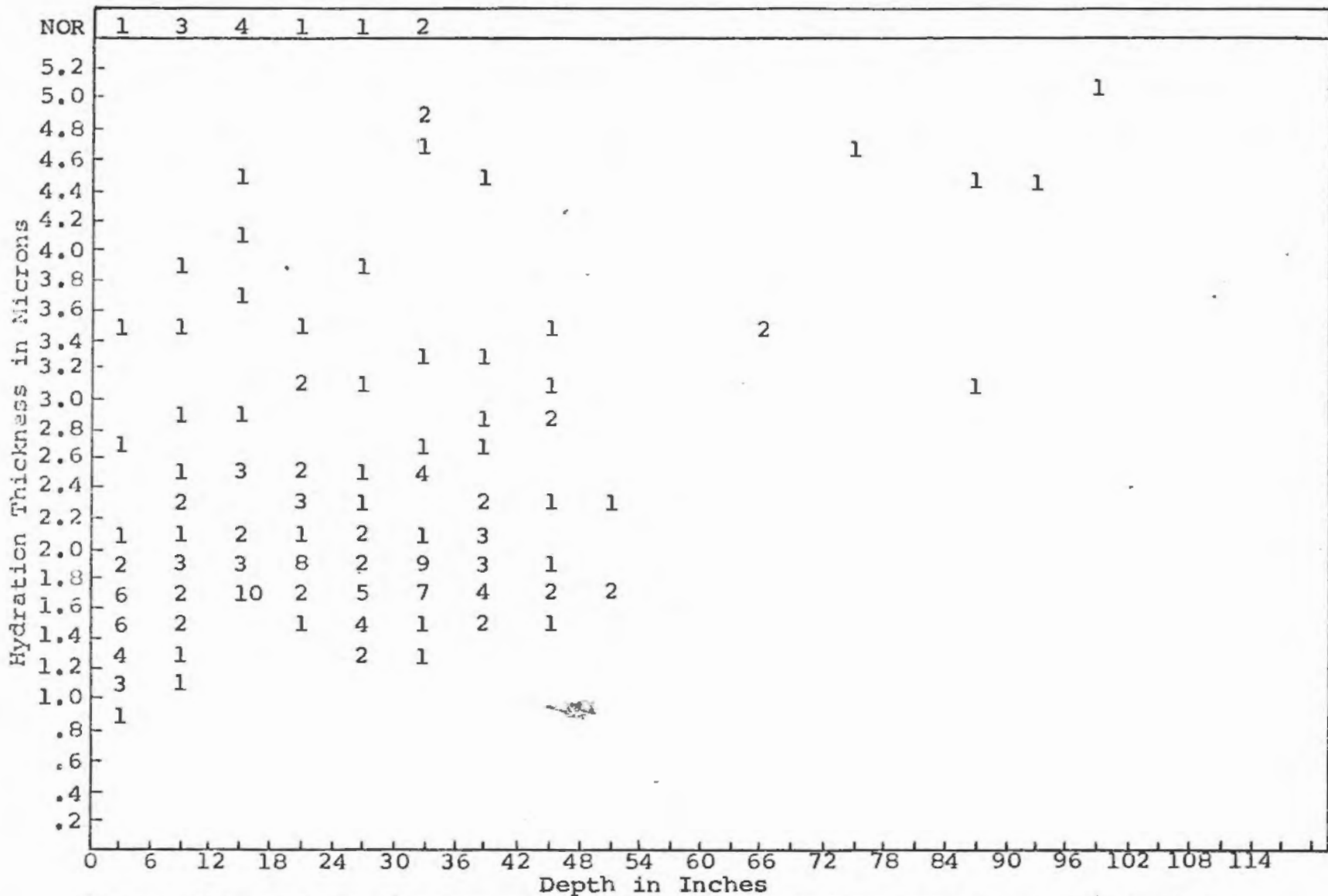


Fig. 5.4. FREQUENCY DISTRIBUTION OF HYDRATION VALUES VS DISPLACEMENT FROM SURFACE

Note: This scatter diagram of all samples (excluding burial lot samples) from SAC-29 shows the frequency distribution of hydration values plotted against depth from the surface of the site.
 NOR designates samples having No Observable Rim.

value for each six-inch level? And from this follows the essential question: does the mean increase uniformly by depth? In other words: is there a consistent change rate of hydration values by soil depth?

Using Fig. 5.4, the mean OH-value of each level (M) is found by: (1) multiplying the number of OH-values within each 2μ class (f) times the class value itself (v); (2) summing these products; and (3) dividing the sum by the total number of OH-values (N). That is:

$$M = \frac{\sum(f \cdot v)}{N}$$

When the mean for each level has been determined along with their respective confidence limits, the results are then displayed in graphical form with a trend line (determined by the method of least squares) to show the fit of the data. The slope of this line is then the change rate of OH-values by depth. Fig. 5.5 is such a display showing the plot of the SAC-29 OH-means for the first nine consecutive levels and the scattered ones thereafter. The vertical extensions from each point are the 80% confidence limits for each mean. In tabular form the results are as follows:

Table 5.5. OH-Thickness vs Displacement from Surface

<u>Depth Level (in.)</u>	<u>Mean (μ)</u>	<u>80% Confidence Limits</u>
0 - 6	1.57	± .16
6 - 12	1.74	± .33
12 - 18	1.91	± .30
18 - 24	2.09	± .21
24 - 30	1.85	± .20
30 - 36	2.01	± .26
36 - 42	2.21	± .24
42 - 48	2.39	± .37
48 - 54	1.90	± .47

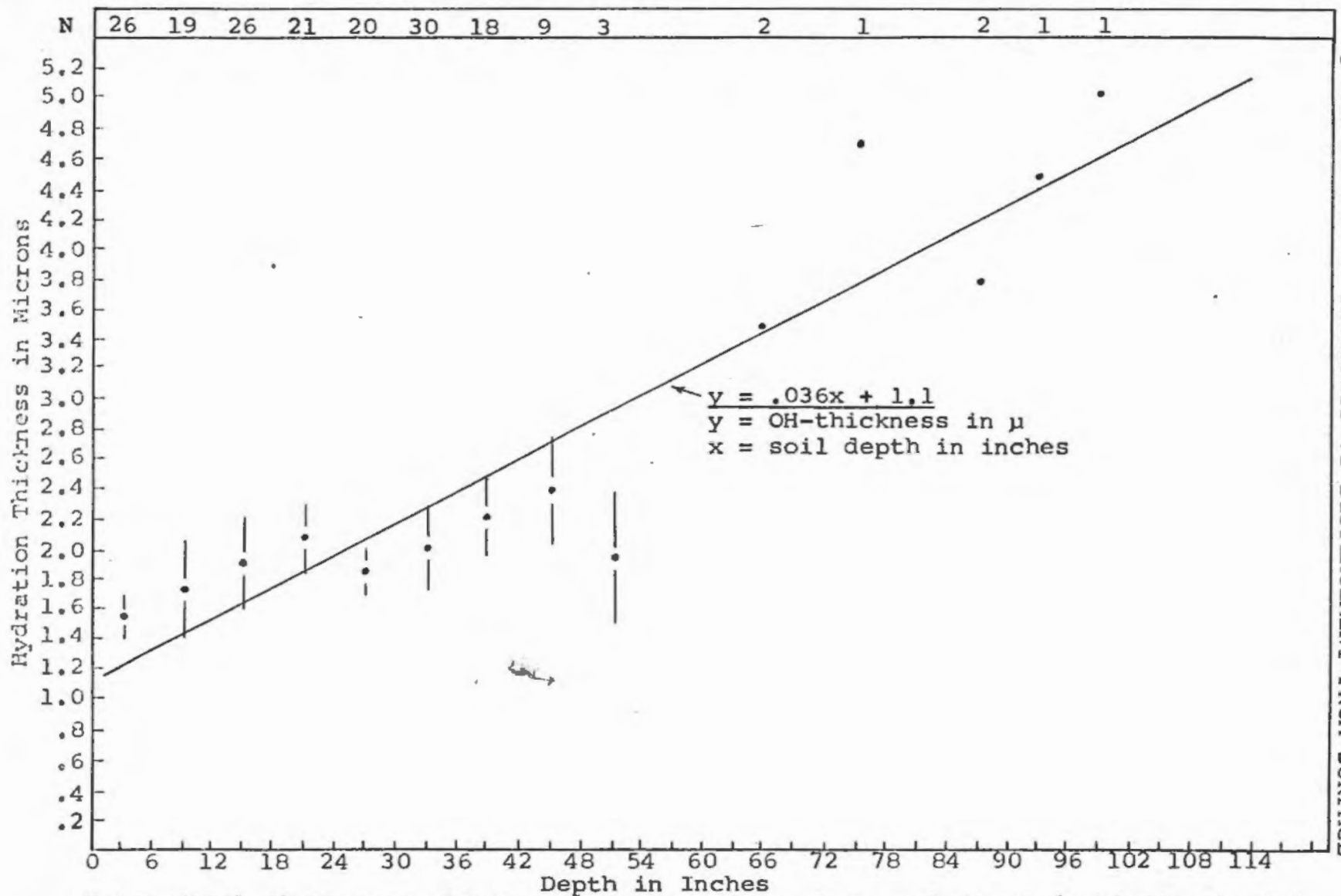


Fig. 5.5. HYDRATION THICKNESS VS DISPLACEMENT FROM SURFACE

Note: Graph shows mean thickness of all samples from each level (excluding burial lots) of SAC-29 plotted against depth from surface of site. There is at least 80% confidence that the true mean lies within the vertical extensions from each point.
 N DESIGNATES THE SAMPLE SIZE FOR EACH LEVEL.

Viewing the data of Table 5.5 before plotting them in Fig. 5.5, one would expect any one mean to have any value between its 80% confidence limits without being exactly in line; however, when the means are actually plotted an important fact becomes obvious: the first four means are nearly exactly in line, as is the case with the next four. In fact, the rate of change is constant for the first eight levels, i.e., a line drawn through the first four point sets is nearly exactly parallel to a line through the next four in Fig. 5.6 reflecting equal rates of change regardless of soil depth. Thus we see for at least the area of the site from which the artifacts were recovered (see Fig. 5.3) that the change is very consistent and occurs at a rate given by the slope .036 in the trend line equation:

$$\underline{y = .036x + 1.1}, \quad \begin{array}{l} y = \text{OH-thickness in } \mu \\ x = \text{soil depth in inches} \end{array}$$

From the slope then the rate of change of hydration by soil depth is .43 μ /foot.

The first conclusion drawn from uniform rate is that the relationship between soil depth and time is exponential, and has the same form as the general diffusion equation: $x^2 = Dt$. Hence from the local OH-diffusion rate, surface soil accumulation for SAC-29 was very close to 1/4 inch per year between 400 years and 1100 years B.P., i.e., between the first and last of the eight well-determined point sets. It should be noted, however, that this does not mean a 1/4 inch difference at any depth equals a difference of one year, for the

change is exponential. In fact, the obvious discontinuity starting between points 4 and 5 in Fig. 5.5 indicates that an absolute correlation between time and soil depth is impossible.

An additional conclusion from Fig. 5.5 is that a net change in depth has occurred relative to the areas where the newer and older artifacts were located. As the last two micron values on the top side of the trend line overlap with the first two on the reverse side, i.e., point set 3 approximately equals 5, and 4 approximately equals 6, the indication is that either the analogous first and second levels above the older areas have been eroded or removed in some manner, or the depth above the younger artifacts has increased by about two levels. Whichever the case, there has been a net change between the two areas. The fact is known, however, that the site was bulldozed in 1956 to level the area (especially the mounded section) for construction purposes. Hence the relative depth above the older artifacts has decreased by the net amount displaced between the two areas. From Fig. 5.5 it appears that the net change was on the order of one foot.

The interpretation for the above is based on the logic that an analysis within a completely undisturbed stratigraphy will produce a completely continuous series of depth-age point sets. A corollary to that logic holds that the removal of disproportionate amounts of material from the site will result in a discontinuity in the depth-age relationship. The first

point in Fig. 5.5 is an average of artifacts found at x , $x + 1$, $x + 2$, (and so on) distances from the original surface but now all located within the first six inches; since point set one contains artifacts of mixed ages, its age will be proportionally higher than in the undisturbed case. This proportionally higher trend will continue until the mixture ceases, at which point the discontinuity will occur in the plot and the depth will swing back to the original or undisturbed trend. The magnitude of the discontinuity (in this case one foot) represents the net change of surface materials, and its depth (about two feet) represents the first depth of generally undisturbed stratigraphy.

Thus from the geotemporal analysis of data provided through hydration analysis the following conclusions have been drawn for SAC-29: (1) hydration increases at a uniform rate of $.43 \mu/\text{foot}$; (2) age increases generally as the square of soil depth; (3) soil accumulation between 400 and 1100 B.P. was approximately $.25 \text{ in}/\text{year}$; (4) there has been a net displacement of surface material on the order of one foot; (5) the stratigraphy above two feet in depth is discontinuous; and (6) the stratigraphy below two feet is generally continuous but with artifact migration between adjacent strata.

B. Culturally Significant Temporal Relationships

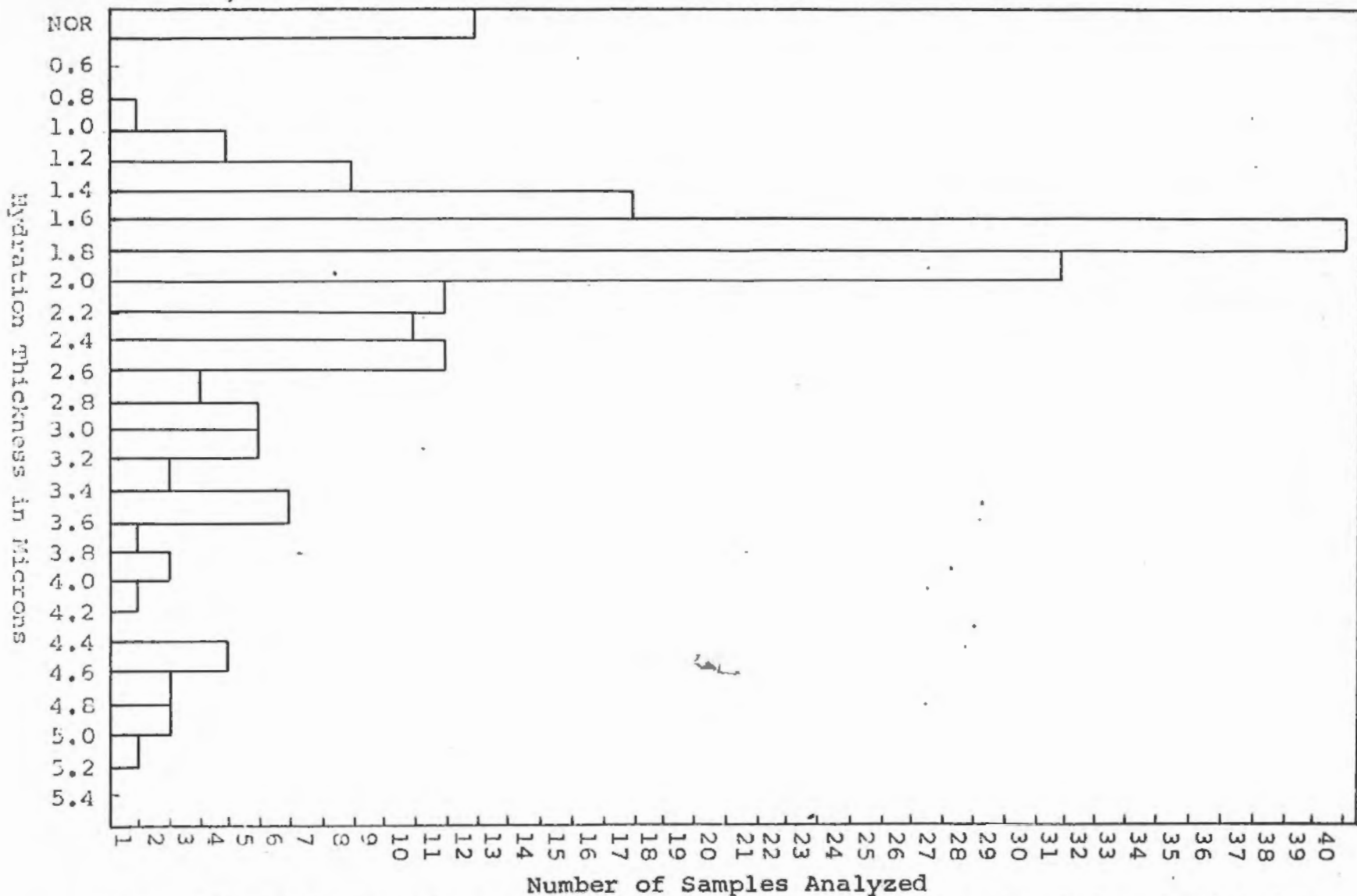
One of the distinct advantages of OH-dating over other methods, e.g., C-14, is the low cost of making the analysis; and hence the practicality of dating large numbers of obsidians.

From this practicality of "mass" dating comes the topic of this section: the SAC-29 occupation intensity through time.

The distribution of a large number of hydration values by frequency provides excellent evidence for the total time range over which a site was occupied, and also the times of maximum and minimum variations in its occupational intensity. Fig. 5.6 is a histogram showing the distribution of the 157 unassociated samples by $.2\mu$ thickness intervals. Such a histogram provides a relative view of the sample intensity by the frequency of values within each $.2\mu$ class interval. By converting the micron values into years B.P. and each class frequency into percentage of samples analyzed, the timeline profile in true perspective becomes readily visible: Fig. 5.7 is such a profile for SAC-29.

From the hydration analysis of artifacts recovered during the 1967 excavation, the total range of occupation at SAC-29 can be seen to cover approximately 5000 years. Beginning around 5133 ± 222 years ago (3164 B.C.), the earliest period of occupation lasted about 1500 years, reaching a maximum intensity in 3886 ± 200 BP and ending around 3600 BP. Following 3600 BP, there is no evidence of occupation until about 3360 BP when the next main period of occupation began. After passing through a secondary maximum in 3000 BP, the second main period reached its highest intensity in 2351 ± 136 BP after which it declined until about 2000 BP. Climbing to a new secondary maximum, the occupation was rather steady from about 1900 BP until 1500 BP when the last marked

FIG. 5.6. DISTRIBUTION OF ARTIFACTS BY HYDRATION THICKNESS



Note: This histogram shows the distribution of all samples (excluding burial lot samples) by hydration thickness.
NOR designates samples having no observable rim of hydration.

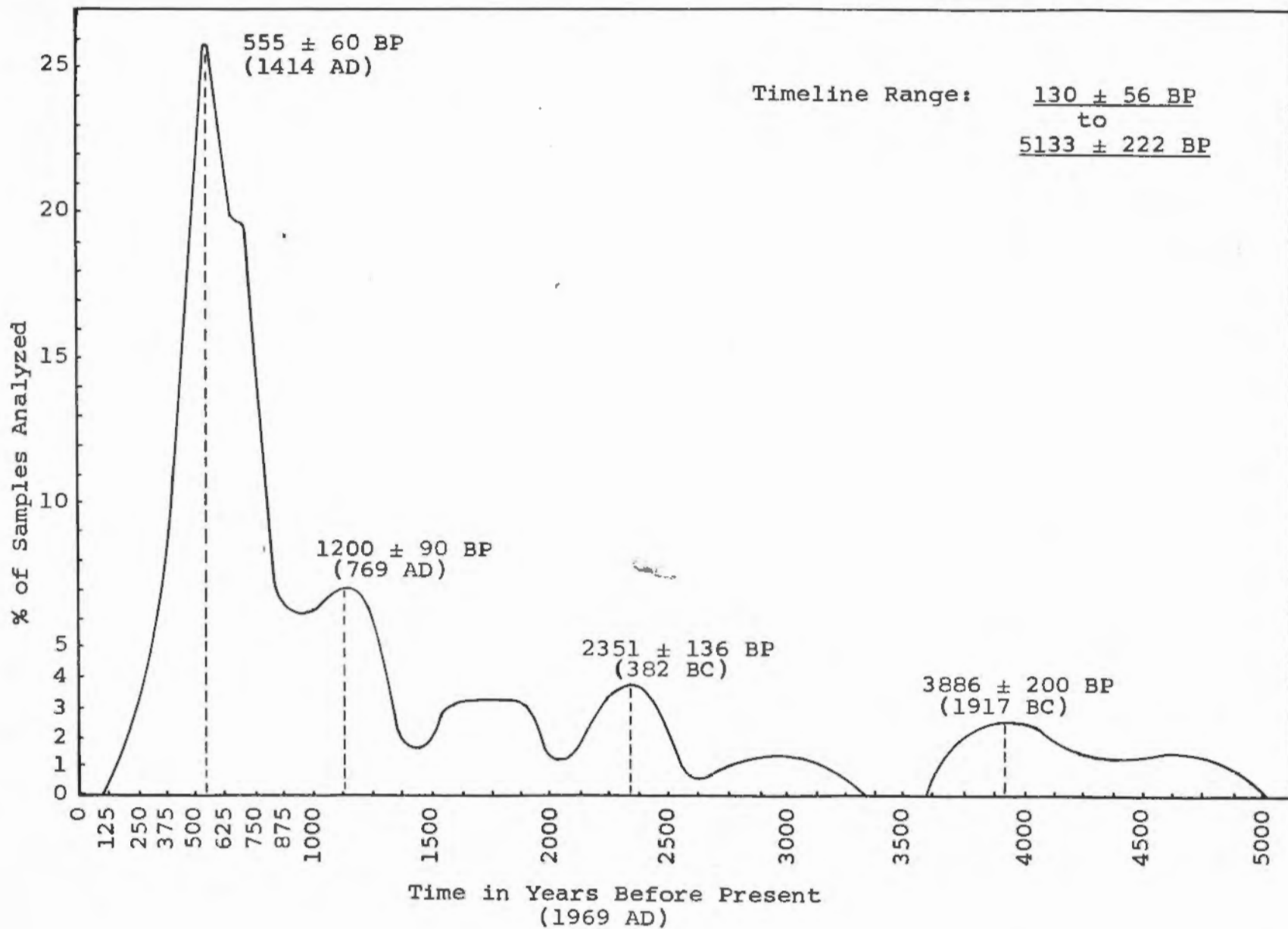


Fig. 5.7: SAC-29 OCCUPATION INTENSITY TIMELINE BY THE PERCENTAGE OF OBSIDIAN ARTIFACTS ANALYZED

decline set in before the third and by far the most intensive period of occupation began. The total time of the second main period beginning in 3360 BP and ending about 1500 BP was on the order of 1900 years. From approximately 1500 BP the final period began to rapidly increase to equal all previous maximums in less than 300 years. Except for a short secondary maximum reached by 1200 ± 90 BP, the phenomenal growth continued with but one slowing (750 BP) to reach the site's most intense occupation in 555 ± 60 BP. Thereafter the evidence indicates a decline so rapid that by 250 BP the intensity had fallen to that of the second main maximum, and by 130 ± 56 BP (1839 BC) the decline was complete.

Thus through the evidence derived from the hydration analysis, there is a strong indication of three main periods of occupation having a total duration on the order of 5000 years. The most recent and by far the most intense period began about 1500 BP and ended in historic times having a total duration on the order of 1400 years, and a maximum at 555 ± 60 BP. The middle period began about 3360 BP and lasted until 1500 BP having a peak intensity in 2351 ± 136 BP and a total duration on the order of 1900 years. Finally, the earliest period of occupation detected began in 5133 ± 222 BP and ended about 3600 BP, having a peak at 3886 ± 200 BP and a total duration on the order of 1500 years.

The above conclusions concerning occupation intensities are based on the assumption that the frequency of obsidian

artifacts at a given period directly reflects the human population for that period. In the great majority of cases this is a valid assumption and there is no reason now evident to reverse this conclusion for SAC-29. However, the reader should not overlook the fact that Fig. 5.7 is a profile directly showing the percentage variation in time for the use of obsidian at the SAC-29, and only indirectly reflecting a synchronic occupational intensity.

Chapter Six

CONCLUSIONS

The main objectives of this thesis, as set forth in the introduction, were (1) to present the hydration phenomenon in theoretical perspective along with a new method for determining hydration rates based on temperature; (2) to develop an optimum procedure (using SSC equipment) for the preparation and analysis of obsidian thin-sections; and (3) to apply the above findings to provide a relative chronology (microns of hydration), and a tentative absolute chronology (years B.P.) for the SAC-29 obsidian artifacts. Secondary objectives then utilized these chronological findings to test the uniform hydration hypothesis; determine the relationship between age and soil depth; estimate the degree of soil disturbance; and, finally, establish the SAC-29 occupation intensity through time.

In the earlier part of Chapter Three, the physical and chemical variations existing between the hydrated and non-hydrated phases were found chiefly attributable to a distinct difference in water content. Non-hydrated rhyolitic obsidian contains on the order of .3% H₂O by weight, whereas the hydrated phase (perlite) contains about 3.5% H₂O. This difference in water concentration provides the driving force from which results a net transport of water into the obsidian interior. Proceeding at 90° to the physical surface, the diffusion front advances at a rate determined chiefly by

the temperature and also by the geometry of the obsidian (a result of chemical composition) and the difference in water content between phases. As the latter two are practically constant throughout rhyolitic obsidians, temperature remains the only significant variable to influence the hydration rate. Consequently, once the relationship between these three variables was determined for rhyolitic obsidian by Friedman et al. (1966), the way was open to develop a theoretical method for determining hydration rates from the environmental temperature. Building upon the foundation set by Friedman, Smith, Long, and Ross, the emphasis of Chapter Three shifted to the main objective of developing a practical system for determining hydration rates. Calibrating OH-rates by C-14 entails many problems and considerable expense, thus a more practical means was deemed a most worthwhile objective.

To be "practical" the system had to operate on a data source which was both readily available and extensive in its coverage: Climatological Data, published by the U.S. Weather Bureau (monthly) qualified as the necessary source of temperature data. The preliminary step in deriving the system was to find an expression equating the diffusion coefficient (D) to the "effective environmental hydration temperature" T_e , or in short the effective temperature. Using the data from Friedman et al. (1966), the expression best fitting that data was found to be: $D = .0424 T_e - .2410$. Next, soil was assumed a priori to be the primary environment of obsidian

artifacts; thus, soil temperatures by depth were investigated to determine the most representative level at which to take continuous temperature measurements: a depth of four inches was found most representative in temperate and tropical climates. After this point, two problems remained: (1) the various monthly temperatures had to be integrated into one temperature (T_e) representing their total effect throughout the year, and (2) a relationship between the rarely reported soil temperatures and the extensively reported atmospheric temperatures was necessary if the system was to be of practical value.

The solution to the first problem was based on the technique of approximate integration in considering the relative effect of each temperature over the total time-temperature area. From Page 32 the expression for finding the effective temperature is:

$$T_e = \frac{t_c}{t_n} \left(\frac{A_1}{A_t} T_1 + \frac{A_2}{A_t} T_2 + \dots + \frac{A_n}{A_t} T_n \right)$$

The solution to the second problem was based on the empirically derived relationship between integrated monthly soil temperatures and integrated monthly atmospheric temperatures. Using the average high and low soil temperatures for each month and the respective average atmospheric highs for the three stations in California measuring soil temperatures, the following relationship was found to have an accuracy within .1° Fahrenheit: $T_e = 4/5 T_a + 11.2$.

With the diffusion coefficient now related through a series of expressions to the atmospheric temperatures the entire system of equations was finally tested against a highly confident rate determined through C-14 calibration near Tulelake, California. The results surprised even the author: there was no detectable difference in the rates determined by the separate methods. From the system of temperature equations using the atmospheric average monthly highs from the Tulelake station, the rate was found to be $D = 3.49 \mu^2/10^3y$; the C-14 calibration by LeRoy Johnson, Jr. also gave $D = 3.49 \mu^2/10^3y$. The C-14 calibrated rate and the rate predicted on theoretical grounds are in agreement: thus the system is conditionally proven by the only highly confident check now known for California.

The verification by one well-determined check does not, however, constitute a firm proof of the system. Such a proof can only result from a number of additional rate verifications agreeing within the specified parameters. Rates calibrated by C-14 from locations at or near Sacramento, Fresno, and Brawley, California are highest on the priority list of needed verifications. These locations are sufficiently different in temperature to give well dispersed point sets along the rate curve, and their hydration rates can and have been determined from soil temperatures.

The weakest bond in the rate-determining system at this time is the relationship between integrated soil and

integrated atmospheric temperature, i.e., $T_e = 4/5 T_a + 11.2$. For the multitude of microclimates found in California, only those of Tulelake, Sacramento, Fresno, and Brawley are known definitely to fit that expression. The latter three locations, of course, are the only stations recording soil temperatures to enable such a comparison, while Tulelake is the only station with a rate verification through C-14. In short, all available data confirms $T_e = 4/5 T_a + 11.2$, but the majority of that data originates from the basin areas of the state; hence the relationship appears quite solid for the basin areas, but to date there is only the Tulelake confirmation for mountainous regions.

The present operational status of the suggested rate determining method is summarized as follows: (1) the entire equation system is conditionally proven for the basin areas of California and definitely proven only for Tulelake; (2) in mountainous regions there is insufficient data to verify the relationship between soil and atmospheric temperatures so results from these regions not based upon soil temperatures will be most tenuous until further verification; finally, (3) until such time as the conditional status of the method in general is terminated through checks via C-14 or other means, any particular rate derived through this method must be considered tentative unless enforced by some particular archaeological evaluation.

100

Turning to the preparation and analysis of thin-sections, the concern at this level is not so much with a particular procedure, as with procedure in general. As one can surmise from Chapter Four, the essential result of the preparation must be a well defined specimen cut at 90° to the absorbing surface; there are of course a variety of ways to achieve such an end. The analysis, however, is a much more restricted and critical matter. The measurements must be in standardized units, and the measuring device must be accurately calibrated against a valid source. The general practice in calibrating utilizes a slide upon which is inscribed divisions in hundredths of a millimeter: from this the measuring device (micrometer ocular) can be calibrated to give results in microns. Thus each analyst uses a particular calibration source for his particular micrometer ocular which results in one particular problem: there is a significant probability that at times some micrometers will be erroneously calibrated. This then necessitates the following recommendations: (1) obsidian hydration laboratories should cooperate in verifying calibration through a set of thin-section specimens having well established rim values; (2) these rim values should be established by at least three laboratories; and (3) this verification should be repeated annually and for each analyst. Such procedure would serve to add considerable credibility to hydration measurements, and have the secondary result of establishing lines of communication between laboratories.

The next recommendation is chiefly important when applying absolute dates to hydration measurements. Since all hydration rates at present are based on rhyolitic obsidian, laboratories receiving obsidians from regions not previously known as a rhyolitic source should submit at least one sample for chemical analysis. Although the vast majority of obsidians in North America are rhyolitic (composed chiefly of orthoclase and quartz), the check would be a wise precaution to insure against a trachyte (chiefly orthoclase and biotite) source.

The final recommendation deals with the publication of hydration measurements. Each hydration measurement should include three parts: (1) the mean rim value in microns; (2) the measurement error in standard deviations (with the included rate error when applicable); and (3) the absolute age in years when applicable. The results of the hydration analysis must include the micron value as it is the primary measurement, and must include the error limits in standard deviations to show the probable range of variation from the mean. To simply show the date in years without somewhere specifying the micron value and error limits would be very poor procedure in any event.

From the third and final main objective i.e., determining the relative and tentative absolute chronology of the SAC-29 artifacts, comes the actual application of the hydration dating method. The results of this analysis, found in Appendix B, provided information regarding SAC-29 which is conveniently divided into two basic categories: geotemporal and cultural interpretations.

Under the geotemporal category an investigation of the

time-soil depth relationship gave the following conclusions: (1) the degree of hydration at SAC-29 increases at the uniform rate of $.43 \mu$ per foot of soil depth; (2) age in years increases generally as the square of the soil depth; (3) soil accumulation at SAC-29 between 400 and 1100 B.P. (during the period of greatest occupation) was on the order of $.25$ inches per year; (4) there was a net displacement of surface material over the site on the order of one foot; (5) the stratigraphy above two feet in depth is discontinuous; and (6) the stratigraphy below two feet is generally continuous, but with considerable artifact migration between strata.

Between the two basic categories comes a topic belonging more to statistics which is important to both geotemporal and cultural interpretations. Under this middle topic falls: (1) the test of the uniform hydration hypothesis; (2) the number of artifacts constituting small and large samples; and (3) the magnitude and nature of the combined error function. The results of the hypothesis test were positive: utilizing the combined standard deviations of 25 artifacts from five burials, a chi-square test (at the 99% confidence level) disclosed that the variation in hydration for the burial obsidians was not significantly greater than the measurement error. Thus similiar obsidians in similiar environments were found to have uniform amounts of hydration.

A secondary result of the statistical inspection of the burial obsidians was the observation that seven samples seems

to be the breaking point between large and small grouped samples for the standard deviations normally encountered in hydration work. The confidence levels tend to decrease for groups below this number, whereas above seven they tend to increase. Thus in dating burial-associated obsidian lots or other grouped samples, it is advisable to have at least seven specimens to insure a high level of confidence.

Regarding the third part of the present topic, as mentioned previously, the error limits must be included in all measurement results. All too often, however, this limit includes only the measurement error when the results are converted to years and ignores the rate error. The nature of the two error factors does not permit such an omission: the two are reciprocal in nature with the percentage measurement error decreasing and the percentage rate error increasing in time. For the Sacramento-Davis microclimate, the rate error was found to be $\pm .15 \mu^2/10^3$ years and the measurement error $\pm .09 \mu$. By converting the rate error to a micron function, and then combining the two errors, the following combined error function was obtained: $E_{m+r} = .012 \sqrt{x^2 + 56.30}$.

Since the difference between the combined error (E_{m+r}) and the measurement error (E_m) at zero microns is zero percent and only up to seven percent at three microns, the static measurement error ($\pm .09\mu$) was decided sufficient at and below three microns of hydration. In short, the measurement results will contain one of two error expressions:

$$\begin{array}{ll} x \pm .09 \mu & (x \leq 3\mu) \\ \text{or} & \\ x \pm .012 \sqrt{x^2 + 56.30} \mu & (x > 3\mu) \end{array}$$

Proceeding now to the second basic category (cultural interpretations), the chief concern is with the occupational intensity of the site through time. Based on the assumption that artifact intensity reflects occupational intensity, the Sacramento-Davis hydration rate ($D = 5.21 \mu^2/10^3\text{years}$) was used to expand 157 artifact hydration measurements into a percentage occupational intensity by absolute age in years B.P. The resulting profile in true time perspective can be seen in Figure 5.7. The occupational history as revealed by the analysis indicates a total time coverage of approximately 5000 years, and is tentatively divided into three main periods:

- I. 130 ± 56 B.P. to 1500 ± 100 B.P.
By far the most intense period of occupation with a peak occupation at about 555 ± 60 B.P.
- II. 1500 ± 100 B.P. to 3360 ± 150 B.P.
The middle period with a peak intensity at about 2351 ± 136 B.P.
- III. 3360 ± 150 B.P. to 5133 ± 222 B.P.
The earliest period of occupation indicated by the analysis with a peak intensity about 3886 ± 200 B.P.

The results of the absolute chronological analysis are, of course, based on the tentative local hydration rate; however, the pattern of the timeline profile will be the same regardless of its absolute placement in time. Preliminary work on projectile styles by William Pritchard and Steve Humpherys is starting to indicate agreement with the dates from the tentative hydration rate; unfortunately, their work

is still in progress and thus inconclusive. In time, hopefully, additional work on materials recovered from the King Brown Site (4-SAC-29) will provide artifact assemblages which reflect the chronological profile derived through this application of obsidian hydration dating.

BIBLIOGRAPHY

- Adams, R.
 1968 Archaeological Research Strategies: Past and Present. Science, Vol. 160, No. 3833, pp. 1187-1192, Washington, D.C.
- Barrer, R.M.
 1951 Diffusion in and through Solids. Corrected edition, Cambridge University Press, Cambridge.
- Bausch, Edward
 1949 The Use and Care of the Microscope. Bausch and Lomb Optical Company, New York.
- Chang, Jen-Hu
 1958 Ground Temperature: Volume II. Blue Hill Meteorological Observatory, Harvard University.
- Clark, Donavan
 1961 The Application of the Obsidian Dating Method to the Archaeology of Central California. Doctoral dissertation, Stanford University.
- 1961 The Obsidian Dating Method. Current Anthropology, Vol. 2, No. 2, pp. 111-114, University of Chicago, Chicago.
- 1964 Archaeological Chronology in California and the Obsidian Hydration Dating Method: Part I. Annual Report for 1963-64, Archaeological Survey, pp. 139-225, University of California, Los Angeles.
- Dixon, K.A.
 1966 Obsidian Dates from Temesco, Valley of Mexico. American Antiquity, Vol.31, No.640, 640-643 pp., Salt Lake City.
- Evans, C. and B.J. Meggers
 1960 A New Dating Method Using Obsidian: Part II, An Archaeological Evaluation of the Method. American Antiquity, Vol.25, No.4, pp. 523-537, Salt Lake City.
- Evans, C.
 1965 Reports of the Norwegian Archaeological Expedition to Easter Island and the East Pacific. School of American Research and the Kon Tiki Museum, Phoenix, Arizona.

Friedman, Irving and R.L. Smith
 1958 The Deuterium Content of Water in Some Volcanic Glasses. Geochimica et Cosmochimica Acta, Vol.15, No.3, pp. 218-228, New York.

1960 A New Dating Method Using Obsidian: Part I, The Development of the Method. American Antiquity, Vol.25, No.4, pp. 476-522, Salt Lake City.

Friedman, I., R.L. Smith and D.L. Clark
 1963 Obsidian Dating. In Science in Archaeology, edited by D. Brothwell and E. Higgs, New York.

Friedman, I., W. Long and R.L. Smith
 1963 Viscosity and Water Content of Rhyolite Glass. Journal of Geological Research, Vol.68, No.24, pp. 6523-6535, Washington, D.C.

1966 Hydration of Natural Glass and Formation of Perlite. Geological Society of America Bulletin, Vol.77, pp. 323-327, New York.

Geiger, Rudolf
 1965 The Climate Near the Ground. Harvard University Press, Cambridge.

Girifalco, L.A.
 1964 Atomic Migration in Crystals. Blaisdell Publishing Company, New York.

Green, Roger
 1962 Obsidian: Its Application to Archaeology. New Zealand Archaeological Association Newsletter, No.5:1.

1964 Sources, Ages, and Exploitation of New Zealand Obsidian. New Zealand Archaeological Association Newsletter, No. 7:3.

Heinrich, E.W.
 1956 Microscopic Petrography. McGraw-Hill, New York.

Johnson, Jr., LeRoy
 1969 The Night Fire Island Site: A New Rate of Obsidian Hydration for Parts of California and Oregon. Unpublished manuscript, University of Oregon Museum of Natural History.

Marshall, R.R.
 1961 Devitrification of Natural Glass. Geological Society of America Bulletin, Vol.72, pp. 1493-1520, New York.

- Meighan, C.W., L.J. Foote and P.V. Aiello
1968 Obsidian Dating in West Mexican Archeology.
Science, Vol.160, pp. 1069-1075, Washington, D.C.
- Michels, J.W.
1965 Lithic Serial Chronology through Obsidian Hydration
Dating. Doctoral dissertation, University of
California (Los Angeles), Los Angeles.
- 1967 Archaeology and Dating by Hydration of Obsidian.
Science, Vol.158, No.3798, pp. 211-214,
Washington, D.C.
- 1969 Testing Stratigraphy and Artifact Reuse through
Obsidian Hydration Dating. American Antiquity,
Vol.34, No.1, pp.15-22, Salt Lake City.
- Minor, Ralph
1956 Physical Measurements: Part II. J.J. Gillick and
Company, Berkeley, California.
- Olsen, W.H.
1963 The Comparative Archaeology of the King Brown Site
4-Sac-29. Masters thesis, Sacramento State College,
Sacramento, California.
- Ross, C.S. and R.L. Smith
1955 Water and Other Volatiles in Volcanic Glass.
American Mineralogist, Vol.40, pp. 1071-1089,
New York.
- Rossi, Bruno
1959 Optics. Addison-Wesley, Reading, Massachusetts.
- Sears, F.W.
1949 Optics. Addison-Wesley, Reading, Massachusetts.
- Speigel, M.R.
1961 Theory and Problems of Statistics. Schaum
Publishing Company, New York.
- Zeuner, Frederick
1958 Dating the Past. Methuen, London.

APPENDIX A

FOOTNOTES

Chapter I

1. "Lithic Serial Chronology through Obsidian Hydration Dating" by J.W. Michels (1965) also contains a fairly complete description of laboratory procedure. A major factor to be emphasized is that the equipment used determines many of the finer procedural details.

Chapter II

1. See "Hydration of Natural Glass and Formation of Perlite" by Friedman, Long and Smith (1966); also see "Archaeology and Dating by Hydration of Obsidian" by Michels (1967).
2. Archaeological Chronology in California and the Obsidian Hydration Dating Method: Part I. Donovan Clark; Annual Report for 1963-64, Archaeological Survey, pp. 139-225, University of California, Los Angeles.
3. "Lithic Serial Chronology through Obsidian Hydration Dating" by J.W. Michels (1965).

Chapter III

1. Tautochrones show the variation of temperature with soil depth for a given time period (Geiger, 1965: 56).

Chapter IV

1. The thermoplastic cement, Lakeside #70, has the following properties (Heinrich, 1956: 3):
 - a. Essentially colorless in thin films
 - b. $n = 1.536$, unchanged with age
 - c. Insoluble in petroleum lubricants
 - d. Easy to apply and grind
 - e. Has superior adhering powers and resistance to shock
 - f. More viscous than Canada balsam, thus preventing spreading of the thin-section during covering
 - g. Melts readily at 140°C to a uniform film, but is likely to form bubbles above 150°C .

Chapter IV (continued)

2. A setting of 2.75 on the hot plate normally is effective for one slide. For more than one, the setting can be adjusted accordingly. Should the Lakeside #70 start to vaporize or boil, the heat should be cut for a few minutes and then reset to a lower point.
3. The following rules for estimating the number of figures to keep in a result should be applied (Minor, 1956: 183):

In sums and differences no more decimal places should be retained than can be trusted in the quantity having the fewest trustworthy decimal places. Also,

Quantities which are to be added or subtracted should be measured accurately to the same decimal place, irrespective of whether they have the same number of significant figures or not.

In products and quotients nor more significant figures should be kept than can be trusted in the factor having fewest trustworthy figures.

Quantities which are to be multiplied or divided should be measured to the same number of significant figures.

4. "An optical instrument consisting of a polarizer [fixed angle] and an analyzer [variable angle] is called a polariscope" (Rossi, 1957: 269).
5. When focusing with the x40 objective, closing on the subject causes the "band patterns" to traverse out from the edge at 90° , and vice versa. When closing, the diffusion boundary will be the first to separate from the patterns, and next will be the outer boundary as the bands are continually traversed out. The two rim boundaries will hold their positions thereafter until the microscope's working field depth is exceeded and they "dissolve out of focus."
6. The variation between ten and five trials per reading over thirty samples was found to be $\pm .02$ microns. The error in reproducibility of measurement over thirty samples is $\pm .09$ microns. The change incurred by decreasing from ten to five trials then varies with the measurement error by more than four standard deviations, and therefore has no more than a .0001 % probability of changing an answer. In short, a ten trial reading is a waste of time and is likely to introduce error.

Chapter V

1. T8N, R4E, SE 1/16 of Section 22 (Olsen, 1962: 10).

APPENDIX B

TABLE I

The 4-SAC-29 Obsidian
Hydration Measurement Results

<u>SSC Slide No.</u>	<u>SAC-29 Cat. No.</u>	<u>SAC-29 Feature</u>	<u>Depth in Soil</u>	<u>OH-Rim in μ</u>	<u>Age in Years B.P.</u>
1	168		18-24	3.56	2435 \pm 137
2	59		24-30	3.87	2877 \pm 147
3	4270			3.58	2463 \pm 137
4	4313		42-48	3.16	1917 \pm 122
5	1657			4.50	3887 \pm 191
6	CS-		27-30	2.29	1006 \pm 77
7	7893		12-18	2.50	1200 \pm 90
8	7160		0- 6	1.95	731 \pm 68
9	1811		42-48	2.89	1610 \pm 105
10	3819		0- 6	1.17	263 \pm 40
11	1860		30-36	4.70	4240 \pm 200
12	3364			3.85	2846 \pm 147
13	3115		36-42	2.14	871 \pm 75
14	2603		12-18	4.16	3322 \pm 160
15	7638		36-42	2.33	1042 \pm 82
16				2.14	879 \pm 75
17	129		0- 6	NOR	
18	4211		0- 6	1.10	192 \pm 40
19	4286		6-12	NOR	
20	7853		30-36	4.86	4534 \pm 205
21	4242		0- 6	1.63	510 \pm 58
22	CS-10			NOR	
23	CS-10		30-33	2.52	1220 \pm 88
24	CS-10		21-24	1.96	738 \pm 68
25	1937		30-33	2.57	1269 \pm 88
26	5581	B-313	15"	2.13	871 \pm 75
27	5577	"	"	2.03	791 \pm 70
28	5578	"	"	2.09	838 \pm 70
29	5583	"	"	2.10	846 \pm 75
30	5584	"	"	2.07	823 \pm 70
31	5580	"	"	2.08	830 \pm 70
32	5582	"	"	2.09	838 \pm 70
33	5579	"	"	2.10	846 \pm 75
34	5585	"	"	2.04	799 \pm 70
35	5589	"	"	2.01	776 \pm 70
36	8291	B-307	3- 4	2.31	1042 \pm 82
37	8292	"	"	2.35	1061 \pm 82
38	3607	B-306	22"	1.87	672 \pm 64
39	6726	B-315	52"	1.81	629 \pm 64
40	6728	"	"	1.84	650 \pm 64

<u>SSC</u> <u>Slide No.</u>	<u>SAC-29</u> <u>Cat. No.</u>	<u>SAC-29</u> <u>Feature</u>	<u>Depth</u> <u>in Soil</u>	<u>OH-Rim</u> <u>in μ</u>	<u>Age in</u> <u>Years B.P.</u>
41	148	B-305	13"	3.13	1881 \pm 122
42	3606	B-306	22"	1.90	693 \pm 68
43	3604	"	"	1.85	659 \pm 64
44	3604	"	"	1.88	679 \pm 64
45	6235	B-304&1		3.52	2378 \pm 137
46	6244	"	24"	2.44	1144 \pm 85
47	6247	"	"	2.06	815 \pm 70
48	6245	B-301	"	2.28	998 \pm 77
49	6336	"	"	2.17	904 \pm 75
50	6243	"	"	2.19	921 \pm 75
51	6249	"	"	1.88	679 \pm 64
52	6250	"	"	1.88	679 \pm 64
53	6248	"	"	1.88	679 \pm 64
54	6239	"	"	1.87	672 \pm 64
55	6242	"	"	2.01	776 \pm 70
56	6237	"	"	1.98	753 \pm 68
57	6246	"	"	2.06	815 \pm 70
58	6238	"	"	2.12	863 \pm 75
59	6240	"	"	2.10	846 \pm 75
60	6241	"	"	2.10	846 \pm 75
61	6251	"	"	2.10	846 \pm 75
62	6252	"	"	2.09	838 \pm 70
63	6253	"	"	2.23	955 \pm 77
64	6254	"	"	2.07	823 \pm 70
65	6255	"	"	2.13	871 \pm 75
66	6256	"	"	2.14	879 \pm 75
67	6257	"	"	2.08	830 \pm 70
68	6258	"	"	2.10	846 \pm 75
69	6259	"	"	2.78	1492 \pm 104
70	4425		52-62	2.51	1210 \pm 88
71	2195		18-24	1.93	716 \pm 68
72	1130			4.64	4133 \pm 197
73	7934		18-24	1.64	516 \pm 58
74	4111		36-42	2.13	863 \pm 75
75	7935		18-24	1.82	636 \pm 64
76	4894		12-18	1.73	575 \pm 60
77	6388		30-36	1.82	636 \pm 64
78	6060		12-18	1.87	672 \pm 64
79	4365		"	2.45	1153 \pm 85
80	4458			1.36	355 \pm 47

<u>SSC</u> <u>Slide No.</u>	<u>SAC-29</u> <u>Cat. No.</u>	<u>SAC-29</u> <u>Feature</u>	<u>Depth</u> <u>in Soil</u>	<u>OH-Rim</u> <u>in μ</u>	<u>Age in</u> <u>Years B.P.</u>
81	3360			1.87	672 \pm 64
82	7790		36-42	1.87	672 \pm 64
83	6061		12-18	1.69	549 \pm 60
84	497		0- 6	1.53	450 \pm 53
85	5558		6-12	1.15	254 \pm 40
86	5254		"	1.78	609 \pm 60
87	4977		0- 6	1.52	456 \pm 53
88	3965		48-54	2.28	998 \pm 77
89	6669		12-18	1.64	516 \pm 58
90	6308		24-30	2.02	784 \pm 70
91	1511		36-42	2.10	846 \pm 75
92	6257	B-301		2.13	863 \pm 75
93	2958		18-24	2.13	863 \pm 75
94	CS-7		24-27	3.06	1797 \pm 117
95	4300		18-24	2.30	1015 \pm 82
96	4480		"	1.99	761 \pm 68
97	778		12-18	2.44	1144 \pm 85
98	7878		0- 6	1.67	535 \pm 58
99	1095		"	1.53	450 \pm 53
100	940		0-36	2.10	846 \pm 75
101	5313		0- 6	1.29	319 \pm 43
102	5665		24-30	2.09	838 \pm 70
103	3361			3.38	2193 \pm 129
104	2624		18-24	2.35	1061 \pm 82
105	5664		24-30	2.44	1144 \pm 85
106	22		6-12	2.31	1024 \pm 82
107	3348		0- 6	3.42	2245 \pm 132
108	6530		6-12	1.43	393 \pm 50
109	7806		36-42	1.68	542 \pm 58
110	3363			1.75	589 \pm 60
111	4998		12-18	1.81	629 \pm 64
112	4284		6-12	2.23	955 \pm 77
113	3675		36-42	3.20	1966 \pm 124
114	7996		30-36	1.61	497 \pm 58
115	CS-6		12-15	2.51	1210 \pm 88
116	4575		12-18	1.66	529 \pm 58
117	6758		36-42	1.76	597 \pm 60
118	2397		18-24	1.82	636 \pm 64
119	3918		30-36	1.67	536 \pm 58
120	7444		18-24	3.01	1739 \pm 105

<u>SSC</u> <u>Slide No.</u>	<u>SAC-29</u> <u>Cat. No.</u>	<u>SAC-29</u> <u>Feature</u>	<u>Depth</u> <u>in Soil</u>	<u>OH-Rim</u> <u>in μ</u>	<u>Age in</u> <u>Years B.P.</u>
121	7915		6-12	1.56	468 \pm 53
122	6232		30-36	2.58	1279 \pm 88
123	5493		18-24	2.36	1070 \pm 82
124	4515		0- 6	1.60	491 \pm 58
125	4169		6-12	1.94	724 \pm 68
126	2442		12-18	2.08	830 \pm 70
127	745		0- 6	1.50	432 \pm 53
128&B	4999		12-18	NOR	
129	6406		24-30	NOR	
130	1254		30-36	NOR	
131	7162		0- 6	1.49	426 \pm 50
132	7061		36-42	1.66	529 \pm 58
133	6415		0- 6	1.55	462 \pm 53
134	2015		24-30	1.69	548 \pm 58
135&B	6573		30-36	NOR	
136	7569		24-30	NOR	
137	7966		42-48	3.42	2245 \pm 132
138	1852		6-12	1.93	716 \pm 68
139	2443		12-18	2.06	815 \pm 70
140	3162		18-24	1.86	666 \pm 64
141	5920		12-18	1.76	597 \pm 60
142	4784			1.82	636 \pm 64
143	4436		12-18	1.75	589 \pm 60
144	7469		12-18	1.76	597 \pm 60
145	7951		6-12	2.83	1546 \pm 98
146	6509		12-18	NOR	
147	1000		"	1.77	604 \pm 60
148	3114		36-42	1.88	679 \pm 64
149	7889		12-18	NOR	
150	7684		102-108	NOR	
151	6759		36-42	1.47	415 \pm 50
152	6351		18-24	NOR	
153	7936		"	1.90	693 \pm 68
154	5110		12-18	2.01	776 \pm 70
155	4533			1.64	516 \pm 58
156	3665		6-12	1.50	432 \pm 53
157	7913		6-12	NOR	
158	8093		42-Sterile	1.90	693 \pm 68
159	4433		12-18	2.95	1670 \pm 102
160	1890		18-24	3.07	1785 \pm 105

<u>SSC</u> <u>Slide No.</u>	<u>SAC-29</u> <u>Cat. No.</u>	<u>SAC-29</u> <u>Feature</u>	<u>Depth</u> <u>in Soil</u>	<u>OH-Rim</u> <u>in u</u>	<u>Age in</u> <u>Years B.P.</u>
161	8304		72-78	4.70	4240 ± 200
162	5559		6-12	3.80	2772 ± 155
163	6309		24-30	1.49	426 ± 50
164	7495		18-24	1.94	724 ± 68
165	1253		30-36	2.03	792 ± 70
166	6074		0-6	1.32	334 ± 47
167	7060		36-42	2.76	1471 ± 95
168	3838		0-6	1.79	617 ± 60
169	6510		12-18	1.64	516 ± 58
170	09		0-6	1.21	281 ± 43
171	6660		42-48	2.94	1659 ± 102
172	2566		6-12	1.81	629 ± 64
173	3362			NOR	
174	4589		12-18	1.78	610 ± 60
175	6473			1.55	462 ± 53
176	6727	B-315		1.80	622 ± 64
177	5667		24-30	1.76	597 ± 60
178	7952			1.76	597 ± 60
179	7233		42-48	1.55	462 ± 53
180	7037		18-24	2.57	1269 ± 88
181	4050		30-36	1.95	731 ± 68
182	7868		36-42	1.53	450 ± 53
183	4535		66	3.50	2351 ± 137
184	4534		66	3.45	2285 ± 132
185	8301	B-307		1.81	629 ± 64
186	8299	"		1.90	693 ± 68
187	8300	"		1.90	693 ± 68
188	8298	"		1.81	629 ± 64
189	3821		0-6	1.29	319 ± 43
190	5663		24-30	1.83	643 ± 64
191	4517		0-6	1.76	597 ± 60
192	4997		12-18	1.80	622 ± 64
193	8293	B-308		1.93	716 ± 68
194	8294	"		1.98	756 ± 68
195	8295	"		1.99	761 ± 68
196	8296	"		1.98	756 ± 68
197	8297	"		1.97	749 ± 68
198	7851		30-36	1.72	568 ± 60
199	3482		12-18	NDR	
200	3416		0-6	1.81	629 ± 64

<u>SSC</u> <u>Slide No.</u>	<u>SAC-29</u> <u>Cat. No.</u>	<u>SAC-29</u> <u>Feature</u>	<u>Depth</u> <u>in Soil</u>	<u>OH-Rim</u> <u>in μ</u>	<u>Age in</u> <u>Years B.P.</u>
201	4242		0-6	1.64	516 \pm 58
202	2977		24-30	1.62	503 \pm 58
203	7018		12-18	NOR	
204	4168		6-12	NOR	
205	942		0-36	1.76	597 \pm 60
206	4235		30-36	1.64	516 \pm 58
207	7802		36-42	2.94	1659 \pm 102
208	4586		12-18	3.64	2544 \pm 140
209	1778		0-6	2.66	1359 \pm 91
210	3301		36-42	NDR	
211	2806		6-12	3.45	2285 \pm 132
212	3126		0-6	2.04	800 \pm 70
213	3462		12-18	4.46	3819 \pm 180
214	3747		30-36	3.24	2016 \pm 124
215	7999		30-36	1.83	643 \pm 64
216	3417		0-6	0.82	130 \pm 30
217	7115		30-36	1.60	491 \pm 58
218	7286		18-24	1.51	438 \pm 53
219	3966		48-54	1.74	582 \pm 60
220	4817			NOR	
221	6912		30-36	NDR	
222	7914		6-12	1.29	319 \pm 43
223	8023		18-24	1.64	516 \pm 58
224	7543		84-90	3.17	1929 \pm 122
225	6954		84-90	4.46	3819 \pm 180
226	7616		96-102	5.17	5131 \pm 218
227	7528		90-96	4.51	3904 \pm 191
228	6861		114-120	LIP	
229	7726		84-90	NDR	
230	1239		30-36	1.74	582 \pm 60
231	3845		42-48	1.71	562 \pm 60
232	2897		0-6	1.01	196 \pm 36
233	7232		42-48	1.71	562 \pm 60
234	7687 (?)		102-108	1.51	438 \pm 53
235	6725	B-315		1.71	562 \pm 60
236	3954		54-60	1.71	562 \pm 60
237	3967		48-54	1.64	516 \pm 58
238	7230		42-48	2.26	981 \pm 77
239	660		36-42	2.30	1015 \pm 82
240	8072		36-42	1.88	679 \pm 64

<u>SSC</u> <u>Slide No.</u>	<u>SAC-29</u> <u>Cat. No.</u>	<u>SAC-29</u> <u>Feature</u>	<u>Depth</u> <u>in Soil</u>	<u>OH-Rim</u> <u>in u</u>	<u>Age in</u> <u>Years B.P.</u>
241	6760		36-42	1.74	582 ± 60
242	8071		36-42	NDR	
243	4051		30-36	1.22	286 ± 43
244	2137		30-36	1.95	731 ± 68
245	7111		30-36	1.99	761 ± 68
246	1625		30-36	1.53	450 ± 53
247	7114		30-36	2.75	1460 ± 95
248	6389		30-36	1.93	716 ± 68
249	2182		30-36	2.42	1125 ± 85
250	2051		30-36	1.97	749 ± 68
251	2138		30-36	1.97	749 ± 68
252	1233		30-36	4.86	4534 ± 205
253	6387		30-36	1.72	568 ± 60
254	3016		30-36	1.88	679 ± 64
255	6692		24-30	1.46	410 ± 50
256	7005		24-30	1.67	536 ± 58
257	5228		24-30	1.20	276 ± 43
258	3095		24-30	1.64	516 ± 58
259	6408		24-30	1.58	480 ± 53
260	5666		24-30	1.90	693 ± 68
261	5785		24-30	1.53	450 ± 53
262	4077		24-30	1.20	276 ± 43

- Note:
- (1) Years B.P. measured from 1969
 - (2) Depth in soil measured in inches
 - (3) NDR = No Distinguishable Rim i.e., rim suspected but thin-section characteristics prevent positive identification of rim or rim location
 - (4) NOR = No Observable Rim i.e., optically sufficient thin-section without a rim.
 - (5) LIP = Lost In Preparation
 - (6) CS = Column Sample
 - (7) B = Burial

APPENDIX C

TABLE I

Micron Equivalents in Years B.P.
Based on $x^2 = 5.21t$ Derived for
the Sacramento-Davis Microclimate

<u>Microns = Years, B.P.</u>		<u>Microns = Years, B.P.</u>	
.5	48	4.0	3071
.6	69	.1	3226
.7	94	.2	3386
.8	123	.3	3549
.9	156	.4	3716
1.0	192	.5	3887
.1	232	.6	4061
.2	276	.7	4240
.3	324	.8	4422
.4	376	.9	4608
.5	432	5.0	4798
.6	491	.1	4992
.7	555	.2	5190
.8	622	.3	5392
.9	693	.4	5597
2.0	768	.5	5806
.1	846	.6	6019
.2	929	.7	6236
.3	1015	.8	6457
.4	1106	.9	6681
.5	1200	6.0	6910
.6	1298	.1	7142
.7	1399	.2	7378
.8	1505	.3	7618
.9	1614	.4	7862
3.0	1727	.5	8109
.1	1844	.6	8360
.2	1966	.7	8616
.3	2090	.8	8875
.4	2219	.9	9138
.5	2351	7.0	9405
.6	2488	.1	9676
.7	2628	.2	9950
.8	2772	.3	10,228
.9	2919		

TABLE II

Micrometer Ocular Conversion
Factors Used for the x40 Objective

<u>Drum Divisions</u>	<u>Microns</u>	<u>Drum Divisions</u>	<u>Microns</u>
0.0	0.0000	30.0	3.525
0.1	0.0117	31.0	3.642
0.2	0.0235	32.0	3.760
0.3	0.0352	33.0	3.878
0.4	0.0470	34.0	3.995
0.5	0.0588	35.0	4.112
0.6	0.0705	36.0	4.230
0.7	0.0823	37.0	4.346
0.8	0.0940	38.0	4.465
0.9	0.1057	39.0	4.582
10.0	1.175	40.0	4.700
11.0	1.292	41.0	4.818
12.0	1.410	42.0	4.935
13.0	1.528	43.0	5.052
14.0	1.645	44.0	5.170
15.0	1.762	45.0	5.288
16.0	1.880	46.0	5.405
17.0	1.998	47.0	5.522
18.0	2.115	48.0	5.640
19.0	2.232	49.0	5.756
20.0	2.350	50.0	5.876
21.0	2.466	51.0	5.992
22.0	2.585	52.0	6.112
23.0	2.702	53.0	6.228
24.0	2.820	54.0	6.345
25.0	2.938	55.0	6.462
26.0	3.055	56.0	6.580
27.0	3.172	57.0	6.698
28.0	3.290	58.0	6.815
29.0	3.406	59.0	6.932

APPENDIX D

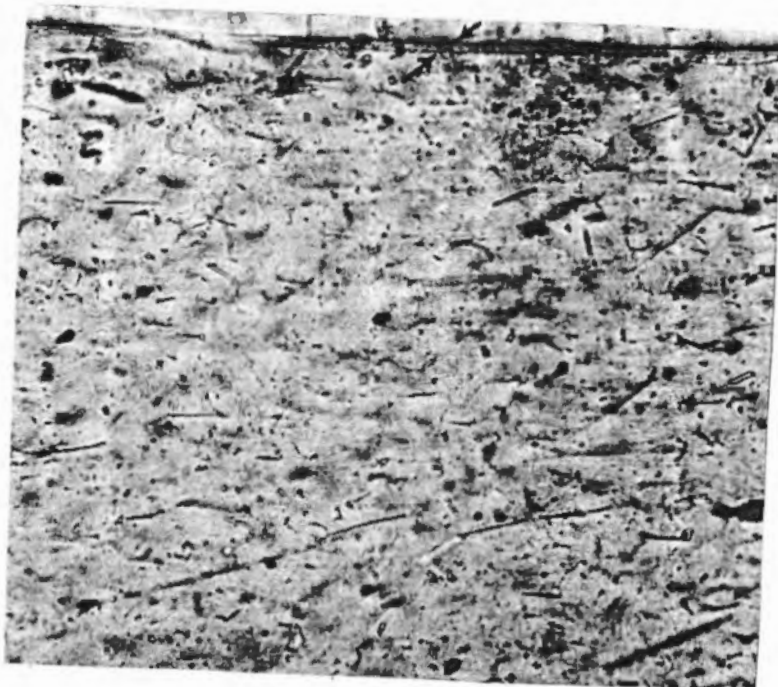


Plate 3.1. Photomicrograph (x400) showing a 2.6 micron hydration rim between the arrows. (From Clark, 1964: Plate 1d).

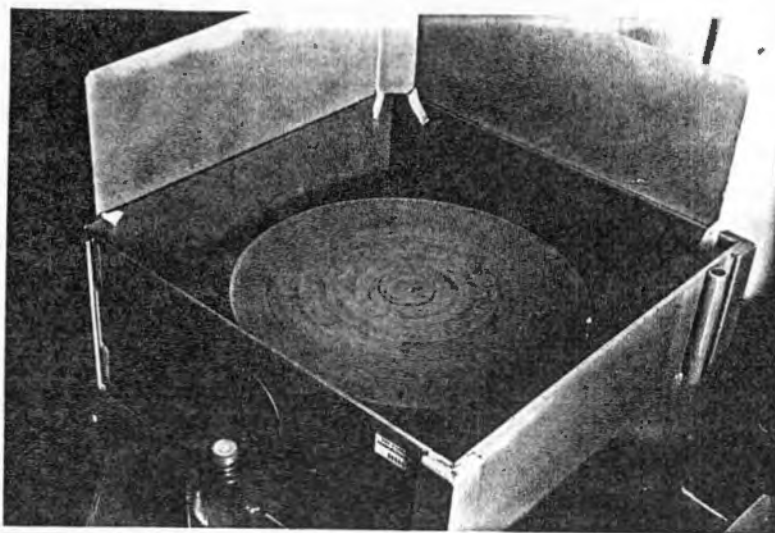


Plate 4.5. Horizontal lap wheel: 90-100 RPM, 12 inch diameter. Abrasive used: #400 corundum powder and water.

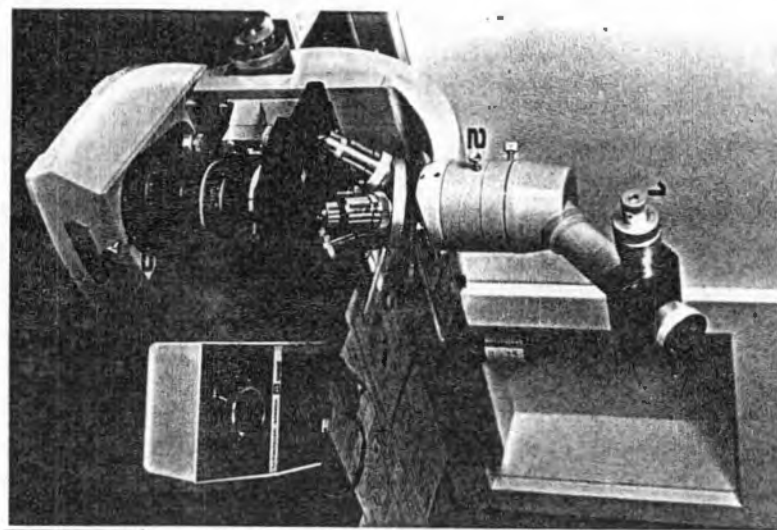


Plate 4.7. Microscope: (#1) Micrometer drum, (#2) Polarizer, (#3) Quartz wedge, (#4) Light condenser, (#5) Analyzer, (#6) Illuminator.

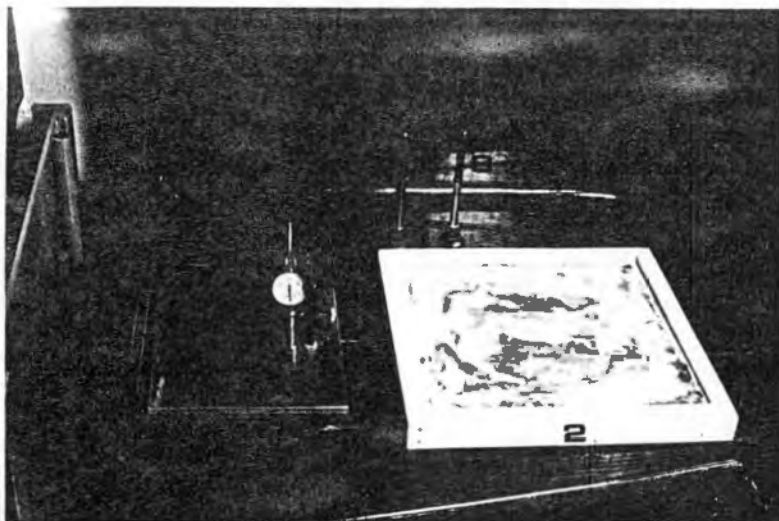


Plate 4.6. (#1) Dial Test Indicator, .001" by graduation, (#2) Pyrex base for #1000 fine abrasive, (#3) Suction darts.

Cat. # _____ SACRAMENTO STATE COLLEGE--DEPARTMENT OF ANTHROPOLOGY Slide # _____		Obsidian Hydration Identification Card	
Site _____	Unit _____	Depth _____	Artifact Type _____
State _____		County _____ Associations _____	
Operator _____	Date _____	Operator _____	Date _____
Micron Determination _____	Micron Determination _____	Micron Determination _____	Micron Determination _____
1. _____	Rim _____	1. _____	Rim _____
2. _____	Average _____	2. _____	Average _____
3. _____	_____	3. _____	_____
4. _____	µm _____	4. _____	µm _____
5. _____	cm _____	5. _____	cm _____
Lens: X10 X40 X100 _____		Lens: X10 X40 X100 _____	
Comments: _____		Comments: _____	
			Negative # _____
			Scale _____

Plate 4.8. Obsidian Hydration Identification Card. Area above "scale" is used for photograph of the artifact.



183

Scale-1/2



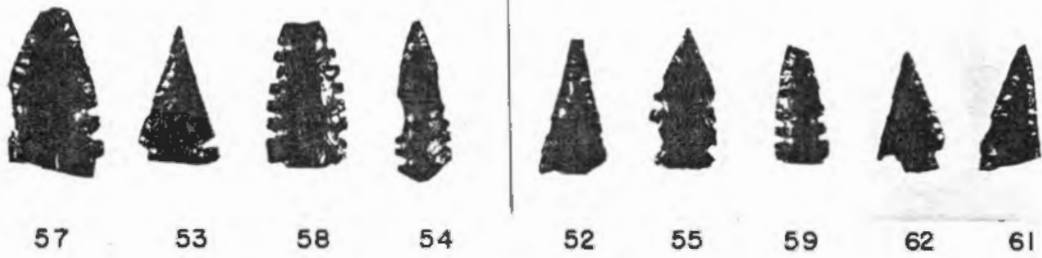
184

Plate 4.9 (a&b). Two examples of disguised sectioning gaps: arrows indicate the position from which the test-section was removed from each artifact. The gap was primarily filled with modeling clay and then finished with Hyplar Paste and Color. The gaps are thus permanently disguised thereby restoring the artifact's physical continuity.

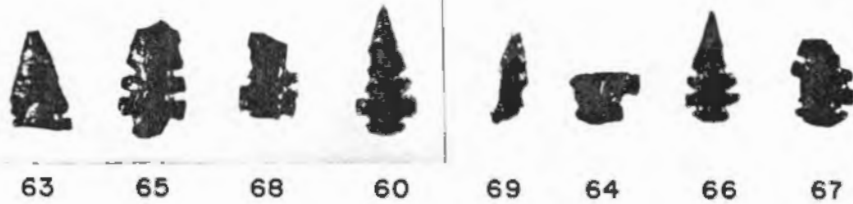
BURIAL - 30184



SCALE 1/2



SCALE 1/2



SCALE 1/2



92

SCALE 3/4

BURIALS - 305, 306, 307 & 308



41

B-305

SCALE - 1/2



38 42 43 44

B-306

SCALE - 1/3



37



36



188



187

186



185



B - 307

SCALE (36,37)-1/2

SCALE (185-8)-3/4



193



195



196



197

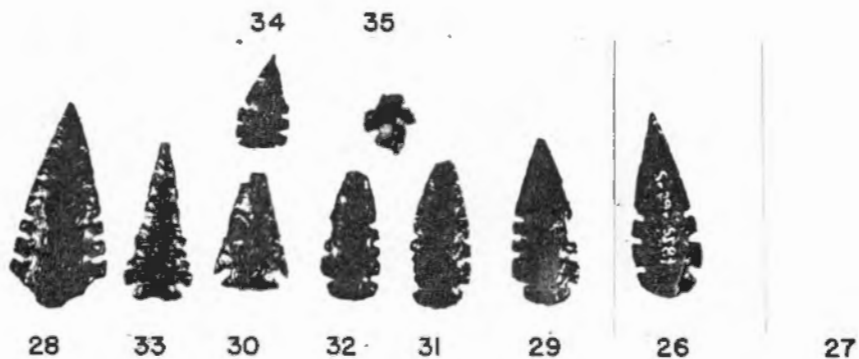


194

B - 308

SCALE - 3/4

BURIALS - 313 & 315



B - 313

SCALE (28-35) - 1/2

SCALE (26, 27) - 3/4



B - 315

SCALE (39, 40) - 1/2

SCALE (176, 235) - 3/4